

Inaugural dissertation
for
obtaining the doctoral degree
of the
Combined Faculty of Mathematics, Engineering and Natural Sciences
of the
Ruprecht - Karls - University
Heidelberg

Presented by
M. Sc. Kristin Frensemeier
born in: Paderborn
Oral examination: 20.07.2022

Dickkopf-1:
An indirect target for oncogenic HPVs
and its role in Cisplatin-mediated apoptosis in
cervical cancer cells

Referees: Prof. Dr. Martin Müller
Prof. Dr. Felix Hoppe-Seyler

Table of Contents

Summary	V
Zusammenfassung	VII
Acknowledgements	IX
Publications and Presentations	XI
1. Introduction	3
1.1 Human papillomaviruses (HPVs).....	3
1.1.1 HPVs and cervical cancer	3
1.1.2 Molecular biology of HPV-associated carcinogenesis	4
1.1.3 The HPV E6 and E7 oncoproteins	6
1.1.4 Cervical cancer and hypoxia	8
1.1.5 Therapy of HPV-positive cervical cancer	9
1.2 Dickkopf-1 (Dkk1): A potential tumor suppressor in cervical cancer.....	11
1.2.1 The Dickkopf (Dkk) family of proteins	11
1.2.2 Dkk1 in canonical Wnt signaling	12
1.2.3 Dkk1 in non-canonical Wnt signaling and beyond	14
1.2.4 The bipartite role of Dkk1 in cancer	14
1.3 Apoptosis.....	15
1.3.1 Mechanisms of apoptosis	16
1.3.2 Interference of HPV E6/E7 with apoptosis	18
1.3.3 JNK/AP-1 signaling in apoptosis	18
1.3.4 Senescence: An alternative stress-induced cell fate	20
1.4 Research objectives.....	20
2. Results	25
2.1 Crosstalk of Dkk1 with the HPV oncogenes.....	25
2.1.1 Dkk1 induction upon HPV E6/E7 silencing	25
2.1.2 Dkk1 is repressed by the HPV oncogenes in a p53-dependent manner	26
2.1.3 Dkk1 is no upstream regulator of the HPV oncogenes	28
2.2 Analysis of hypoxic Dkk1 regulation.....	28
2.2.1 Hypoxic Dkk1 repression in HPV-positive and HPV-negative cells	28
2.2.2 OXPPOS inhibition mimics hypoxic Dkk1 regulation	30
2.2.3 Transient Dkk1 repression under hypoxia	31

2.2.4	The ambiguous role of p53 for hypoxic Dkk1 repression	32
2.3	Analysis of epigenetic regulation of Dkk1 in cervical cancer cell lines	33
2.3.1	Cell line-dependent epigenetic regulation of Dkk1	34
2.3.2	Epigenetic silencing plays no major role in hypoxic Dkk1 repression	35
2.4	The role of Dkk1 in the cellular response towards Cisplatin	36
2.4.1	Dose- and cell line-dependent induction of Dkk1 by Cisplatin	36
2.4.2	Dkk1 expression induces apoptosis in a Dkk1-negative HeLa variant	38
2.4.3	Dkk1 sensitizes HeLa cells towards Cisplatin-mediated apoptosis	39
2.4.4	RNAi-induced Dkk1 repression impairs Cisplatin-mediated apoptosis	40
2.4.5	Cisplatin resistance of Dkk1 knockout HeLa cells	42
2.4.6	Induction of senescence in Dkk1 KO HeLa cells	43
2.5	Canonical Wnt signaling and the Dkk1-dependent Cisplatin response	44
2.5.1	Dkk1 counteracts Wnt3a-induced canonical Wnt signaling	45
2.5.2	The Dkk1-dependent Cisplatin response is uncoupled from Wnt activation	45
2.6	Affymetrix gene expression analyses of Cisplatin-treated HeLa cells.....	47
2.6.1	Identification of global gene alterations	47
2.6.2	Differential activation of AP-1 signaling factors	49
2.6.3	Validation of EGR-1 and Bim as potential AP-1 targets	51
2.7	The role of JNK signaling in the Dkk1-dependent Cisplatin response.....	53
2.7.1	JNK activation is required for Cisplatin-induced apoptosis in HeLa cells	53
2.7.2	JNK signaling in Cisplatin-mediated apoptosis in SiHa and CaSki cells	55
3.	Discussion.....	59
3.1	Dkk1 expression in cervical cancer cells.....	59
3.1.1	HPV-oncogene driven Dkk1 repression	59
3.1.2	Dkk1 expression in hypoxic cervical cancer cells	60
3.1.3	The role of p53 in regulating Dkk1 expression	61
3.1.4	Epigenetic Dkk1 regulation	63
3.2	The pro-apoptotic role of Dkk1 in the Cisplatin response of cervical cancer cells.....	64
3.2.1	Cisplatin-induced Dkk1 induction and apoptosis	64
3.2.2	Dkk1 depletion protects against Cisplatin-induced apoptosis	66
3.2.3	Dkk1 KO HeLa cells acquire a senescent phenotype	67
3.2.4	Cellular mechanisms behind the Dkk1-dependent Cisplatin response	68
3.2.5	JNK signaling activation in Cisplatin-induced apoptosis	71
3.3	Implications of Dkk1 and JNK/AP-1 in cancer therapy	73

3.4	Conclusions	75
4.	Materials and Methods	79
4.1	Reagents	79
4.2	DNA-related methods.....	79
4.2.1	Plasmid transformation	79
4.2.2	Plasmid DNA isolation	80
4.2.3	Agarose gel electrophoresis	81
4.2.4	Plasmid DNA validation	82
4.2.5	Molecular cloning strategies	82
4.3	Cell-related methods	84
4.3.1	Cell culture	84
4.3.2	Long-term preservation of cells	84
4.3.3	Transfection with siRNA	85
4.3.4	Plasmid Transfection	86
4.3.5	Preparation of Dkk1 CM	86
4.3.6	Chemical treatments	87
4.3.7	CRISPR/Cas9-mediated generation of HeLa Dkk1 KO clones	88
4.3.8	TUNEL assay	88
4.3.9	Caspase 3/7 Assay	89
4.3.10	Senescence Assay	89
4.3.11	Colony Formation Assay	90
4.3.12	TOP-/FOPflash luciferase assay	90
4.4	RNA-related methods	92
4.4.1	RNA isolation	92
4.4.2	Reverse transcription	92
4.4.3	Quantitative real-time PCR (qRT-PCR)	92
4.4.4	Gene expression analyses on Affymetrix GeneChips	94
4.5	Protein-related methods	95
4.5.1	Protein isolation and protein sample preparation	95
4.5.2	Protein sample preparation from cell supernatants	96
4.5.3	SDS polyacrylamide gel electrophoresis (SDS-PAGE)	96
4.5.4	Immunoblots	97
4.6	Statistical Analyses	97

Appendix.....	101
List of Figures	101
List of Tables	102
Abbreviations.....	102
References.....	106

Summary

Oncogenic human papillomavirus (HPV) types cause cervical cancer. The continuous expression of the viral *E6/E7* oncogenes controls the malignant phenotype of HPV-positive cancer cells, as they interfere with major tumor-suppressive pathways and thereby induce uncontrolled cell proliferation and cellular resistance towards apoptosis. The low vaccination rates with the prophylactic vaccines protecting against oncogenic HPV infections as well as the overall poor therapeutic response of advanced or recurrent cervical carcinomas emphasize the importance to improve our concepts of HPV-associated carcinogenesis as a basis to develop more efficient therapeutic options.

The overall aim of this thesis was to characterize the regulation and functional role of the putative tumor suppressor protein Dickkopf-1 (Dkk1) in cervical cancer cells. My studies revealed that Dkk1 levels are strongly restricted by HPV oncogene expression. Mechanistically, E6 was found to be a key driver in this process by interfering with the ability of p53 to activate Dkk1 expression. Moreover, epigenetic mechanisms as well as metabolic changes at hypoxic conditions, such as the inhibition of oxidative phosphorylation (OXPHOS), were shown to be additional driving forces in silencing Dkk1 expression levels in cervical cancer cells.

Further, I could demonstrate that Dkk1 levels are a critical determinant for the Cisplatin response of cervical cancer cells: While treatment with Dkk1 conditioned medium sensitized HeLa cells towards Cisplatin treatment, RNAi- or CRISPR/Cas9-induced Dkk1 repression or depletion efficiently protected cervical cancer cells from Cisplatin-induced apoptosis. Despite the well-characterized role of Dkk1 in antagonizing canonical Wnt signaling, the Dkk1-dependent Cisplatin response was not associated with alterations of this pathway.

Instead, transcriptome analyses using Affymetrix GeneChip arrays uncovered that multiple members of the AP-1 protein family were less efficiently induced upon Cisplatin treatment in Dkk1 knockout HeLa cells compared to parental HeLa cells. Functional studies revealed that Dkk1 expression was required to induce pro-apoptotic JNK signaling, which acts upstream of AP-1 and is necessary to trigger an efficient apoptotic Cisplatin response in cervical cancer cells.

Collectively, this work discloses that Dkk1 expression in cervical cancer cells is negatively controlled by oncogenic HPVs through E6-mediated p53 degradation. Moreover, it shows that Dkk1 repression provides Cisplatin resistance in cervical cancer cells, which is mechanistically caused by the impairment of Cisplatin-induced pro-apoptotic JNK signaling.

Zusammenfassung

Onkogene Typen humaner Papillomviren (HPV) verursachen das Zervixkarzinom. Die kontinuierliche Expression der viralen *E6/E7*-Onkogene hält den malignen Phänotyp HPV-positiver Krebszellen aufrecht, indem die E6- und E7-Proteine mit zentralen Tumorsuppressor-Signalwegen interferieren und dadurch die unkontrollierte Proliferation sowie die Apoptoseresistenz der Wirtszelle fördern. Sowohl die geringen Impfraten mit den prophylaktisch wirkenden HPV-Vakzinen, als auch die insgesamt schlechte Therapierbarkeit fortgeschrittener oder rezidivierender Zervixkarzinome unterstreichen die Notwendigkeit eines besseren Verständnisses der HPV-assoziierten Karzinogenese, um effizientere therapeutische Optionen zu entwickeln.

Das übergeordnete Ziel dieser Arbeit war es, die Regulation und funktionelle Rolle des putativen Tumorsuppressor-Proteins Dickkopf-1 (Dkk1) in Zervixkarzinomzellen zu charakterisieren. Meine Studien ergaben, dass die Dkk1-Expressionsspiegel durch die HPV-Onkogene stark reprimiert werden. Hierfür spielt die HPV E6-vermittelte negative Regulation von p53 eine entscheidende Rolle, da dadurch die p53-abhängige Aktivierung der Dkk1-Expression verhindert wird. Weiterhin wurde deutlich, dass auch epigenetische Mechanismen sowie metabolische Veränderungen unter Hypoxie, wie die Inhibierung der oxidativen Phosphorylierung (OXPHOS), zu einer Dkk1-Repression in Zervixkarzinomzellen führen können.

Zudem zeigte sich, dass die Dkk1-Expressionslevel eine kritische Determinante für den Phänotyp von Zervixkarzinomzellen unter Cisplatinbehandlung sind: Während Dkk1-konditioniertes Medium HeLa-Zellen gegenüber Cisplatin sensibilisierte, schützte eine durch RNAi- oder CRISPR/Cas9-induzierte Dkk1-Reprimierung bzw. Depletion Zervixkarzinomzellen effizient vor der pro-apoptotischen Wirkung von Cisplatin. Trotz der etablierten Funktion von Dkk1 als Inhibitor des kanonischen Wnt-Signalwegs, korrelierte die Dkk1-abhängige Antwort der Zellen auf Cisplatin nicht mit Veränderungen dieses Signalwegs.

Transkriptomanalysen mittels „Affymetrix GeneChips“-Arrays deckten vielmehr auf, dass mehrere Mitglieder der AP-1 Proteinfamilie in Dkk1 „knockout“ HeLa-Zellen weniger effizient induziert wurden als in parentalen HeLa-Zellen. Funktionelle Analysen ergaben, dass Dkk1 eine wichtige Rolle für die Induktion des pro-apoptotischen JNK/AP-1-Signalwegs spielt und die Aktivierung von JNK für eine effiziente pro-apoptotische Wirkung von Cisplatin in Zervixkarzinomzellen notwendig ist.

Zusammenfassend zeigt diese Arbeit, dass die Dkk1-Expression in Zervixkarzinomzellen durch die HPV E6-vermittelte Degradierung von p53 effizient gehemmt wird. Zudem führt eine Dkk1-Reprimierung zu einer verminderten Aktivierung des pro-apoptotischen JNK-Signalwegs und erhöht dadurch die Cisplatinresistenz in Zervixkarzinomzellen.

Acknowledgements

First of all, I would like to express my gratitude to Prof. Dr. Felix Hoppe-Seyler for giving me the opportunity to join his research group and to complete my PhD project in such an interesting field. Thank you for your excellent guidance, constant support and helpful feedback whenever it was needed. Further, I deeply thank Prof. Dr. Karin Hoppe-Seyler for always giving me valuable support with novel insights for my project and great ideas for all experimental problems.

I also would like to thank Prof. Dr. Martin Müller for taking the time to be my first referee and for supporting my TAC meetings with many critical questions and helpful discussions. Likewise, I am grateful to Prof. Dr. Suat Özbek for his helpful comments and great ideas as my TAC member and for joining my thesis examination committee. I also want to acknowledge Dr. Tim Waterboer for his supporting role as my thesis committee member.

In addition, I appreciate the help of everyone who scientifically contributed to the accomplishment of this thesis. I thank the Microarray Unit of the DKFZ Genomics and Proteomics Core Facility for providing the Affymetrix Gene Expression Arrays and excellent related services, as well as Dr. Damir Kronic, as part of the DKFZ Light Microscopy Core Facility, for his expertise in generating the macros for analyses using ImageJ.

A special thanks goes to all present and former members of the Hoppe-Seyler group. I am deeply grateful to Claudia Lohrey, Julia Bulkescher and especially Angela Holzer towards the end of my PhD work for their excellent technical support and their patience in answering all my questions. To all of them, and also to Anja Herrmann, Dongyun Yang, Tobias Strobel, Nora Heber, Milica Velimirović, Alicia Avenhaus, Felicitas Bossler, Svenja Adrian, Julia Mändl and Maria Weber: A huge thanks for the great time we had in- and outside the lab. You all contributed to the warm and enjoyable working atmosphere which I highly appreciated during my PhD time. I also want to thank Tom Holz for his help with all IT-related problems.

Finally, I owe my thanks to all people who have supported me - even many times from the distance - during the good and not so good times: my parents, my sisters Julia and Lisa with their families, my friends and especially Paul. Thank you for always encouraging me and cheering me up whenever I needed it. I am very lucky to have you all in my life.

Publications and Presentations

Publications

Braun JA, Herrmann AL, Blase JI, **Frensemeier K**, Bulkescher J, Scheffner M, Galy B, Hoppe-Seyler K, Hoppe-Seyler F. Effects of the Antifungal Agent Ciclopirox in HPV-Positive Cancer Cells: Repression of Viral E6/E7 Oncogene Expression and Induction of Senescence and Apoptosis. *Int J Cancer*. (IF 2020: 7.4); 2020; 146(2):461-474.

Frensemeier K, Holzer A, Hoppe-Seyler K, Hoppe-Seyler F. Dickkopf-1 (Dkk1) is an indirect target for oncogenic HPVs and regulates the Cisplatin sensitivity of HPV-positive cancer cells in a JNK-dependent manner. Manuscript under review.

Presentations

Frensemeier K, Hoppe-Seyler K, Hoppe-Seyler F. Repression of Dickkopf-1 in normoxic and hypoxic HPV-positive cancer cells. Helmholtz International Graduate School for Cancer Research. PhD Poster Presentation. 20.11.2020, Heidelberg, Germany. Poster Presentation.

Frensemeier K, Hoppe-Seyler K, Hoppe-Seyler F. Repression of Dickkopf-1 in normoxic and hypoxic HPV-positive cancer cells. 14th International PhD Student Cancer Conference. 16.-18.06.2021, CRUK Beatson Institute, Glasgow, Virtual Edition. Poster Presentation.

Frensemeier K, Hoppe-Seyler K, Hoppe-Seyler F. HPV oncogene-mediated repression of Dickkopf-1 in cervical cancer and its role in cisplatin resistance. Helmholtz International Graduate School for Cancer Research. PhD Retreat. 06.07.2021, DKFZ Heidelberg, Virtual Edition. Poster Presentation.

CHAPTER 1

INTRODUCTION

1. Introduction

1.1 Human papillomaviruses (HPVs)

With an estimated number of almost 20 million new cases and 10 million deaths in 2020, cancer represents a major health burden and belongs to the leading causes of death worldwide.¹ The progress in cancer prevention, treatment and comprehension of tumor biology contradicts the rising numbers of incidences and cancer-related mortalities.¹ This is at least in part explicable by an increased human life span,² changes in lifestyle, including obesity, smoking, alcohol consumption and physical activity,³ as well as by other environmental factors such as UV light or exposure to chemical mutagens or radiation.⁴ Additionally, pathogenic infections are considered major risk factors for carcinogenesis.⁵ In 2018, 13 % of all cancer cases were attributable to infections including those caused by the bacterium *Helicobacter pylori* or by hepatitis B and hepatitis C viruses, but also by human papillomaviruses (HPVs).⁶ Notably, HPV infection is associated with the development of almost 5 % of all cancer incidences worldwide.⁶

1.1.1 HPVs and cervical cancer

Papillomaviruses (PVs) are non-enveloped DNA viruses, which are transmitted via physical skin-to-skin contact, thereby infecting cutaneous and mucosal epithelia.⁷ In total, more than 200 different PV types have been identified of which more than 150 belong to five different genera of human PVs.⁸ The majority of these belong to the low-risk group, which are mainly causative for benign anogenital or cutaneous warts.⁹ In contrast, at least 12 high-risk HPV types of the alpha genus are classified as carcinogenic¹⁰ and they are responsible for the development of oropharyngeal and anogenital cancers (Figure 1).¹¹ Best studied is the role of HPV infection in the development of cervical cancers, which are almost exclusively HPV-positive and which account for more than 80 % of all HPV-attributable cancers.^{6,7} Among women, cervical cancers contribute to 13.3 % of all cancers worldwide and they represent the fourth leading cause of death.¹ Of the HPV types causing cervical cancer, HPV16 is the predominant one (60 %), followed by HPV18 (15 %).¹² Notably, more than 80 % of females become infected with a high risk HPV type during lifetime, but in the majority of cases the infection is cleared by the immune system.⁹

Although HPV infection is considered a necessary step for cervical carcinogenesis, additional factors drive the malignant transformation of HPV-associated tumors.¹⁰ These include the long-term use of oral contraceptives, a high number of child births and tobacco smoking.¹³⁻¹⁶

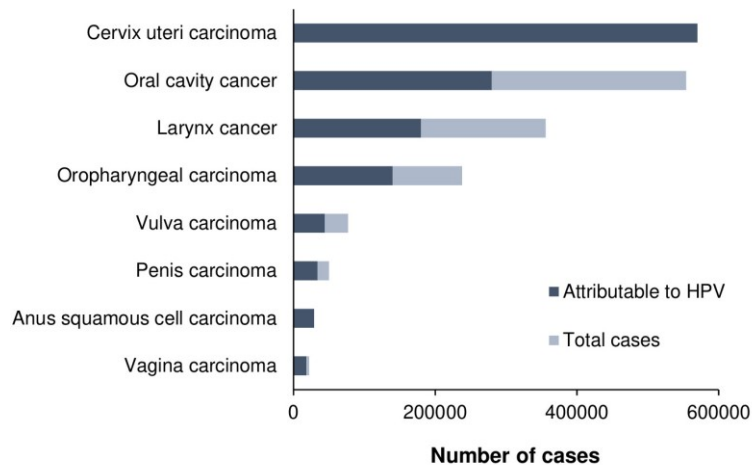


Figure 1 | Cancers attributable to HPV infection in 2018. Data from GLOBOCAN 2018.⁶

In theory, cervical cancer is almost entirely preventable. Routine screenings have resulted in a decline of incidences and their associated deaths in large parts of the world.^{1,17} Moreover, since 2006, three different prophylactic HPV vaccines have been licensed and they are expected to reduce the number of cervical cancer cases in the next decades. While the first developed vaccine Cervarix (GlaxoSmithKline) contains antigens of the predominant oncogenic HPV types 16 and 18, two follow-up Gardasil vaccines (Merck) protect against infection with two or seven additional HPV types, respectively - thereby covering the majority of carcinogenic HPVs.¹⁸ Both, Cervarix and Gardasil vaccines, strongly decreased the incidence of HPV16- and HPV18-caused infections in young girls in countries with an efficient vaccine program.¹⁹ However, the majority of cervical cancer cases arises from low- or middle-income countries in Eastern Europe, Africa or Central Asia,¹ where routine screening programs are barely applied and vaccines are often unavailable due to financial restraints.^{1,20} Moreover, the current vaccines are also not targeting persistent infections and the onset of cervical cancer usually occurs decades after infection.⁷ Thus, cervical cancer as well as other HPV-induced cancers are expected to remain a major health burden worldwide for decades.

1.1.2 Molecular biology of HPV-associated carcinogenesis

The double-stranded, circular genome of HPVs is composed of almost 8000 base pairs and encompasses two late (L1, L2) and six early (E1, E2, E4, E5, E6) open reading frames (ORFs), as well as one long control region (LCR), also referred to as the upstream regulatory region (URR), composed of regulatory elements for genome replication and transcription (Figure 2A).²¹ Gene expression of early (E) and late (L) genes is dependent on the progression of the viral life cycle, and is controlled by the activity of multiple viral promoters and complex splicing processes, giving rise

to a variety of gene products from a relatively small number of genes.¹¹ L1 and L2 encode the major and minor capsid proteins, respectively, which package the viral genome.²² While E1 and E2 are mainly involved in viral replication, and, like L1 and L2, are highly conserved among different HPVs, E4, E5, E6 and E7 are more diverse and their expression and function depend on the papillomavirus type.⁷ E5 expression is restricted to the alpha type of HPVs and functions in protecting the host cells from apoptosis, thereby stimulating cell proliferation and immune evasion in the early phases of infection.²³ In contrast, E4 is stronger expressed at late stages and contributes to an efficient virus assembly and release.²¹ The expression and functions of E6 and E7 strongly differ in between low and high-risk HPV types and the oncogenic properties of E6 and E7 are described in more detail in chapter 1.1.3.

HPVs infect keratinocytes of the multi-layered stratified epithelium in skin and mucosa and their replication and viral life cycle is closely linked to the epithelial differentiation (Figure 2B).²⁴ For infection, the virus needs to access the replicating stem cells in the basal layer of the epithelium, which usually occurs through (micro-)wounds.²¹ Upon binding to heparan sulfate proteoglycans (HSPGs) on the cell surface,²⁵ the L2 capsid protein is cleaved by furin proteases,²⁶ which ultimately leads to the internalization of the viral genome via endocytosis.²⁷ After infection, the expression of E1 and E2 drives the initial viral genome amplification at low levels to ensure the maintenance of viral episomes in the basal layer.

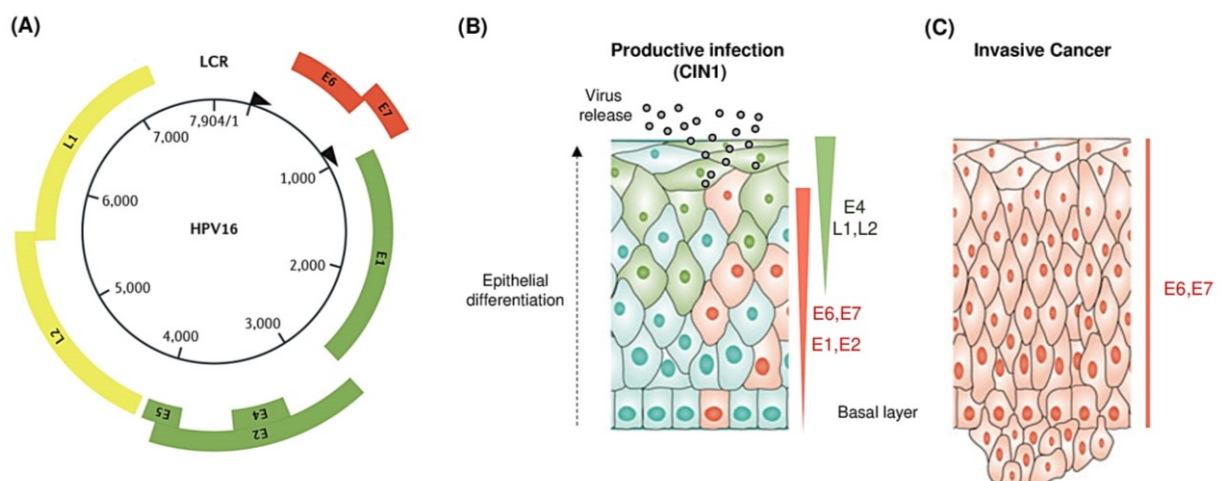


Figure 2 | HPV genome organization and life cycle in the progression to cancer. (A) Genome organization of high-risk HPV type 16. E: early genes, L: late genes, LCR: long control region. Arrows indicate the localization of two major promoters. (B) During productive infection (CIN1: cervical intraepithelial neoplasia I) expression of early (E) and late (L) genes is linked to the epithelial differentiation from the basal layer to the epithelial surface where newly assembled virions are released. (C) In invasive cancer, E6 and E7 drive epithelial cell proliferation. Modified from Schiffmann et al. (2007).⁷

The infected basal epithelial cells differentiate and migrate to upper epithelial layers, which leads to E6 and E7 activation to induce an increase in viral replication and cellular proliferation. In the most upper layers, close to the epithelial surface, E4, L1 and L2 expression results in the production and the release of new virions.^{7,21}

Persistent infection with high risk HPV types can result in enhanced proliferation in the basal epithelial layers, a phenotype which is classified as cervical intraepithelial neoplasia 1 (CIN1) (Figure 2B).⁷ If this is not cleared by the immune system, the proliferating cells can progress to the upper epithelial layers, which usually is accompanied by the disruption of the viral life cycle. At this stage, the lesion is classified as moderate to severe dysplasia (CIN2 and CIN3, respectively) which is the preliminary stage of invasive cervical cancer (Figure 2C).⁷ In these latter stages, the viral gene-expressing episomes are frequently integrated into the host cell genome, which occurs randomly at fragile sites.²⁸ For this purpose, the circular HPV genome is typically interrupted within the E2 ORF, resulting in the functional depletion of the E2, as well as of the E4, E5 and L2 ORFs.²⁹ While of HPV16-positive cervical cancers about 70 % harbor integrated HPV sequences, HPV18-related genomes are almost completely integrated into the host genome.⁹

1.1.3 The HPV E6 and E7 oncoproteins

E6 and E7 of high risk HPV types are the key drivers of HPV-associated carcinogenesis and the progression from CIN1 to invasive cervical cancer is accompanied by an increased expression of the two oncogenes.³⁰ During episomal expression in early-stage infections, E2 can bind to the *E6/E7* promoter regions and thereby represses their expression.³¹ This mechanism is blocked upon viral integration into the host genome due to the loss of E2, thus allowing for an increased *E6/E7* transcription.³² Additionally, integration of the *E6/E7* ORFs usually occurs in multiple or tandem repeats at a single locus, which can form “super enhancer” elements and thus further promotes HPV oncogene expression.³³

E6 and *E7* pre-mRNAs are expressed as bicistronic transcripts from a common promoter and alternative splicing processes give rise to the E6 and E7 oncoproteins,³⁴ which - dependent on the HPV type - have a molecular weight of approximately 150 and 100 kDa, respectively.³⁰ The precise regulation of *E6/E7* expression is mediated via a multitude of transcription factors which bind to the URR 5' of the *E6/E7* ORFs. Two major regulators of HPV oncogene expression are SP1 and activator protein 1 (AP-1) and the latter exerts its regulatory role on HPV *E6/E7* gene induction via two AP-1 binding sites within its URR.³⁵ Continuous expression of the two oncoproteins is

indispensable for the growth of cervical tumors both *in vivo* and *in vitro*.^{30,36} While the interference with E6 activity by peptide aptamers or E6-specific RNA interference (RNAi) induces apoptosis in HPV-positive cervical cancer cells,³⁶⁻³⁸ E2 expression and E6/E7-targeting RNAi both promote the induction of senescence, an irreversible, proliferative arrest.^{39,40} Accordingly, E6 and E7 should represent ideal targets for the development of novel therapeutics.

On the molecular level, E6 and E7 of oncogenic HPV types drive the malignant transformation and tumor progression by modulating the function and expression of a variety of host cell proteins. This includes the interference with the function of two major tumor suppressors: the retinoblastoma protein (pRb) and p53 (Figure 3). In more detail, HPV E7 binds to and targets pRb, as well as the related pocket protein family members p107 and p130, for proteasomal degradation.⁴¹ In the absence of E7, pRb sequesters and thereby prohibits the activity of E2F transcription factors, which are key drivers of the G₁-S cell cycle transition by inducing the cell cycle regulators p16^{INK4A}, cyclin A and cyclin E.⁴² However, E7-mediated pRb degradation results in the release and activation of E2F, thereby enhancing cell cycle progression.⁴³ More recently, E7-induced degradation of the p107 and p130 pocket proteins has further been linked to the disruption of the cell-cycle repressive DREAM (dimerization partner, RB-like, E2F and multi-vulval class B) complex, which further can promote cell cycle activity.⁴⁴ The majority of cells would counteract these unscheduled, E7-mediated proliferative signals with an induction of p53-mediated apoptosis or cell cycle arrest.³⁰ However, concomitant HPV E6 expression in HPV-positive cancer cells leads to the proteolytic degradation of p53 via the formation of a trimeric complex with the ubiquitin ligase E6-associated protein (E6AP) and thus prohibits the induction of p53-dependent pathways.⁴⁵

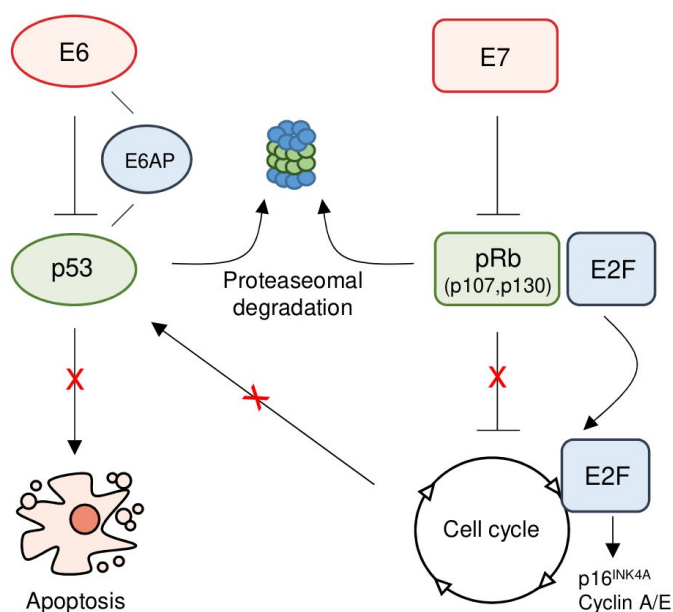


Figure 3 | Cooperative effect of HPV E6 and E7 to disrupt tumor suppressor pathways. HPV E7 contributes to cell cycle deregulation by binding and targeting retinoblastoma protein (pRb) and its related pocket proteins p107 and p130 for proteasomal degradation, which results in the release of E2F transcription factors and subsequent activation of cell cycle inducing genes, such as p16^{INK4A} and cyclin A/E. Concomitant E6 expression protects against proliferation-mediated pro-apoptotic signals by E6-associated protein (E6AP)-dependent proteasomal degradation of p53.

Other pathways by which the HPV oncogenes promote the malignant tumor growth include the E6-mediated activation of telomerase activity in order to prevent replicative senescence⁴⁶ or the E7-induced aberrant centrosome duplication, which leads to aneuploidy and increased chromosomal instability.⁴⁷ Moreover, via its C-terminal PDZ binding motif, HPV E6 binds to and deregulates a multitude of PDZ domain-containing proteins.⁴⁸

Collectively, the E6/E7 proteins from high-risk HPV types hijack a variety of cellular tumor suppressive pathways and thus contribute to the establishment of the major cancer hallmarks, including the evasion of growth suppressors, sustained proliferation, cell death resistance and replicative immortality.⁴⁹

1.1.4 Cervical cancer and hypoxia

Hypoxia is defined by an oxygen (O₂) concentration below 1.5-2 % and is a common characteristic of a large variety of solid cancers.⁵⁰ In tumor tissue, hypoxic regions arise by the reduced oxygen supply due to the long distances between tumor cells and blood vessels, which are caused by intensive cellular proliferation and abnormal tumor vessel formation.⁵⁰ While in normal cells, hypoxia often results in cell death, in tumor cells, low oxygen concentrations can induce genomic and proteomic changes that help the cells to adopt to the hypoxic environment. The transcription factor hypoxia-inducible factor 1 α (HIF-1 α), which is stabilized under hypoxic conditions, regulates the transcription of a large number of genes involved in cell growth and survival, angiogenesis and metabolic adaptations.⁵¹ For instance, hypoxic cells need to increase their glycolysis rates to ensure a sufficient adenosine triphosphate (ATP) production, since hypoxia leads to the repression of oxygen-dependent oxidative phosphorylation (OXPHOS). To this end, HIF-1 α upregulates a number of glycolytic enzymes, as well as the expression of glucose transporters, and thereby supports the metabolic shift from aerobic respiration to anaerobic glycolysis.⁵²

Cervical cancer tissues are characterized by a heterogeneous oxygen distribution and while in normal cervical tissue the median oxygen concentration is ~5 %, it is strongly decreased to ~1.3 % in cervical cancers.⁵³ Remarkably, these values strongly differ from the standard conditions of the majority of *in vitro* studies at 21 % O₂. Our group previously found that the expression levels of HPV E6 and E7 are efficiently but reversibly repressed under chronic hypoxia.⁵⁴ Mechanistically, this is linked to the hypoxia-induced activation of the PI3K (phosphatidylinositol-3-kinase)/mTORC2 (mammalian target of rapamycin complex 2)/AKT axis, which is further dependent on cellular glucose availability.⁵⁵

In contrast to normoxic cells, where RNAi-mediated E6/E7 repression results in the induction of a senescent phenotype, hypoxic cells adopt a dormant state besides E6/E7 downregulation, which is reversible upon re-oxygenation.⁵⁴ In addition to the global increase of therapy resistance in hypoxic cells,⁵⁰ HPV oncogene repression under hypoxia may further reduce the efficiency of E6/E7-targeting therapies and the dormant phenotype may also result in altered resistance towards chemotherapeutics, as these preferably act on proliferating cells.⁵⁴

1.1.5 Therapy of HPV-positive cervical cancer

1.1.5.1 Treatment options

The choice of treatment for cervical cancer depends on the stage of tumor progression. While precancerous lesions can be surgically removed by conisation or hysterectomy, in early-stage cervical cancers this removal is usually combined with radiation and/or neo-adjuvant chemotherapy.⁵⁶ For advanced or recurrent tumors, platinum-based therapies, including Cisplatin or Carboplatin, in combination with radiotherapy, are considered as the treatments of choice.⁵⁷ Their efficiencies may further be enhanced in combination with cell cycle-targeting drugs such as paclitaxel or 5-fluorouracil.^{56,58,59} Targeted therapeutic approaches, such as employing the programmed death-1 (PD-1)-specific antibody pembrolizumab⁶⁰ or the vascular endothelial growth factor receptor (VEGFR)-neutralizing antibody bevacizumab,⁶¹ represent alternatives to increase the response towards chemo-, radio- and/or radiochemotherapy.

1.1.5.2 Cisplatin: Mechanism of action and therapy resistance

The platinum compound Cisplatin [*cis*-diamminedichloroplatinum(II)] was first synthesized in 1844 by M. Peyrone and was originally identified in the 1960's to inhibit prokaryotic cell division⁶² until it was approved for cancer treatment in 1987.⁶³ Cisplatin is composed of a platinum core which is bound to two amine and two chloride ligands (Figure 4).⁶³ Although the cellular uptake of Cisplatin is not completely understood, several membrane transporters, such as copper-transporting ATPases or the copper transporter 1 (Ctr1), were shown to mediate the entry of Cisplatin into the cell.⁶⁴

In comparison to extracellular regions, the chloride concentrations in the cytosol are relatively low (~2-10 mM compared to 100 mM), which induces spontaneous aquation reactions on the chloride ligands, resulting in their substitution by water molecules and thereby generating highly reactive electrophiles. These can bind to the nucleophilic N7 reactive center of DNA purine bases, which leads to the formation of DNA inter- and intra-strand adducts.⁶⁵

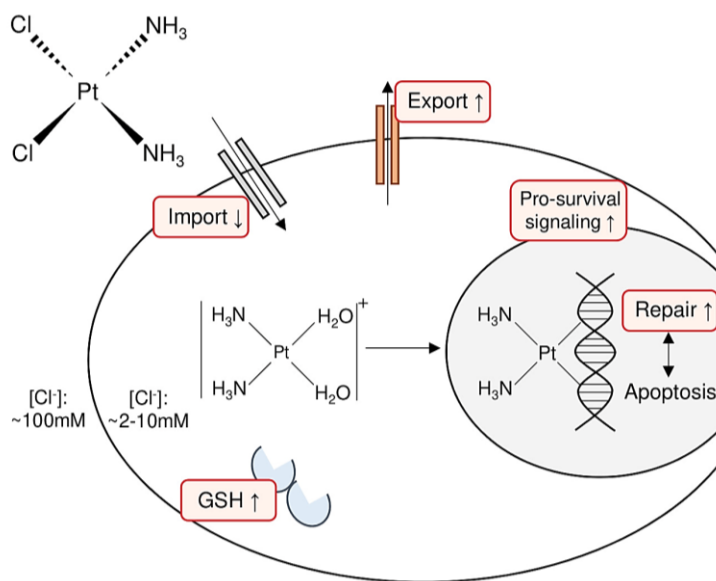


Figure 4| Schematic representation of Cisplatin-related cellular mechanisms.

Cisplatin is composed of a platinum core (Pt) bound to two amine (NH₃) and two chloride (Cl) ligands. Upon cellular import, the chloride ions are substituted by water molecules due to decreased intracellular chloride [Cl⁻] concentrations compared to extracellular regions, which enables Cisplatin to bind to DNA. Cisplatin-induced DNA lesions are either repaired or transmitted into apoptotic signals. Increased DNA repair, as well as decreased drug import, increased drug export or neutralization by nucleophilic scavengers, such as glutathione (GSH) provide the cell with resistance towards Cisplatin-induced apoptosis (indicated in red).

Cisplatin-induced cytotoxicity is mainly caused by severe DNA damage mediated by DNA 1,2-intrastrand d(GpG) and d(ApG) crosslinks, which trigger the recruitment of damage recognition proteins in order to transduce damage-induced signals to a variety of downstream pathways.⁶⁶ These include, among others, the activation of cell cycle checkpoints, such as the ATR (Ataxia telangiectasia and Rad3-related) kinase which phosphorylates and activates Chk1, a kinase involved in p53 activation and cell cycle arrest.⁶⁷ During this process, the cell is either able to repair the Cisplatin-induced DNA lesions or to activate the irreversible apoptotic machinery, a decision which is ultimately based on the integration of a multitude of pro-survival and pro-apoptotic signaling pathways.⁶⁶

Cisplatin resistance, either intrinsic or acquired after prolonged treatments, represents a major hurdle for cervical cancer therapy.⁶⁸ Mechanistically, this can be linked to a decreased intracellular accumulation of the drug due to defects in the cellular uptake or an increased efflux mediated by export transporters, as well as to an increased activity of nucleophilic scavenger proteins in the cytoplasm (e.g. glutathione (GSH) or metallothioneins), which sequester Cisplatin and thus proscribe its binding to DNA (Figure 4). Moreover, enhanced DNA damage repair or deficiencies in pro-apoptotic signaling can further enhance the activation of pro-survival pathways and thereby prohibit Cisplatin-induced apoptosis.^{68,69} Examples of such pathways include the inactivation of the tumor suppressor p53,⁷⁰ as mediated for example by E6/E6AP-dependent degradation in

cervical cancer cells,⁴⁵ or the deregulated activation of mitogen activated protein kinase (MAPK) family proteins.⁷¹

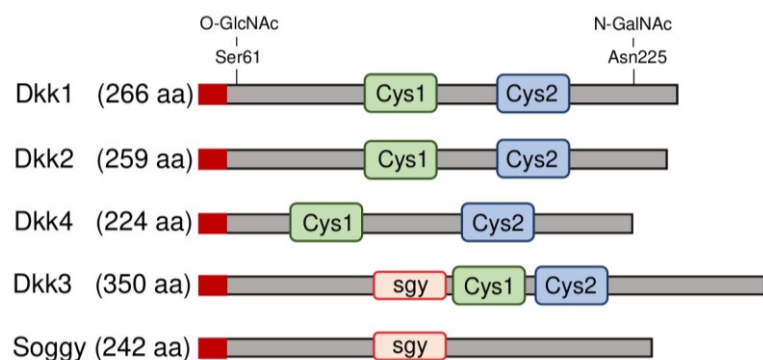
1.2 Dickkopf-1 (Dkk1): A potential tumor suppressor in cervical cancer

In 1998, Dickkopf-1 (Dkk1) was originally identified as a secreted Wnt antagonist and major inducer of head formation in *Xenopus* during embryonic development.⁷² One year later, the human homologue of Dkk1 was characterized from the medium of SK-LMS-1 leiomyosarcoma cells.⁷³ Since its discovery, a plethora of studies have elucidated its physiological role not only in embryogenesis, but also in cellular homeostasis and in cancer, with the best established function being its Wnt-inhibitory activity.⁷⁴

1.2.1 The Dickkopf (Dkk) family of proteins

Dkk1 is the founding and best studied member of the Dickkopf (Dkk) family of proteins, consisting of the four central members Dkk1, Dkk2, Dkk3 and Dkk4, as well as the Dkk3-related factor Dickkopf-like 1 (Dkk1l or soggy) (Figure 5).⁷⁵ With 224-350 amino acids (aa) in length, the predicted molecular weights for Dkk1, -2 and -4 are 24 to 29 kDa, and 38 kDa for Dkk3. All Dkks contain an amino (N)-terminal signal sequence, which most likely functions in their cellular secretion.⁷⁴ They further share two conserved cysteine-rich domains at their N-terminus (Cys1) and carboxy (C)-terminus (Cys2), which contain in total 10 disulfide bonds.⁷⁶ While Cys1 is unique to Dkk proteins, the Cys2 domain forms a colipase-like fold, which serves as a potential interface for protein interactions.⁷⁷ Outside of these conserved domains, sequence similarities are less pronounced, with Dkk3 and its related factor soggy being the most divergent of the protein family members. The *DKK1*, -2 and -4 genes are located on chromosomes 10q11, 4q25 and 8p11, respectively, and thus form part of one chromosomal paralogy group, which has early evolved in vertebrates. In contrast, the gene encoding Dkk3 is located on 11q15.3 which does not belong to the same paralogous group.⁷⁴ Additionally, unlike Dkk1, -2 and -4, the functions of Dkk3 and soggy are unrelated to Wnt signaling.⁷⁵

Figure 5| Domain structure and lengths (aa: amino acids) of Dkk1-4 and the Dkk3-related factor soggy. Depicted are N-terminal signaling sequences (red), cysteine-rich domains Cys1 and Cys2 and soggy (sgy) domains. For Dkk1, O- and N-linked glycosylation sites are indicated. Figure generated based on Niehrs et al. (2006).⁷⁴



Besides their expression during embryonic development,^{78,79} the abundance and localization of the Dkk proteins in adult tissues differs in between family members. While Dkk4 expression is generally low with some enrichment in brain and esophagus, Dkk3 can be detected in a wide range of tissues with an enrichment in the heart muscle and Dkk2 levels are most abundant in the cervix. Dkk1 shows comparably enhanced expression in the placenta, cervix and urinary bladder (Human Protein Atlas).⁸⁰ The protein sequences of all Dkks contain cleavage sites for furin type proteases and for Dkk2, -3 and -4 smaller molecular weight proteins can be observed in sodium dodecyl sulfate-polyacrylamide gel electrophoresis (SDS-PAGE), which are putatively cleaved fragments.⁷⁴ In contrast, Dkk1 is usually detectable by multiple bands with a higher apparent molecular weight in SDS-PAGE.^{73,74} Causative for this shift are the three N-linked glycans at Asparagine (Asn) 225 and at least two O-linked glycans at Serine (Ser) 61 on the Dkk1 protein in humans (Figure 5).⁷⁶

1.2.2 Dkk1 in canonical Wnt signaling

During embryogenesis, Dkk1 is required for the development of proper head structures, as shown in *Xenopus* and zebrafish embryos,^{72,81} as well as in *DKK1* null mice embryos.⁸² This function is associated to its Wnt inhibitory activity, as a concomitant inhibition of Wnt and bone morphogenetic protein (BMP) signaling is required for head induction.⁸³ However, the Wnt pathway is not only implicated in a variety of developmental processes, but is also linked to tissue homeostasis in adults and is often found to be deregulated in a multitude of cancers.⁸⁴ One of the key functions of Dkk1 in adult tissues is its repressive effect on bone formation, which is mediated by its Wnt inhibitory role in osteoblast differentiation.⁸⁵

In humans, the Wnt network is composed of 19 different, conserved Wnt ligands which, in their secreted form, can bind to at least 15 different Wnt receptors and co-receptors and thereby determine the induction of different downstream pathways.⁸⁶ Usually, these pathways are divided into a canonical, β -catenin-dependent and a non-canonical, β -catenin-independent branch. Wnt1 and Wnt3a are prototypical activators of the canonical Wnt pathway, which bind to Wnt-specific G protein-coupled Frizzled (Fzd) receptors and Lrp5/6 co-receptors (Figure 6A). This leads to the dimerization of the two receptors, followed by the phosphorylation of Lrp5/6, which triggers the recruitment of Dishevelled (Dvl) proteins to the cellular membrane. These polymerized Dvl proteins sequester and inactivate the Wnt-related destruction complex by binding to its scaffold protein Axin.⁸⁴ In addition, major components of this complex include the adenomatous polyposis coli (APC) protein and the kinases glycogen synthase kinase 3 β (GSK-3 β) and casein kinase 1 α (CK1 α).⁸⁷ The inactivation of the destruction complex results in the intracellular stabilization of

β -catenin and its translocation into the nucleus, where it induces T-cell factor (TCF)/lymphoid enhancer factor (LEF)-dependent transcription.⁸⁴ Notably, Dkk1 contains two active TCF/LEF binding sites in its promoter, which lead to Dkk1 transactivation as a negative feedback response towards canonical Wnt activity.⁸⁸ Dkk1 antagonizes the canonical Wnt pathway by binding to the LRP5/6 co-receptor, thereby prohibiting the formation of the trimeric Wnt/Fzd/LRP5/6 complex (Figure 6B). This allows the destruction complex components GSK-3 β and CK1 α to phosphorylate and target β -catenin for proteasomal degradation, which disables TCF/LEF-mediated transcription.⁷⁴ In more detail, Dkk1 binds to Lrp5/6 in a dual fashion via its conserved N-terminal Cys1 and C-terminal Cys2 domains.⁸⁹ While the colipase-like Cys2 domain is sufficient to antagonize Wnt signaling,⁹⁰ the Cys1 domain is likely involved in increasing the Dkk1-Lrp5/6 binding affinity and thus in enhancing the Wnt-inhibitory effect.^{89,91}

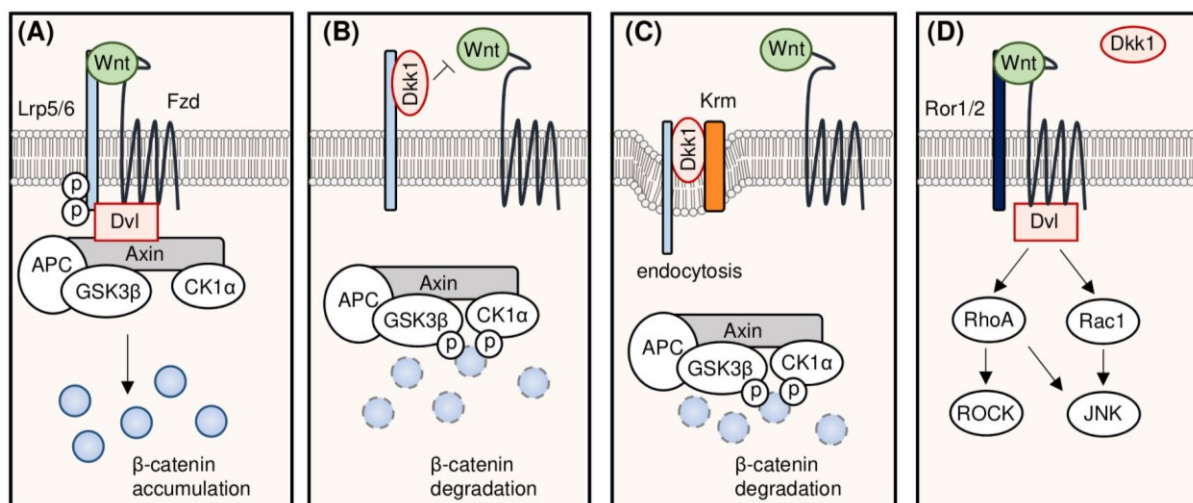


Figure 6 | Modulation of Wnt signaling by Dkk1. (A) Wnt ligands form a complex with Frizzled (Fzd) receptors and Lrp5/6 co-receptors, which leads to dual Lrp5/6 phosphorylation and sequestration of Dishevelled (Dvl). Dvl recruits the destruction complex composed of Axin, adenomatous polyposis coli (APC), glycogen synthase kinase 3 β (GSK-3 β) and casein kinase 1 α (CK1 α) to the cell membrane, resulting in β -catenin accumulation. (B) Dkk1 interacts with Lrp5/6 and prohibits the binding of Wnt ligands, which enables the destruction complex to phosphorylate and target β -catenin for degradation. (C) Alternatively, Dkk1 forms a trimeric complex with Kremen (Krm) and Lrp5/6, which is endocytosed and thereby blocks the activation of β -catenin-dependent Wnt signaling. (D) Presence of Dkk1 may activate the non-canonical Wnt/PCP (planar cell polarity) pathway, which is activated by Wnt ligand binding to Fzd and a co-receptor, such as Ror1/2, resulting in Dvl sequestration, followed by RhoA or Rac1 activation, which can induce Rho kinase (ROCK) and/or c-Jun N-terminal kinase (JNK), respectively.

In addition to Lrp5/6, the Dkk1-Cys2 domain can interact with the transmembrane proteins Kremen 1 and Kremen 2 (Krm1 and Krm2) (Figure 6C).⁹² In the presence of Dkk1, Lrp5/6 forms a trimeric complex with Dkk1 and Kremen, which is internalized via clathrin-dependent endocytosis⁹³ and thereby blocks the activation of canonical Wnt signaling. Importantly, the cooperative function on Wnt antagonism of Kremen and Dkk1 seems to be dependent on the

cellular context as both, essential and non-essential roles of Kremen have been described for Dkk1-mediated Wnt inhibition.^{94,95}

1.2.3 Dkk1 in non-canonical Wnt signaling and beyond

Besides the precisely studied mechanisms by which Dkk1 interferes with the β -catenin-dependent Wnt pathway, an emerging number of studies suggests that Dkk1 is also able to signal via β -catenin-independent mechanisms. Two major non-canonical Wnt pathways which do not involve β -catenin are the Wnt/Calcium (Ca^{2+}) and the Wnt/planar cell polarity (PCP) pathway, which both, alike canonical Wnt signaling, are activated by Wnt ligand binding to Fzd receptors.⁸⁴ The Wnt/ Ca^{2+} branch activates phospholipase C (PLC) which modulates intracellular Ca^{2+} levels and as a result drives the transcriptional induction of Ca^{2+} -dependent genes.⁸⁴ Wnt/PCP signaling requires a co-receptor, such as Ror1/2 or Ryk, which forms a complex with Fzd upon Wnt ligand binding and thereby recruits and activates Dvl (Figure 6D). This triggers the small GTPases Rac1 or RhoA to activate Rho kinase (ROCK) or c-Jun N-terminal kinase (JNK). Transcriptional responses of Wnt/PCP signaling include the regulation of cell polarity and/or the activation of the JNK downstream effectors ATF-2 or Jun, which both form part of AP-1 transcription factor complexes.^{84,96}

Evidence that Dkk1 can activate JNK signaling and thus potentially signals through the Wnt/PCP pathway emerged in embryogenesis-, as well as in carcinogenesis-related studies. For example, both, the prototypic activator of the Wnt/PCP pathway Wnt11, as well as Dkk1, are able to trigger JNK activation in embryonal cardiogenesis without affecting canonical Wnt activities.⁹⁷ (The role of Dkk1-mediated JNK activation for carcinogenesis will be covered in more detail in chapter 1.2.4) Moreover, a pro-apoptotic role for Dkk1 has not only been reported in the context of cancer-related studies,⁹⁸ but also during developmental vertebrate limb formation and digit patterning.⁹⁹ More recently, CKAP4 (cytoskeleton-associated protein 4) was identified as a novel Dkk1 receptor, which triggers the PI3K/AKT signaling cascade and thus might contribute to enhanced cell proliferation.¹⁰⁰ Consequently, Dkk1 may be able to signal through binding to additional, so far unknown receptors or interaction partners, which could include non-canonical Wnt or Wnt-independent pathways.

1.2.4 The bipartite role of Dkk1 in cancer

In recent years, Dkk1 has been linked to the development and progression of a variety of cancer types, however the expression and function of Dkk1 are highly tumor- and tissue type-dependent

and discrepant data about its potential tumor suppressive or oncogenic function exist.¹⁰¹ Due to its key role in adult bone homeostasis, it is not surprising that one of the major oncogenic functions of Dkk1 is associated to bone-related cancers.⁸⁵ In multiple myeloma, increased Dkk1 levels in patients' tissues and sera are linked to the development of osteolytic lesions,¹⁰² and this phenotype is commonly shared by metastatic prostate and breast cancer types with increased Dkk1 expression.^{103,104} However, independent from its bone-related effects, Dkk1 overexpression is also a characteristic for hepatocellular, esophageal or gastric carcinomas, amongst others.¹⁰⁵ Dkk1 levels in the sera of patients have been suggested to function as a biomarker for early detection and prognosis in hepatocellular and pancreatic cancers^{106,107} and anti-Dkk1 antibodies, such as BHQ880 and DKN-01, are currently in clinical trials for the treatment of multiple myeloma and gynecologic, gastric or esophageal cancers.^{108,109}

In stark contrast, in several other cancer entities, Dkk1 represents a repressed and potent tumor suppressor, which likely limits the use of Dkk1-inhibitory drugs to a subset of cancers. For example, *DKK1* transcription is epigenetically silenced in brain tumor-, gastrointestinal tumor- and cervical cancer cells.¹¹⁰⁻¹¹³ In addition, the Dkk1 promoter contains a putative p53 response element approximately 2.1 kb upstream of its transcription start site, which might link the tumor suppressive role of Dkk1 to p53-mediated apoptotic responses.¹¹⁴ Discrepant data also exist regarding the role of Dkk1-mediated canonical Wnt inhibition for its tumor suppressive function. While the apoptosis-sensitizing effect of Dkk1 in glioma cells, as well as a correlation of Cisplatin resistance and decreased Dkk1 expression are proposed to be mediated through the inhibition of Wnt/ β -catenin signaling,^{98,115} in mesothelioma and placental choriocarcinoma, Dkk1-induced apoptosis was described to be dependent on JNK activation.^{116,117} In HeLa cervical cancer cells, Dkk1 appears to act as a pro-apoptotic tumor suppressor in a Wnt-independent manner, as Dkk1 overexpression reduces the tumorigenicity of HeLa cells in xenografts without affecting TCF/LEF-mediated transcriptional activity.¹¹⁸

1.3 Apoptosis

Apoptosis is defined as a form of programmed cell death and plays a major role in health and disease. During embryogenesis, the cellular turnover mediated by apoptosis is critically involved in the development of healthy organisms.¹¹⁹ Moreover, in adult tissue apoptosis is a major driver of cellular homeostasis¹²⁰ and plays key roles in the host immune response, as well as in the DNA damage response.^{121,122} Consequently, a deregulated control in between cell death and cell growth is causative for the development of a variety of diseases, including cancer.¹²³ While evasion of

apoptosis is considered as one of the hallmarks of cancer,⁴⁹ apoptotic cell death also represents a preferable way of therapy-induced tumor cell elimination, as the apoptotic process does not trigger an inflammatory response.¹²⁴ Therefore, a better understanding of the mechanisms behind apoptosis mediated by therapeutic interventions may improve the efficacy of cancer treatments.

1.3.1 Mechanisms of apoptosis

On cellular level, the induction of cell death by apoptosis is characterized by cell and nuclei shrinkage, which includes the condensation and breakup of chromatin, as well as membrane blebbing and the formation of apoptotic bodies.¹²⁵ These contain cellular content such as organelles or nuclear fragments and are removed by phagocytosis.¹²⁰ Biochemical characteristics of the apoptotic process include the translocation of phosphatidylserine from the inner to the outer layer of the cell membrane, the fragmentation of DNA and the activation of caspases, which are cysteine-aspartic proteases cleaving a variety of apoptotic effector proteins which finally orchestrate cell death.¹²³ In the absence of apoptotic stimuli, caspases are expressed as catalytically inactive zymogens, and their activation occurs through sequential proteolytic cleavage, which is executed by the activation of an initiator caspase.¹²⁶

Dependent on the type of stimuli, apoptosis is induced via two different signaling branches (Figure 7). The extrinsic or death receptor pathway is activated by the binding of extracellular ligands to death receptors, which belong to the tumor necrosis factor (TNF) receptor gene superfamily. Prototypical examples of ligand/receptor pairs include the Fas ligand (FasL)/Fas receptor (FasR), TNF α /TNF receptor (TNFR) or TNF-related apoptosis-inducing ligand (TRAIL)/death receptor 4/5 (DR4 or DR5).^{127,128} Upon ligand binding, the respective death receptors trimerize, which results in the sequestration of adaptor proteins to its cytoplasmic domain (e.g. FADD to Fas/FasR).¹²³ The adaptor proteins interact with procaspase 8, which results in the formation of the death-inducing signaling complex (DISC) and thereby triggers the auto-catalytic induction of the initiator caspase 8.¹²⁹ Activated caspase 8 can either directly induce the activity of the effector caspases 3 and 7, or it can interfere with the second branch of apoptosis signaling, the intrinsic or mitochondrial pathway.¹³⁰

This latter pathway is usually induced by internal, stress-induced stimuli, such as DNA damage, oxidative stress or growth factor withdrawal and is fine-tuned by the cooperative interactions between proteins of the Bcl-2 family. Members of this protein family can act either as anti-apoptotic factors (e.g. Bcl-2 or Bcl-xL) or pro-apoptotic Bcl-2 homology 3 (BH3)-only proteins (e.g. BAD, BID

or BIM). Apoptotic stimuli modulate their abundance, cellular localization and stability, which ultimately determines the oligomerization and activity of a third group of Bcl-2 family proteins, the pro-apoptotic pore-formers BAX and BAK.¹³¹ BAX- or BAK-mediated pore formation within the mitochondrial outer membrane, also referred to as mitochondrial outer membrane permeabilization (MOMP), results in the release of the pro-apoptotic factors cytochrome c (CytC) or Smac (second mitochondria-derived activator of caspase) from the mitochondrial intermembrane region.¹³² In the cytosol, cytochrome c oligomerizes with apoptotic protease activating factor 1 (APAF-1) and the inactive form of the initiator caspase 9 to form the apoptosome, which serves as a platform for caspase 9 activation and thereby triggers the activation of caspases 3, 6 and 7.¹³³ Cytosolic Smac interacts with inhibitor of apoptosis proteins (IAPs) to interfere with their negative regulation on caspase maturation and thus further facilitates apoptosis induction.¹³⁴ Hence, both extrinsic and intrinsic pathways lead to the activation of the effector caspases 3, 6 and 7, which, amongst other substrates, cleave and inactivate the DNA repair-associated protein poly (ADP-ribose) polymerase (PARP) into a 89 kDa and 24 kDa fragment, which in turn promotes caspase-mediated DNA fragmentation.¹³⁵ Due to their key role in apoptosis, caspase and PARP cleavage are considered useful markers for apoptosis induction in cellular assays.^{136,137}

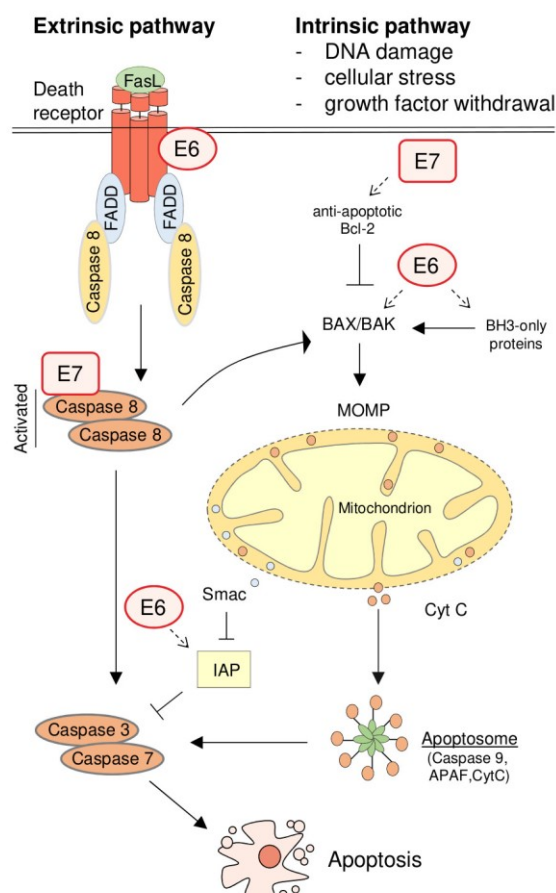


Figure 7 | Extrinsic and intrinsic apoptosis pathways and interference with HPV E6/E7. Extrinsic pathway (left panel): Death ligands (e.g. FasL) bind to death receptors leading to intracellular binding of death receptor adaptor proteins (e.g. FADD), which results in caspase 8 recruitment and activation. Caspase 8 activates caspases 3/7 which trigger apoptosis. Intrinsic pathway (right panel): Stress signals activate pro-apoptotic BH3-only proteins and inhibit anti-apoptotic Bcl-2 proteins to allow BAX and BAK to induce mitochondrial outer membrane permeabilization (MOMP), resulting in the release of cytochrome c (CytC) and Smac. BAX and BAK may further be induced by caspase 8. CytC release induces the formation of the apoptosome, composed of APAF-1 (apoptotic protease-activating factor 1), CytC and caspase 9, resulting in caspase 9 activation, followed by caspase 3/7 activation and apoptosis. Smac blocks the activity of inhibitor of apoptosis (IAP) proteins to impede caspase 3/7 activation. The HPV E6/E7 oncoproteins interfere with several components of the apoptotic machinery, thereby providing the host cell with increased apoptosis resistance (interactions indicated in red).

1.3.2 Interference of HPV E6/E7 with apoptosis

HPV oncogene expression provides the host cell with apoptosis resistance, as an efficient infection and the viral life cycle require the virus to evade pro-apoptotic signals as a part of the host defense mechanism.¹¹ These anti-apoptotic properties may also play a major role in the resistance towards therapy-induced apoptosis (Figure 7).¹³⁸ As previously described, HPV E6-mediated degradation of the tumor suppressor p53 prevents the cell to undergo apoptosis (chapter 1.1.3).³⁰ Importantly, p53 is critically involved in the DNA damage response by transactivating a plethora of genes involved in DNA repair, cell cycle arrest and apoptosis.^{139,140} HPV E6 confers apoptosis resistance via p53-dependent mechanisms, as it interferes for instance with the pro-apoptotic p53/PUMA/BAX axis¹⁴¹ or the induction of the p53-responsive pro-apoptotic protein survivin.¹⁴²

However, E6-mediated apoptosis resistance is not solely dependent on p53. In response to UV-induced DNA damage, both low- and high-risk HPV type E6 proteins inhibit apoptosis in p53 wild type as well as in p53 null cells.¹⁴³ E6 can also promote the E6AP-mediated degradation of the pro-apoptotic protein BAK in a p53-independent manner (Figure 7).¹⁴⁴ Moreover, HPV E6 expression was reported induce the expression of c-IAP2, which acts anti-apoptotic in normal human oral keratinocytes and in cervical cancer cells.¹⁴⁵ In the context of the extrinsic pathway of apoptosis, HPV E6 binds via its PDZ-domain to the death receptor TNFR1, thus preventing its interaction with its cytosolic adaptor protein TRADD.¹⁴⁶ Additionally, E6 interacts with the FasR-related adaptor protein FADD, thereby inducing its degradation and interfering with TRAIL-induced apoptosis.^{147,148}

In comparison with HPV E6, less is known about HPV E7-mediated apoptosis resistance, as one of the key roles of E7 is its interference with the cell cycle as described in chapter 1.1.3, which rather augments pro-apoptotic signaling.³⁰ However, there is some evidence that HPV E7 inhibits TNF α -induced apoptosis by the attenuation of caspase 8 activity (Figure 7).¹⁴⁹ Moreover, E7 binds to and interferes with the pro-apoptotic activity of the Siva protein, which results in the release of anti-apoptotic Bcl-X_L from its negative regulation by Siva.¹⁵⁰

1.3.3 JNK/AP-1 signaling in apoptosis

The JNK pathway represents a major signaling pathway in the response to cellular stress. JNK was originally found to be a UV-responsive kinase which binds to the activation domain of its prototypic target protein c-Jun, thereby inducing c-Jun phosphorylation on Ser63 and Ser73.¹⁵¹

Different stimuli, such as pro-inflammatory cytokines, growth factors and cytotoxic or genotoxic reagents can induce JNK activity, which may result in the induction of apoptosis.¹⁵²⁻¹⁵⁴

At least ten different JNK isoforms are derived by alternative splicing from three JNK genes, of which JNK1 and JNK2 are ubiquitously expressed and JNK3 is mainly found in testis, brain and heart.¹⁵⁵ The selection of the splice site determines whether JNK is expressed in its 54 kDa or 46 kDa isoform, the latter lacking a C-terminal extension.¹⁵⁶ Together with ERK (extracellular signal-regulated kinase) and p38, JNK forms part of the MAPK family. The typical, sequential activation of the MAPK cascade involves the binding of extracellular ligands to TNFRs¹⁵⁷ or the activation of the Rho family GTPases Rac or Cdc42,¹⁵⁸ which trigger MAP kinase kinase kinases (MAP3Ks) to phosphorylate and activate MAP kinase kinases (MAP2Ks). MAP2Ks in turn phosphorylate and activate ERK, p38 or JNK MAPKs.¹⁵⁹ Fourteen out of twenty MAP3Ks are implemented in JNK activation by phosphorylation of the MAP2Ks MKK4 or MKK7.¹⁶⁰

In its activated form, JNK typically phosphorylates a variety of apoptosis-related transcription factors, including the AP-1 transcription factor complex components c-Jun, JunB, JunD and ATF2.¹⁶¹ AP-1 complexes are considered as decision makers between cellular survival and death and their transcriptional response is determined by the differential homo- or heterodimerization of proteins of the Jun (c-Jun, JunB, JunD), Fos (c-Fos, FosB, Fra-1, Fra-2), activating transcription factor (ATF2, ATF3, B-ATF) and Maf (e.g. v-Maf, c-Maf, MafB) protein families via their basic region-leucine zipper (bZIP) domains.¹⁶² Jun:Jun homodimers as well as Jun:Fos heterodimers can bind to AP-1 recognition elements (5'-TGAG/CTCA-3') of gene promoters, which are also referred to as TREs (phorbol 12-O-tetradecanoate-13-acetate (TPA) response elements).¹⁶³ While FOS proteins are unable to form homodimers and thus only dimerize with JUN, ATF proteins can form both homodimers as well as heterodimers with JUN and they regulate gene transcription by binding to cAMP responsive elements (CREs) of gene promoters.¹⁶² MAF-related proteins form homo- and heterodimers with other bZIP proteins and they can bind to Maf recognition elements (MAREs).¹⁶⁴

As the AP-1 complex is to a large extent driven by MAPK activity,¹⁶⁵ it is not surprising that it is also induced by stress stimuli such as pro-inflammatory cytokines, growth factors and UV radiation.¹⁶⁵ Via an auto-regulatory process, JNK-induced phosphorylation stabilizes c-Jun, which further augments *JUN* transcription via an AP-1 binding site in its promoter.¹⁶⁶ Both, JNK and AP-1 are associated to apoptosis, although discrepancies regarding their pro- and anti-apoptotic

activities are reported in between stress stimuli and cell or tissue types.^{154,162} Dependent on the composition of the AP-1 complex, pro- or anti-apoptotic proteins may be activated to drive or resist apoptosis induction, respectively.¹⁶²

1.3.4 Senescence: An alternative stress-induced cell fate

Cellular stress induced by UV light, oxidants, chemotherapeutics or radiation is not only responsible for the induction of apoptosis, as it also can cause the cells to undergo a permanent cell cycle arrest, referred to as senescence.¹⁶⁷ Cellular senescence was first described in 1961 by Hayflick and Moorhead, who found that primary human cells have a limited replication capacity *in vitro*.¹⁶⁸ Each round of replication is associated with the loss of telomeres at the end of chromosomes which function in protecting the genetic material. Advanced telomere erosion triggers the DNA damage response, which results in the induction of senescence.¹⁶⁹ Likewise, DNA damage caused by cellular stress, oncogene expression or cancer therapy may result in a senescent phenotype.¹⁷⁰

Senescent cells are characterized by an enlarged and flat cell morphology and by an elevated lysosomal content. Based on this feature, senescence-associated β -galactosidase activity (Sa- β -gal), which is activated at a pH of 6.0, is commonly used as a marker for senescence along with the expression of senescence-associated proteins such as p16^{INK4A}, p21 or hypophosphorylated pRb.¹⁷⁰ Moreover, senescent cells secrete a plethora of pro-inflammatory cytokines and chemokines, including the interleukins (IL) IL-6 and IL-8 or the transforming growth factor β (TGF β), which in concert form the senescence-associated secretory phenotype (SASP).¹⁷¹ Thus, in contrast to apoptotic cell clearance, which does not stimulate inflammation,¹²⁴ senescence is associated to a pro-inflammatory phenotype, which may or may not be beneficial for the treatment of cancer. On the one hand, the SASP contributes to senescence induction of neighbouring cells via paracrine mechanisms, also known as bystander senescence,¹⁷² and thereby stimulates the elimination of senescence-associated cells by the immune system.¹⁷³ On the other hand, some SASP factors are known to be pro-tumorigenic and may favour a more malignant phenotype of cancer cells.¹⁶⁷

1.4 Research objectives

Dkk1 has been proposed to function as a tumor suppressor in cervical cancer cells. Moreover, previous proteome analyses from our lab revealed that Dkk1 is regulated in parallel with the HPV oncogenes in cervical cancer cells under hypoxic conditions, raising the question of a potential crosstalk of Dkk1 with HPV E6/E7 in HPV-positive cancer cells. The present thesis aims to elucidate the following aspects:

- I. Do HPV E6 or E7 modulate Dkk1 expression in HPV-positive cancer cells under both, normoxic and hypoxic conditions?

Dkk1 expression will be assessed upon RNAi-induced silencing of the HPV oncogenes in HPV-positive cervical cancer cells. This will further be combined with RNAi targeting p53, as p53 is a well-established HPV E6 target and was previously described to transcriptionally activate *Dkk1* expression. Hypoxic Dkk1 downregulation in parallel with HPV E6/E7 will be validated in HPV-positive as well as HPV-negative cancer cell lines.

- II. Which additional factors drive Dkk1 regulation in cervical cancer cells?

The effects of epigenetic drugs on Dkk1 expression will be evaluated at normoxic and hypoxic conditions to investigate a potential epigenetically driven Dkk1 regulation in cervical cancer cells. Moreover, hypoxic Dkk1 regulation in terms of time- and glucose-dependence will be analyzed in more detail.

- III. Is Dkk1 functionally involved in Cisplatin-induced apoptosis in cervical cancer cells?

Ectopic Dkk1 expression as well as Dkk1 silencing, achieved by either RNAi or CRISPR/Cas9-mediated gene knockout (KO), will be combined with Cisplatin treatment in cervical cancer cells, followed by different apoptosis assays.

- IV. Which factors or pathways mechanistically underlie possible Dkk1-linked effects on the phenotypic response of cervical cancer cells towards Cisplatin?

Gene expression analyses of parental HeLa and Dkk1 KO HeLa cells will be performed on Affymetrix GeneChips and complemented by subsequent functional analyses of candidate factors involved in this regulation.

The overall aim of delineating the regulatory and functional principles for Dkk1 in cervical cancer cells is to gain novel insights into the mechanisms of HPV-associated carcinogenesis, which may also serve as a basis for developing novel approaches to improve cervical cancer therapies.

CHAPTER 2

RESULTS

2. Results

2.1 Crosstalk of Dkk1 with the HPV oncogenes

Previous studies have suggested a tumor suppressive role for Dkk1 in cervical cancer cells.¹¹⁸ Given the central role of the HPV oncogenes in cervical carcinogenesis and considering the parallel regulation of Dkk1 and HPV E6/E7 in hypoxic SiHa cervical cancer cells,⁵⁵ it was interesting to study whether there is a direct crosstalk of the HPV oncogenes with Dkk1.

2.1.1 Dkk1 induction upon HPV E6/E7 silencing

To analyze whether Dkk1 is a possible downstream target of HPV E6/E7, Dkk1 expression levels were measured after RNAi-mediated silencing of the viral oncogenes in HPV18-positive HeLa and in HPV16-positive SiHa and Caski cervical cancer cells. Due to complex alternative splicing processes of the HPV E6/E7 transcript,³⁴ siRNA-mediated silencing of E6 alone can be achieved, while targeting the exon encoding for E7 leads to repression of both E6 and E7. Interestingly, Dkk1 protein levels were strongly increased after depletion of E6 alone or E6 and E7 in combination in all three tested cell lines (Figure 8A). This was in parallel with an induction of p53 which is negatively regulated in cervical cancer cells by E6-mediated proteasomal degradation.⁴⁵

Notably, intracellular Dkk1 induction upon silencing of the HPV oncogenes was accompanied by increased amounts of Dkk1 levels in the cell supernatant in all three cell lines (Figure 8B), indicating that the secreted Dkk1 amounts also underlie a negative regulation by the HPV oncogenes. In this latter experiment, HPV E7 was used as a control to show that the supernatant did not comprise intracellular content compared to the cell lysate, as HPV E7 expression is restricted to the cytosol and the nucleus.¹⁷⁴

Corresponding to the immunoblot results, the concentrations of *DKK1* mRNA were significantly increased in HeLa, SiHa and CaSki cells in qRT-PCR analyses after both, E6 or E6/E7 silencing (Figure 8C). As E6/E7 transcript levels were analyzed with primers targeting all splicing-derived transcripts, repression of E6 alone was not detectable on mRNA level due to primer recognition of alternative transcripts. However, the same cellular samples of siE6- or siE6/E7-transfected cells were used for protein and RNA extractions and therefore E6 repression can be verified by the reduced E6 and increased p53 protein levels in immunoblots (Figure 8A).

Overall, these findings show that under normoxic conditions, expression of the HPV oncogenes efficiently restricts Dkk1 levels in HPV-positive cervical cancer cells.

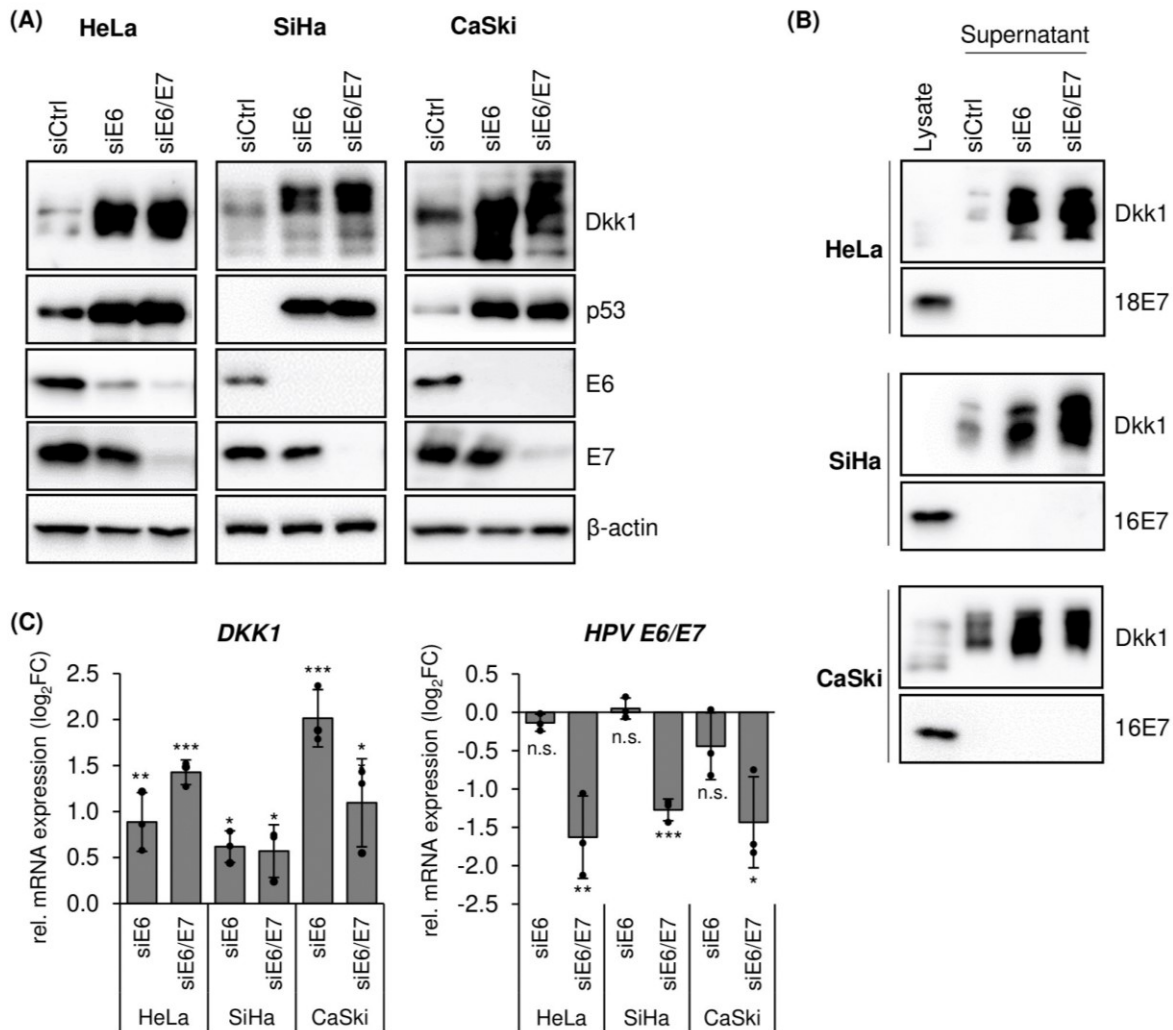


Figure 8 | Silencing of the HPV oncogenes induces Dkk1 expression in cervical cancer cells. (A) HeLa, SiHa and CaSki cells were transfected with control siRNA (siCtrl), siRNA against E6 (siE6) or against E6 and E7 (siE6/E7) (HPV18 and HPV16-specific siRNAs for HeLa cells or SiHa and CaSki cells, respectively). Protein levels of Dkk1, p53 and HPV E6/E7 were analyzed by immunoblots. β -actin: loading control. (B) Dkk1 levels in the cell supernatant after E6 or E6/E7 silencing compared to protein levels in the cell lysate. HPV E7 is not secreted and therefore indicates that the supernatants do not contain intracellular content. (C) Transcript levels of *Dkk1* (left panel) and *HPV E6/E7* (right panel) were tested in qRT-PCR and are indicated as mean \log_2 -transformed fold changes (\log_2FC) relative to siCtrl-transfected cells ($\log_2FC=0$) with standard deviations. Statistical significances are depicted by asterisks (*: $p<0.05$, **: $p<0.01$, ***: $p<0.001$, n.s.: not significant).

2.1.2 Dkk1 is repressed by the HPV oncogenes in a p53-dependent manner

Since silencing of E6 alone was sufficient to increase Dkk1 levels in cervical cancer cells (Figure 8) and the Dkk1 promoter was previously described to contain a p53 response element,¹¹⁴ I questioned whether Dkk1 repression in cervical cancer cells was mediated by E6-induced degradation of p53.³⁰ To this end, I combined RNAi-mediated silencing of E6 or E6/E7 with RNAi targeting p53 in HeLa and SiHa cells. In contrast to E6 or E6/E7 repression alone, which strongly increased p53 and Dkk1 protein expression, upon concomitant silencing of p53, Dkk1 protein levels remained largely unchanged in both cell lines (Figure 9A).

Further, qRT-PCR analyses showed that the downregulation of p53 in combination with a depletion of E6 or E6/E7 also interfered with the induction of *Dkk1* transcript levels (Figure 9B). This supports the notion that *Dkk1* is an indirect downstream target of HPV E6, which acts by blocking the p53-mediated transactivation of *Dkk1* expression. Remarkably, knockdown of p53 alone did not affect *Dkk1* expression on the protein or on the RNA level (Figures 9A, 9B), suggesting that p53 is not a major regulator for the basal *Dkk1* expression in HPV-positive cervical cancer cells.

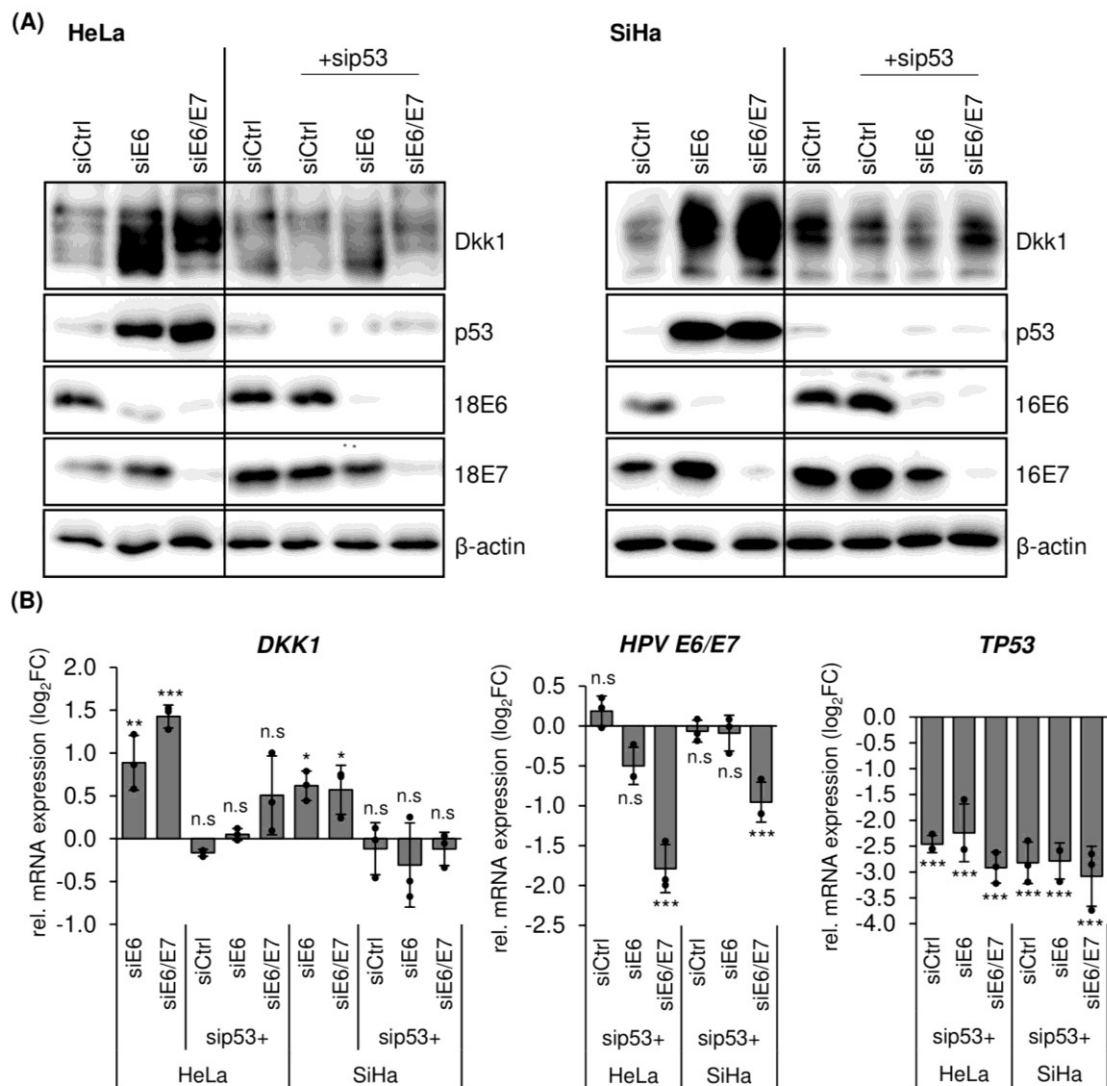


Figure 9 | siE6/E7-mediated induction of *Dkk1* is dependent on p53 stabilization. (A) In addition to control siRNA (siCtrl), siE6 or siE6/E7, HeLa (left panel) and SiHa cells (right panel) were transfected in parallel with siRNA targeting p53. Protein expression of *Dkk1*, p53 and HPV18 (HeLa) or HPV16 (SiHa) E6/E7 was analyzed by immunoblots compared to E6 or E6/E7 repression alone. β-actin: loading control. (B) *Dkk1* (left panel), HPV E6/E7 (central panel) and *TP53* (encoding p53) (right panel) mRNA expression was determined by qRT-PCR and is shown by mean log₂-transformed fold changes (log₂FC) relative to siCtrl-treated cells (log₂FC=0) with standard deviations. Statistical significances are indicated by asterisks (*: p<0.05, **: p<0.01, ***: p<0.001, n.s.: not significant).

2.1.3 Dkk1 is no upstream regulator of the HPV oncogenes

Vice versa, in view of its parallel repression with HPV E6/E7 under hypoxia,⁵⁵ it was interesting to test whether Dkk1 acts as a direct upstream regulator of the oncogenes. However, silencing of Dkk1 with two individual siRNAs alone (siDkk1 #1; siDkk1 #2) or in combination (siDkk1 #1+#2) did not affect HPV E6 or E7 protein expression in HeLa or SiHa cells (Figure 10A). Additionally, *E6/E7* mRNA levels were not significantly changed upon efficient *DKK1* repression in both cell lines (Figure 10B), indicating that Dkk1 levels do not affect HPV oncogene expression, at least under normoxic conditions.

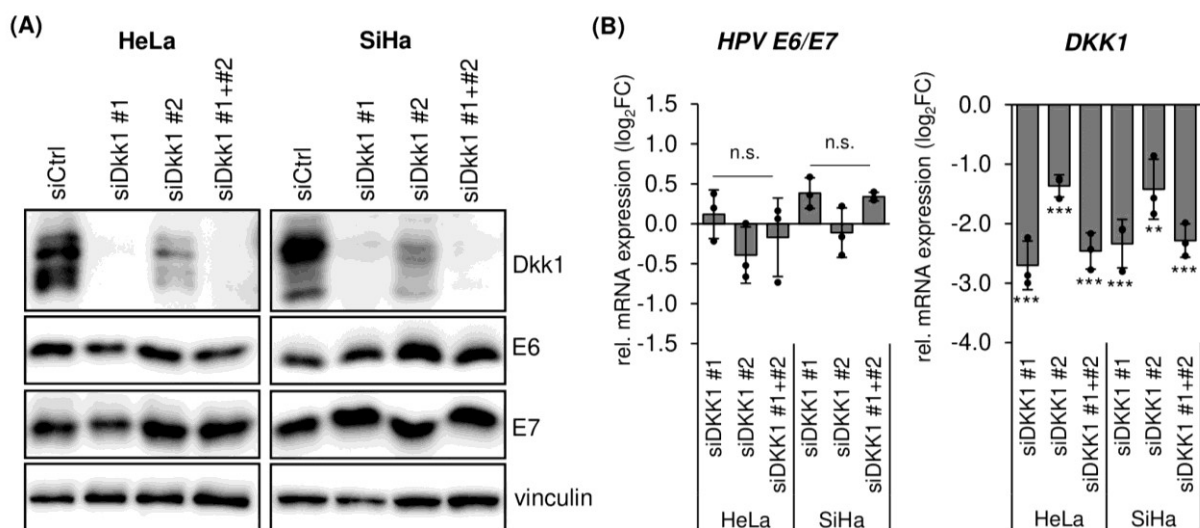


Figure 10| Dkk1 downregulation does not affect HPV E6 or HPV E7 expression. (A) HeLa (left panel) and SiHa cells (right panel), transfected with two different siRNAs against Dkk1 alone (siDkk1 #1; siDkk1 #2) or as a pool (siDkk1 #1+#2), were analyzed for Dkk1 and HPV E6/E7 protein expression by immunoblots. Vinculin: loading control. (B) *HPV E6/E7* (left panel) and *DKK1* (right panel) mRNA expression was determined by qRT-PCR after Dkk1 silencing. Shown are mean log₂-transformed fold changes (log₂FC) with standard deviations relative to siCtrl-transfected cells (log₂FC=0). Statistical significances are depicted by asterisks (**: $p < 0.01$, ***: $p < 0.001$, n.s.: not significant).

2.2 Analysis of hypoxic Dkk1 regulation

2.2.1 Hypoxic Dkk1 repression in HPV-positive and HPV-negative cells

Both, the HPV oncogenes and Dkk1, have previously been shown to be repressed under hypoxia in a glucose- and AKT-dependent manner in SiHa cells.⁵⁵ This parallelism is contradictory to the inverse correlation of Dkk1 with the HPV oncogenes under normoxia, since RNAi-mediated E6/E7 repression induced its expression (Figure 8). I therefore aimed to further validate the regulation of Dkk1 under hypoxic conditions in HPV-positive HeLa and CaSki cells, as well as in HPV-negative HCT116 colon cancer and A549 lung cancer cells.

Hypoxic treatments stabilized the hypoxia marker HIF-1 α in all cell lines (Figures 11A, 11B) and prohibited HPV E7 expression in HeLa and CaSki cells (Figure 11A). Moreover, Dkk1 was efficiently repressed in HPV-positive as well as HPV-negative cell lines in accordance with the previously obtained data from SiHa cells.⁵⁵ This clearly defines Dkk1 as a hypoxia-regulated factor.

High glucose concentrations in the cell medium (25 mM glucose) counteracted the hypoxic Dkk1 expression, although the effect was less pronounced in CaSki cells (Figure 11A). In contrast, AKT inhibition using the small molecule inhibitor AKTiVIII reverted Dkk1 downregulation under hypoxia in CaSki cells, but not in the other cell lines tested (Figures 11A, 11B). The functionality of the AKT inhibitor was validated by downregulation of Ser473-phosphorylated AKT, which is a marker for AKT activity.¹⁷⁵

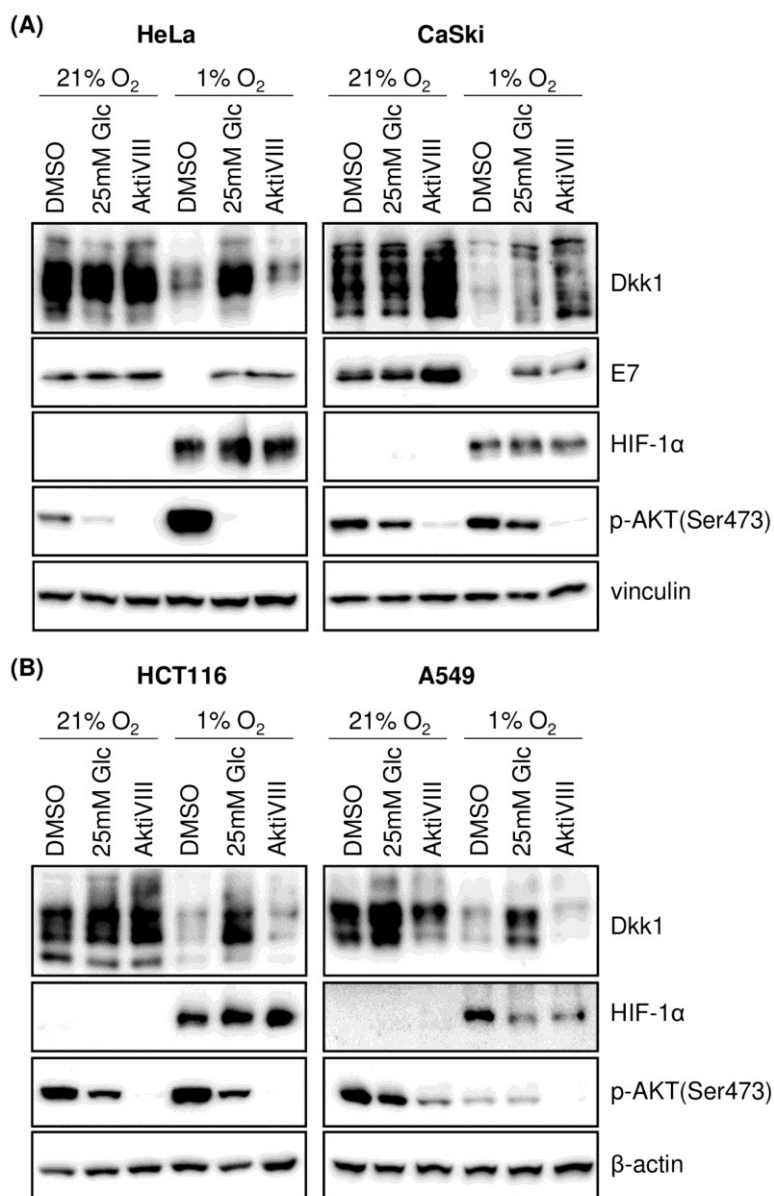


Figure 11 | Hypoxic Dkk1 regulation in HPV-positive and HPV-negative cancer cells. (A) HPV-positive HeLa (left panel) and CaSki cells (right panel) were cultured under normoxia (21 % O₂) or hypoxia (1 % O₂) in the presence of 5 mM glucose medium with solvent control (DMSO), 25 mM glucose medium (25 mM Glc) or 10 μ M of the AKT inhibitor AKTiVIII for 24 h. Protein expression of Dkk1 and HPV E7, as well as the expression of the hypoxia marker hypoxia-inducible factor 1 α (HIF-1 α) and Ser473-phosphorylated AKT (p-AKT) are depicted in immunoblots. Vinculin: loading control. (B) Analogous experiments were performed in HPV-negative HCT116 colon cancer (left panel) and A549 lung cancer cells (right panel). β -actin: loading control.

Overall, since Dkk1 repression under hypoxia is observed in HPV-positive as well as in HPV-negative cancer cell lines, these results suggest that hypoxic Dkk1 regulation is uncoupled from HPV oncogene expression and that it may be rather a result of metabolic changes, as it was shown to be critically dependent on the availability of glucose in most of the cell lines.

2.2.2 OXPHOS inhibition mimics hypoxic Dkk1 regulation

Hypoxia is characterized by a metabolic switch from O₂-dependent OXPHOS to O₂-independent glycolysis.⁵² To test the hypothesis, that Dkk1 downregulation under hypoxia is mediated by OXPHOS inhibition, I analyzed whether chemical inhibition of this pathway leads to Dkk1 repression in a glucose-dependent manner also under normoxic conditions. To this end, HeLa and SiHa cells were treated for 24 h or 48 h with the OXPHOS inhibitors Rotenone or Metformin in the presence of 5 mM ("low glucose", corresponding to normal serum concentrations in humans) or 25 mM glucose ("high glucose") supplemented medium. Both drugs inhibit the activity of complex I of the mitochondrial respiratory chain.¹⁷⁶

Under low glucose, Dkk1 expression was reduced after 24 h in both cell lines when OXPHOS was impaired, which was even stronger pronounced after 48 h (Figure 12). In contrast, after treatment with both OXPHOS inhibitors under high glucose, the cells were protected from Dkk1 repression after 24 h and a downregulation was observed only after treatments for 48 h. This observation may be explicable by an increased cellular glucose consumption after prolonged OXPHOS inhibition, which consequently leads to decreased glucose levels in the medium.

Notably, with the exception of prolonged Metformin treatment in combination with high glucose medium in HeLa cells, HPV E7 was repressed in parallel with Dkk1 after OXPHOS inhibition, which is in line with a previous report, showing that Metformin efficiently represses HPV oncogene expression in a glucose-dependent manner.¹⁷⁷

From these results, it can be concluded that an impaired OXPHOS, as is the case under hypoxic conditions, decreases Dkk1 levels in parallel with HPV E6 and E7 in HeLa and SiHa cells, and that this effect can be counteracted by increased glucose availability.

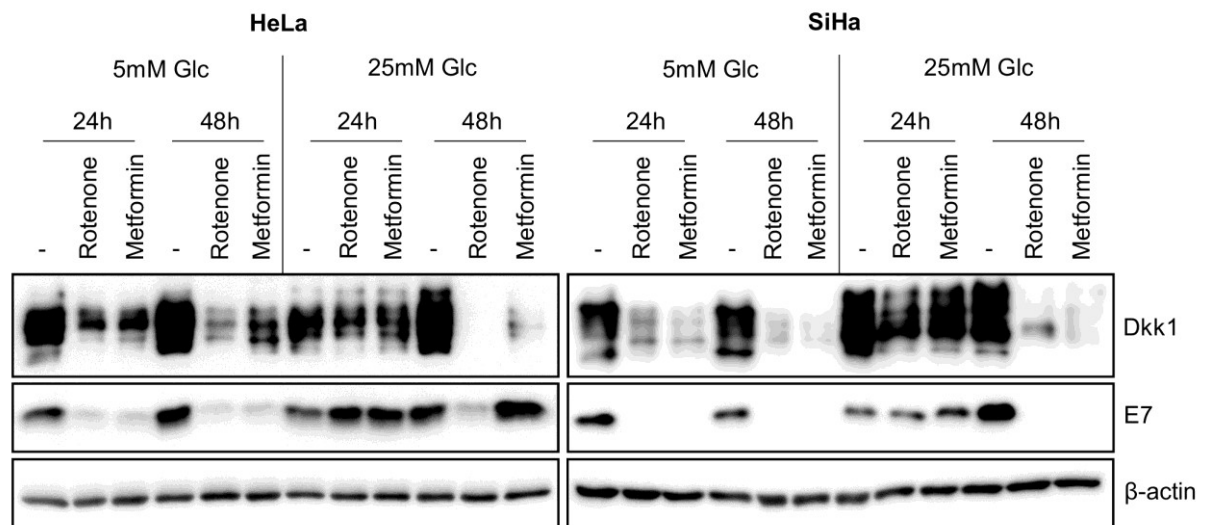


Figure 12 | OXPPOS inhibition represses Dkk1 in a glucose-dependent manner. HeLa (left panel) and SiHa cells (right panel) were cultured for 24 h or 48 h in medium supplemented with either 5 mM or 25 mM glucose (Glc), without or in the presence of the OXPPOS inhibitors Rotenone (20nM) or Metformin (2.5 mM for HeLa and 5 mM for SiHa cells). Protein expression of Dkk1 and HPV E7 was determined by immunoblots. β -actin: loading control.

2.2.3 Transient Dkk1 repression under hypoxia

HPV oncogene-induced Dkk1 repression under normoxia was dependent on p53 reconstitution after E6/E7 silencing (Figure 9). Alike Dkk1, regulation of p53 was previously shown to be uncoupled from E6/E7 expression under hypoxia: Besides the efficient downregulation of the two oncogenes, p53 levels are repressed after short-term hypoxic treatments, while after prolonged hypoxia (up to 72 h), p53 expression is strongly enhanced.^{54,178} This raises the question whether Dkk1, as a potential p53 target gene,¹¹⁴ is regulated in an analogous manner.

In a time course in HeLa cells, Dkk1 protein expression was efficiently repressed after 14-24 h of hypoxic incubation and was found to be re-induced after 48 h in parallel with p53 (Figure 13A). At the same time, HPV E6/E7 protein levels remained suppressed even after prolonged hypoxic treatments. This biphasic Dkk1 regulation was further reflected on transcript level by qRT-PCR (Figure 13B), suggesting that p53 may be a key driver of Dkk1 expression under hypoxic conditions.

It was further interesting that HIF-1 α , a critical transcription factor for hypoxia-regulated genes,⁵¹ showed a parallel regulation with p53 and Dkk1 (Figure 13A), suggesting that the cells could undergo a major HIF-1 α - or p53- mediated transcriptional reprogramming under hypoxia in a time-dependent, biphasic manner.

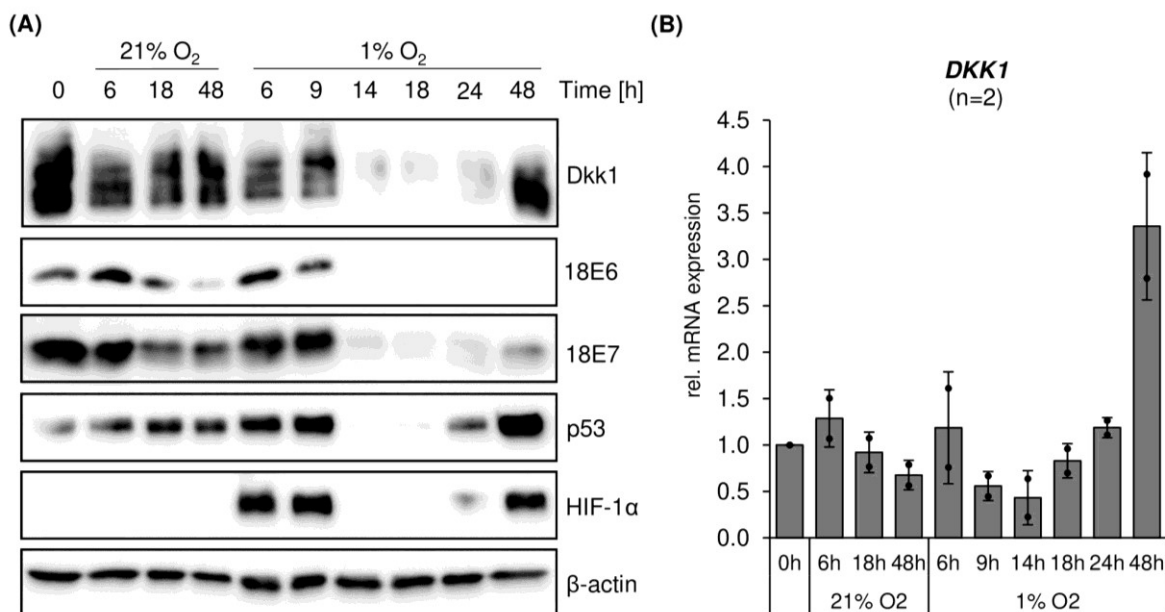


Figure 13| Dkk1 is transiently repressed in parallel with p53 under hypoxia. (A) Time course experiments were performed in HeLa cells under normoxia (21% O₂) or hypoxia (1% O₂). Immunoblots depict the protein expression levels of Dkk1, HPV18 E6/E7, p53 and the hypoxia marker HIF-1α at the indicated timepoints. β-actin: loading control. (B) *DKK1* mRNA expression was analyzed by qRT-PCR at the indicated time points under 21 % and 1 % O₂. Gene expression is shown as a mean relative to the start of the time course (0 h) and error bars depict standard deviations of experiments (n=2).

2.2.4 The ambiguous role of p53 for hypoxic Dkk1 repression

To investigate whether p53 expression is the primary driver of hypoxic Dkk1 regulation, HeLa cells were treated for 18 h or 48 h at normoxic or hypoxic conditions upon RNAi-induced p53 silencing. While the treatments under normoxia did not affect the protein expression of Dkk1, p53 or HPV 18E7 at both time points, 18 h of hypoxic incubation in siCtrl-transfected cells resulted as expected in decreased levels of these proteins, as well as an induction of HIF-1α (Figure 14A). In line with the previous data (Figure 13), Dkk1 and p53 levels were re-induced after prolonged hypoxic treatment, which was accompanied by an increased stabilization of HIF-1α and the continuous repression of 18E7 (Figure 14A). Interestingly, upon RNAi-induced p53 silencing, Dkk1 re-expression was abolished after 48 h of hypoxic incubation, which suggests that p53 drives Dkk1 protein expression at prolonged hypoxic conditions.

To verify this result, I next compared *DKK1* mRNA expression of siCtrl- and sip53-transfected HeLa cells under normoxic and hypoxic conditions. Intriguingly, *DKK1* transcript levels were strongly increased after 48 h of hypoxic incubation in both, siCtrl- and sip53-transfected cells despite efficient *TP53* silencing in the latter cells (Figure 14B), which differs from the results obtained on the protein level. This finding raises the question whether in concert with p53,

additional factors may be involved in the regulation of Dkk1 expression under hypoxia, for instance by modulating Dkk1 transcript or protein stability.

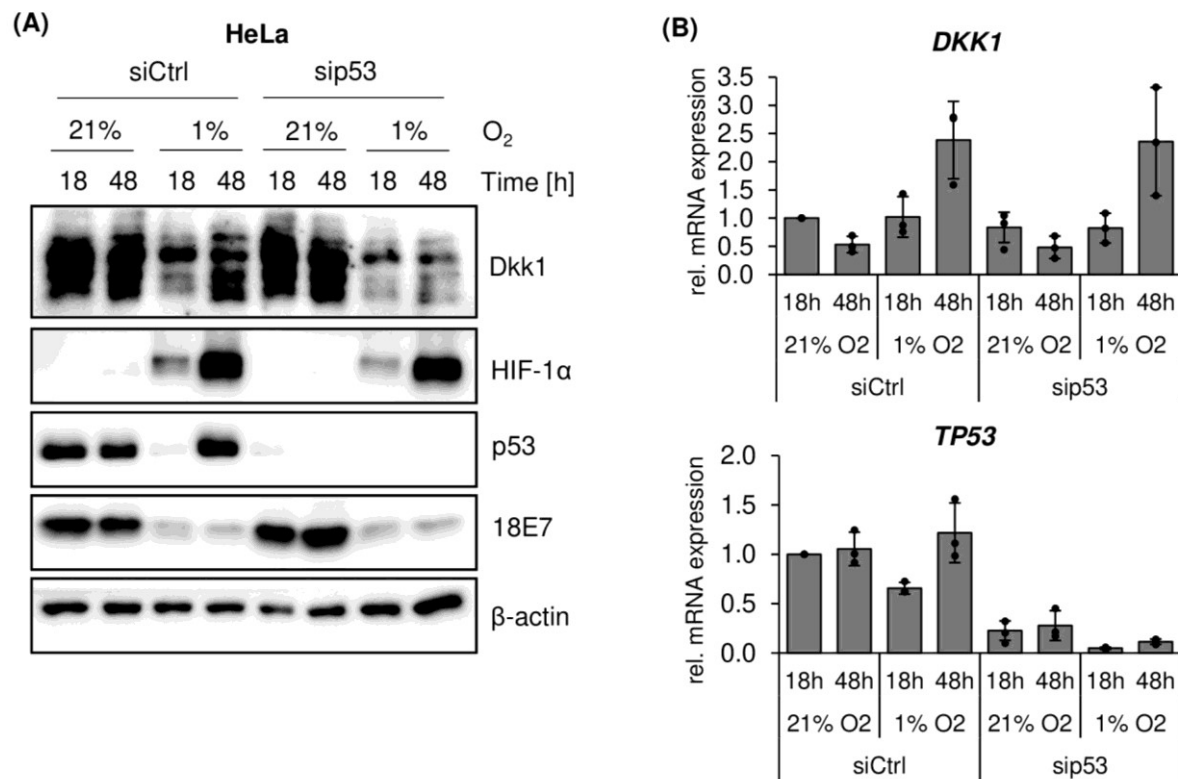


Figure 14 | p53 affects Dkk1 regulation under hypoxia on the protein but not on the transcript level. (A) HeLa cells were transfected with control siRNA (siCtrl) or sip53 and cultured at 21 % or 1 % O₂ for 18 h or 48 h. Immunoblots depict protein expression of Dkk1, HIF-1α, p53 and 18E7. β-actin: loading control. (B) Transcript levels of *DKK1* (upper panel) and *TP53* (encoding p53) (lower panel) after treatments as described above. Mean expressions with standard deviations are shown relative to siCtrl-transfected cells after 18 h at 21 % O₂.

2.3 Analysis of epigenetic regulation of Dkk1 in cervical cancer cell lines

DNA methylation at CpG islands and histone modifications, including acetylation and methylation, represent major epigenetic mechanisms which influence the gene activity in mammalian cells.¹⁷⁹ Dkk1 was previously reported to be epigenetically silenced not only in cervical cancer cells,¹¹¹ but also in gastrointestinal cancers and in multiple myeloma.^{112,113} It was therefore interesting to investigate whether in addition to HPV E6- or metabolic-driven Dkk1 repression, alternative, potential epigenetic mechanisms regulate Dkk1 levels in HPV-positive cancer cells under normoxic or hypoxic conditions.

2.3.1 Cell line-dependent epigenetic regulation of Dkk1

To study the impact of DNA methylation and histone acetylation on Dkk1 expression, HeLa, SiHa and CaSki cells were treated with increasing doses of the hypomethylating agent 5-Azacytidine (5-Aza)¹⁸⁰ or the histone deacetylase (HDAC) inhibitor Trichostatin A (TSA).¹⁸¹ Dkk1 protein levels were assessed after 72 h of 5-Azacytidine or 24 h of TSA treatments by immunoblots and in parallel *DKK1* transcript levels were analyzed using qRT-PCR. The efficiency of 5-Azacytidine treatment is indicated by the loss of DNA methyltransferase 1 (DNMT1) (Figure 15A) and of TSA treatment by an increase of tubulin acetylation in contrast to total tubulin expression (Figure 15B).

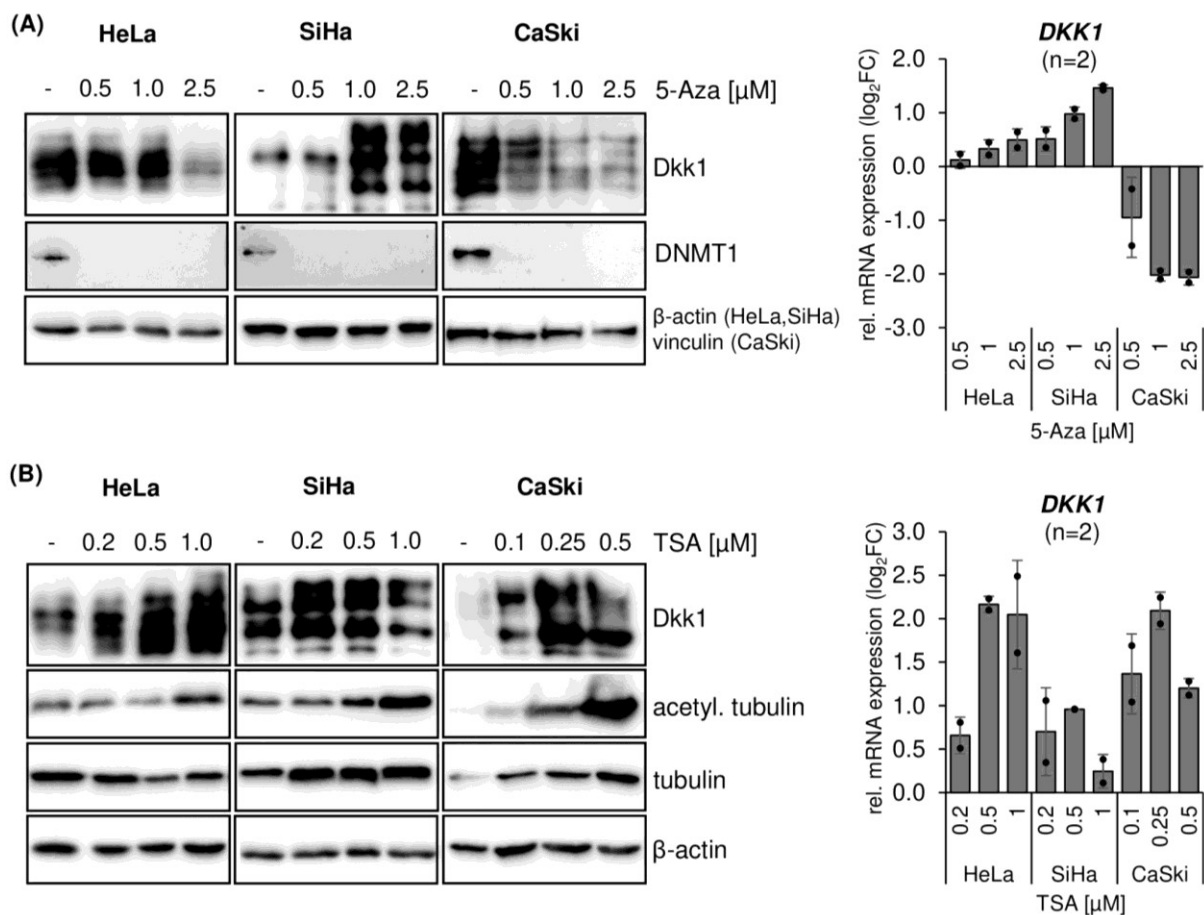


Figure 15| The effect of 5-Azacytidine and Trichostatin A on Dkk1 regulation. (A) Left panel: HeLa, SiHa and CaSki cells were treated with three different doses of 5-Azacytidine (5-Aza) for 72 h and protein expression of Dkk1 and DNA methyltransferase 1 (DNMT1) as a positive control were compared to their expressions in untreated cells. β -actin, vinculin: loading controls. Right panel: *DKK1* transcript levels were determined by qRT-PCR and are indicated by their mean expression relative to untreated cells as \log_2 -transformed fold changes (\log_2 FC). Error bars indicate standard deviations in between experiments (n=2). (B) Analogous protein (left panel) and mRNA expression (right panel) analyses were performed after treatment of HeLa, SiHa and CaSki cells with increasing doses of the histone deacetylase (HDAC) inhibitor Trichostatin A (TSA) for 24 h, and staining for acetylated (acetyl.) tubulin compared to total tubulin was used as a positive control. β -actin: loading control.

In accordance with the results from Lee et al. (2008),¹¹¹ Dkk1 protein expression was not increased by 5-Azacytidine in HeLa cells and transcript levels were only slightly induced (Figure 15A). In the same study it was reported that the Dkk1 promoter of SiHa cells was unmethylated,¹¹¹ however in the present work, 5-Azacytidine treatment strongly induced Dkk1 expression in SiHa cells, suggesting that Dkk1 is also repressed via DNA methylation in this cell line. Strikingly, in CaSki cells, Dkk1 protein and mRNA levels were downregulated after exposure to 5-Azacytidine, although DNA methylation is usually defined as an epigenetic repressive mark.¹⁷⁹

In contrast to the inhibition of methylation, Dkk1 protein and mRNA levels were induced upon treatment with TSA in HeLa cells (Figure 15B). An increase of Dkk1 expression after HDAC inhibition was also detected in SiHa and CaSki cells, although the TSA-mediated induction of Dkk1 in SiHa cells was less pronounced (Figure 15B) compared to the induction observed after 5-Azacytidine treatment (Figure 15A).

In conclusion, these observations support the notion that Dkk1 expression can be epigenetically regulated by histone acetylation or DNA methylation, however, the resulting effects vary substantially between different cell lines.

2.3.2 Epigenetic silencing plays no major role in hypoxic Dkk1 repression

Due to the strong influence of epigenetic marks on Dkk1 expression under normoxia (Figure 15), I next aimed to test whether they also have a regulatory role for the hypoxic Dkk1 downregulation in cervical cancer cells. For this purpose, HeLa, SiHa and CaSki cells were treated with 5-Azacytidine or TSA for 24 h under normoxic or hypoxic conditions. For hypoxic treatments, the 5-Azacytidine-exposed cells had been treated in advance for 48 h with the hypomethylating agent at 21 % O₂ to ensure an efficient inhibition of DNA methylation.

Dkk1 expression upon exposure to the two compounds under normoxia largely reflected the results as described above (Figure 15): Dkk1 expression was mainly affected by the inhibition of histone deacetylation and not by prohibition of DNA methylation in HeLa cells, while in SiHa cells both agents lead to an increase of Dkk1 protein levels and in CaSki cells, 5-Azacytidine decreased and TSA increased Dkk1 expression (Figure 16). In contrast, under hypoxic conditions, which were verified by HIF-1 α stabilization, Dkk1 expression remained suppressed after exposure to both agents in all three cell lines, which argues against a major regulatory role of DNA methylation or histone deacetylation for the repression of Dkk1 under hypoxia.

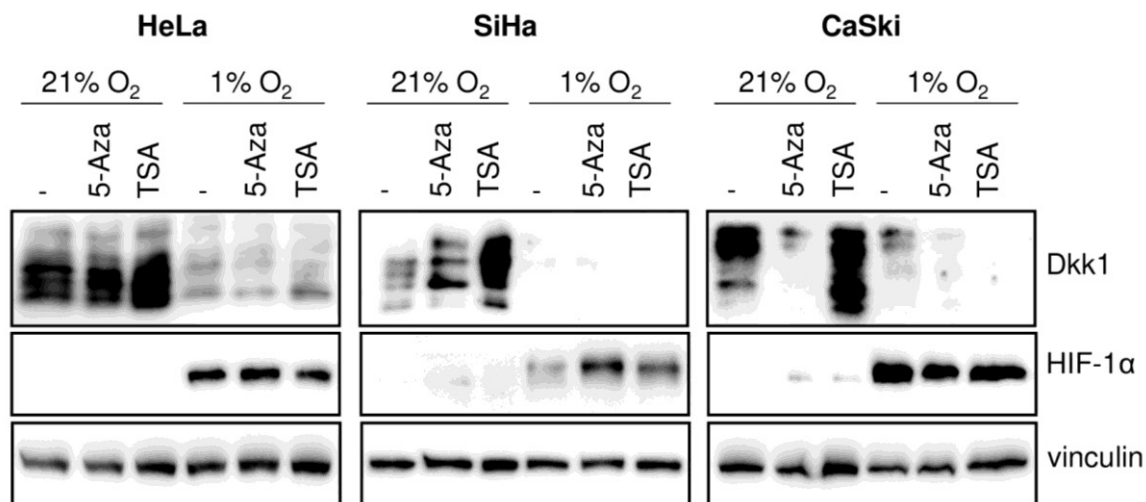


Figure 16| 5-Azacytidine or TSA treatments do not counteract hypoxic Dkk1 repression. HeLa (left panel), SiHa (central panel) and CaSki cells (right panel) were incubated for 24 h at 21 % or 1 % O₂ while being treated with 1 μM 5-Azacytidine (5-Aza) or 0.5 μM (CaSki: 0.25 μM) Trichostatin A (TSA). 5-Aza exposure was preceded by 48 h of pre-treatment with the component under normoxic conditions. Protein expression of Dkk1 and the hypoxic marker HIF-1α were analyzed by immunoblots. Vinculin: loading control.

2.4 The role of Dkk1 in the cellular response towards Cisplatin

The results obtained above reveal that Dkk1 is efficiently suppressed in HPV-positive cervical cancer cells under normoxic and, at least in part, under hypoxic conditions. Earlier studies have associated decreased Dkk1 levels with an increased tumorigenicity in HeLa cells and Dkk1 overexpression sensitized the same cells to UV-induced apoptosis.¹¹⁸ Consequently, it was interesting to investigate whether a reduced Dkk1 expression in cervical cancer cells may also contribute to their resistance towards clinically used therapeutics.⁵⁷ To this end, I chose to analyze the role of Dkk1 expression in Cisplatin-mediated apoptosis, due to the central role of Cisplatin-based therapies for the treatment of advanced or recurrent cervical cancers in the clinic.⁵⁹

2.4.1 Dose- and cell line-dependent induction of Dkk1 by Cisplatin

To investigate the effect of Cisplatin on Dkk1 expression, HeLa, CaSki and SiHa cells were treated with increasing concentrations of the drug for 24 h. As SiHa cells are known to be more resistant towards Cisplatin compared to HeLa cells,¹⁸² they were treated with 10, 15 or 20 μM instead of 5, 10 or 15 μM Cisplatin, which was used for HeLa and CaSki cells (Figure 17).

Cisplatin induced apoptosis in all three cervical cancer cell lines, which is depicted in immunoblots by an increase of the apoptosis marker cleaved (cl.) PARP (Figure 17A). Compared to HeLa and CaSki cells, the amount of cl. PARP was relatively lower in SiHa cells despite of using higher Cisplatin concentrations.

The Dkk1 expression levels showed cell-dependent differences: While in HeLa and CaSki cells, Cisplatin treatment lead to an increase of Dkk1 protein concentrations, Dkk1 levels were decreased in SiHa cells. Notably, exposure to 15 μM Cisplatin also prohibited Dkk1 induction in HeLa cells, which may be a consequence of the severe apoptosis levels indicated by the high amounts of cl. PARP. In HeLa and CaSki cells, the analysis of *DKK1* transcripts further reflected the results obtained on protein level: In HeLa cells *DKK1* expression was significantly induced upon treatment with 5 or 10 μM Cisplatin and in CaSki cells, all tested concentrations increased *DKK1* transcript levels (Figure 17B). Interestingly, despite its repression on the protein level, 10 μM Cisplatin induced the amount of *DKK1* transcripts also in SiHa cells.

Overall, the observation that Cisplatin can induce Dkk1 expression raises the question whether increased Dkk1 levels may be functionally connected to Cisplatin-mediated apoptosis in cervical cancer cells.

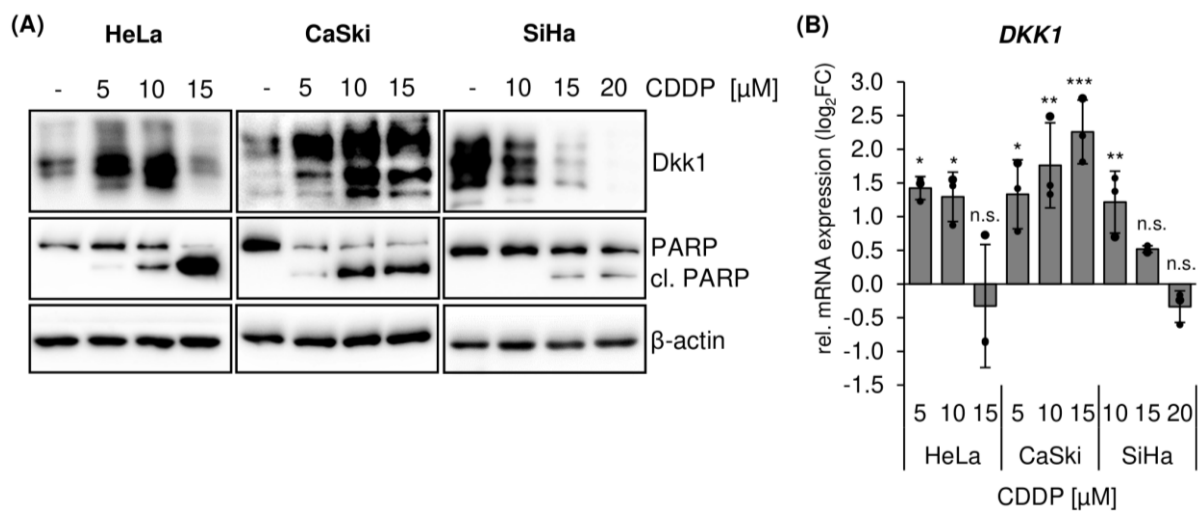


Figure 17 | Effect of Cisplatin on Dkk1 expression in cervical cancer cells. (A) HeLa (left panel), CaSki (central panel) and SiHa cells (right panel) were treated with the indicated Cisplatin (CDDP) concentrations for 24 h. Protein expression of Dkk1 and PARP (cleaved (cl.) and uncleaved forms) are shown in immunoblots. β -actin: loading control. (B) *DKK1* transcript levels of CDDP-treated cells as described above were analyzed by qRT-PCR and are depicted as mean \log_2 -transformed fold changes ($\log_2\text{FC}$) with standard deviations relative to untreated cells ($\log_2\text{FC}=0$). Statistical significances are indicated by asterisks (*: $p < 0.05$, **: $p < 0.01$, ***: $p < 0.001$, n.s.: not significant).

2.4.2 Dkk1 expression induces apoptosis in a Dkk1-negative HeLa variant

Previous reports have suggested that Dkk1 expression can sensitize cancer cells to apoptosis induced by DNA-damaging agents, such as Cisplatin.^{98,118} It was therefore interesting to elucidate whether an enhanced Dkk1 expression also exerts pro-apoptotic effects in cervical cancer cells. To this end, I made use of a laboratory HeLa variant, in the following referred to as HeLa*, which - among other dissimilarities in gene expression¹⁸³ - differed from the herein thus far described HeLa cells by undetectable Dkk1 protein levels (Figure 18A).

HeLa* cells were transfected with increasing amounts of a Dkk1 expression plasmid (pCS2-hDkk1-Flag) or vector control (pCS2). Ectopic Dkk1 expression resulted in enhanced levels of the apoptosis markers cl. PARP and cl. Caspase 9 (Figure 18A), indicating a pro-apoptotic role for Dkk1 in this cell line. In accordance, TUNEL (terminal deoxynucleotidyl transferase dUTP nick end labeling) assays revealed a significant increase of apoptotic cells as a result of enhanced Dkk1 levels (Figure 18B).

In conclusion, the induction of apoptosis mediated by Dkk1 re-expression in a Dkk1-negative HeLa variant, along with the previous notion that Cisplatin can enhance Dkk1 levels in cervical cancer cells (Figure 17), further give rise to the question whether Dkk1 plays a role for Cisplatin-induced apoptosis in these cells.

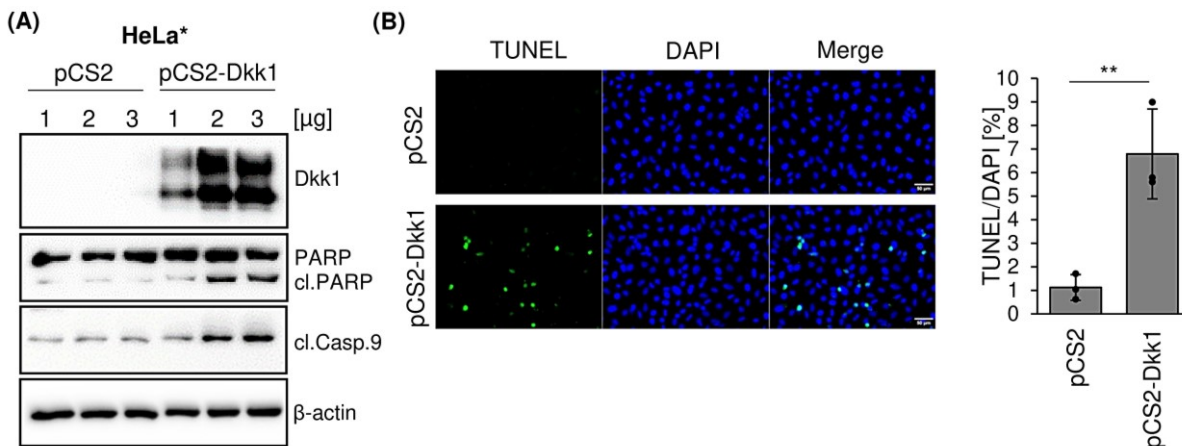


Figure 18 | Apoptosis induction in HeLa* cells upon Dkk1 overexpression. (A) The HeLa* variant, which exhibits undetectable Dkk1 protein levels, was transfected with increasing amounts of vector control (pCS2) or a Dkk1 expression plasmid (pCS2-hDkk1-Flag) and protein levels of Dkk1, PARP (cleaved (cl.) and uncleaved forms) and cl. Caspase 9 (Casp.9) were assessed by immunoblots. β-actin: loading control. (B) TUNEL assays of HeLa* cells transfected with 2 μg pCS2 or pCS2-hDkk1-Flag (scale bar: 50 μm) (left panel). TUNEL-positive cells were quantified relative to the total number of cells, as counted by the number of DAPI stainings (right panel). Indicated are mean percentages with standard deviations and the statistical significance is shown by asterisks (**: p<0.01).

2.4.3 Dkk1 sensitizes HeLa cells towards Cisplatin-mediated apoptosis

As a secreted factor, Dkk1 is known to exert its signaling functions via cell surface receptors in an autocrine or paracrine manner.⁷⁴ To further explore the role of exogenously added Dkk1 on the apoptotic response in HeLa cells, I generated Dkk1 conditioned medium (Dkk1 CM) by transfecting the HeLa* variant with the Dkk1 expression plasmid pCS2-hDkk1-Flag (Figure 19A).

Dkk1 overexpression was not only detectable in cell lysates of HeLa* cells upon transfection, but also in their cell supernatant (SN) (Figure 19B). For subsequent experiments, this supernatant was transferred as Dkk1 CM to HeLa cells (Figure 19A). Control conditioned medium (Ctrl CM) was generated in an analogous manner by transfection of the vector control pCS2.

Notably, in Dkk1 CM-treated HeLa cells, intracellular Dkk1 levels strongly increased, indicating an efficient cellular uptake of Dkk1. Unlike observed for HeLa* cells (Figure 18), the increase of Dkk1 expression was not associated with apoptosis induction *per se*, as treatment with Dkk1 CM alone did not enhance cl. PARP or cl. Caspase 9 levels (Figure 19C). Importantly, however, upon parallel treatment with Cisplatin, expression of both apoptosis markers was enhanced after exposure to Dkk1 CM compared to Ctrl CM, suggesting that Dkk1 CM sensitizes HeLa cells to Cisplatin-mediated apoptosis.

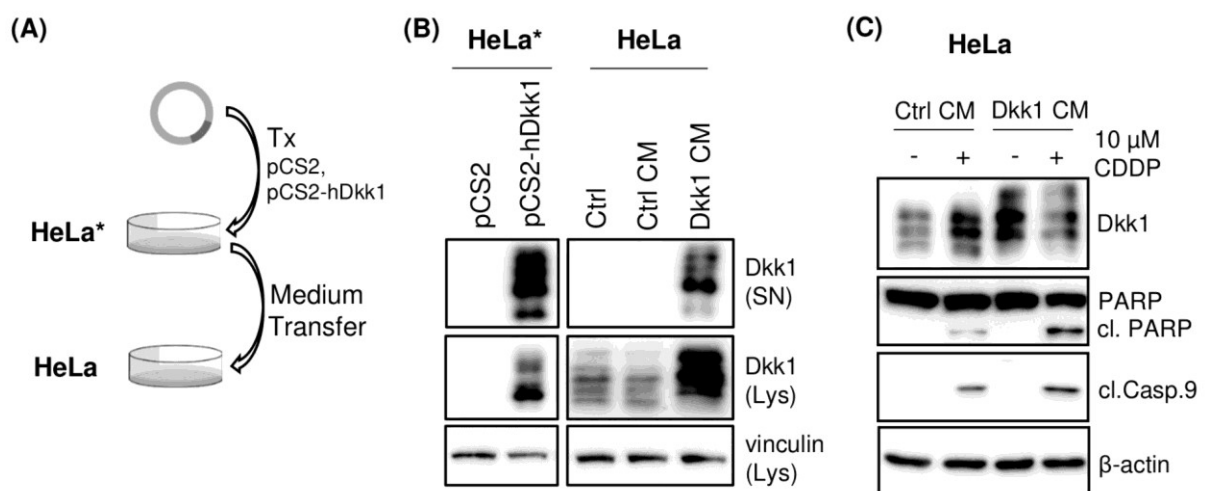


Figure 19 | Dkk1 conditioned medium enhances Cisplatin-induced apoptosis in HeLa cells. (A) Dkk1 conditioned medium (Dkk1 CM) and control medium (Ctrl CM) were produced by transfecting the HeLa* variant (not expressing detectable levels of Dkk1) with a Dkk1 expression plasmid (pCS2-hDkk1-Flag) or vector control (pCS2), respectively, and then transferred to HeLa cells for ensuing experiments. (B) Immunoblots depict Dkk1 levels in the supernatants (SN) and cell lysates (Lys) in the HeLa* variant after transfection (left panel) and in HeLa cells after treatment with standard cell culture medium (Ctrl), Ctrl CM or Dkk1 CM (right panel). Vinculin: loading control.

(figure legend continued on next page)

(see figure on previous page)

(C) HeLa cells were pre-incubated for 48 h with Ctrl CM or Dkk1 CM and subsequently treated for 24 h with Cisplatin (CDDP) or left untreated in the presence of Ctrl CM or Dkk1 CM, respectively. Protein expression of intracellular Dkk1, PARP (cleaved (cl.) and uncleaved forms) and cl. Caspase 9 (Casp.9) was analyzed by immunoblots. β -actin: loading control.

2.4.4 RNAi-induced Dkk1 repression impairs Cisplatin-mediated apoptosis

If Dkk1 has a pro-apoptotic role for cervical cancer cells in the response towards Cisplatin, then Dkk1 downregulation should provide these cells with increased resistance to the drug. To test this hypothesis, I performed RNAi-mediated repression of Dkk1 in combination with Cisplatin treatment in HeLa, CaSki and SiHa cervical cancer cells.

Surprisingly, as observed for HeLa and CaSki cells, Cisplatin efficiently induced Dkk1 expression also in siCtrl-transfected SiHa cells (Figure 20A), which is in conflict with the previous finding that Cisplatin decreased Dkk1 protein levels in this particular cell line under slightly different experimental conditions (Figure 17A). Importantly, however, transient downregulation of Dkk1 using a pool of two different *DKK1*-targeting siRNAs (siDkk1 #1+#2) reduced the apoptosis rates in all three cell lines after being treated with two different doses of Cisplatin, as indicated by the decreased levels of cl. PARP and cl. Caspase 9, compared to cells transfected with siCtrl (Figure 20A).

TUNEL assays further corroborate that Cisplatin-induced apoptosis is impaired upon Dkk1 silencing. Compared to ~16 % of TUNEL-positive signals in siCtrl-transfected HeLa cells, only ~2.4 % of the siDkk1-transfected cells were stained positive for apoptosis under the same experimental conditions (Figure 20B). In accordance, TUNEL stainings in SiHa cells also indicate that Cisplatin-mediated apoptosis was reduced upon Dkk1 silencing in this cell line (Figure 20C), although quantifications revealed that the effect was not significant and less pronounced compared to HeLa cells.

Overall, the impaired apoptosis induction by Cisplatin upon Dkk1 downregulation in all three cell lines strongly suggests a critical role for Dkk1 in Cisplatin-mediated apoptosis in cervical cancer cells.

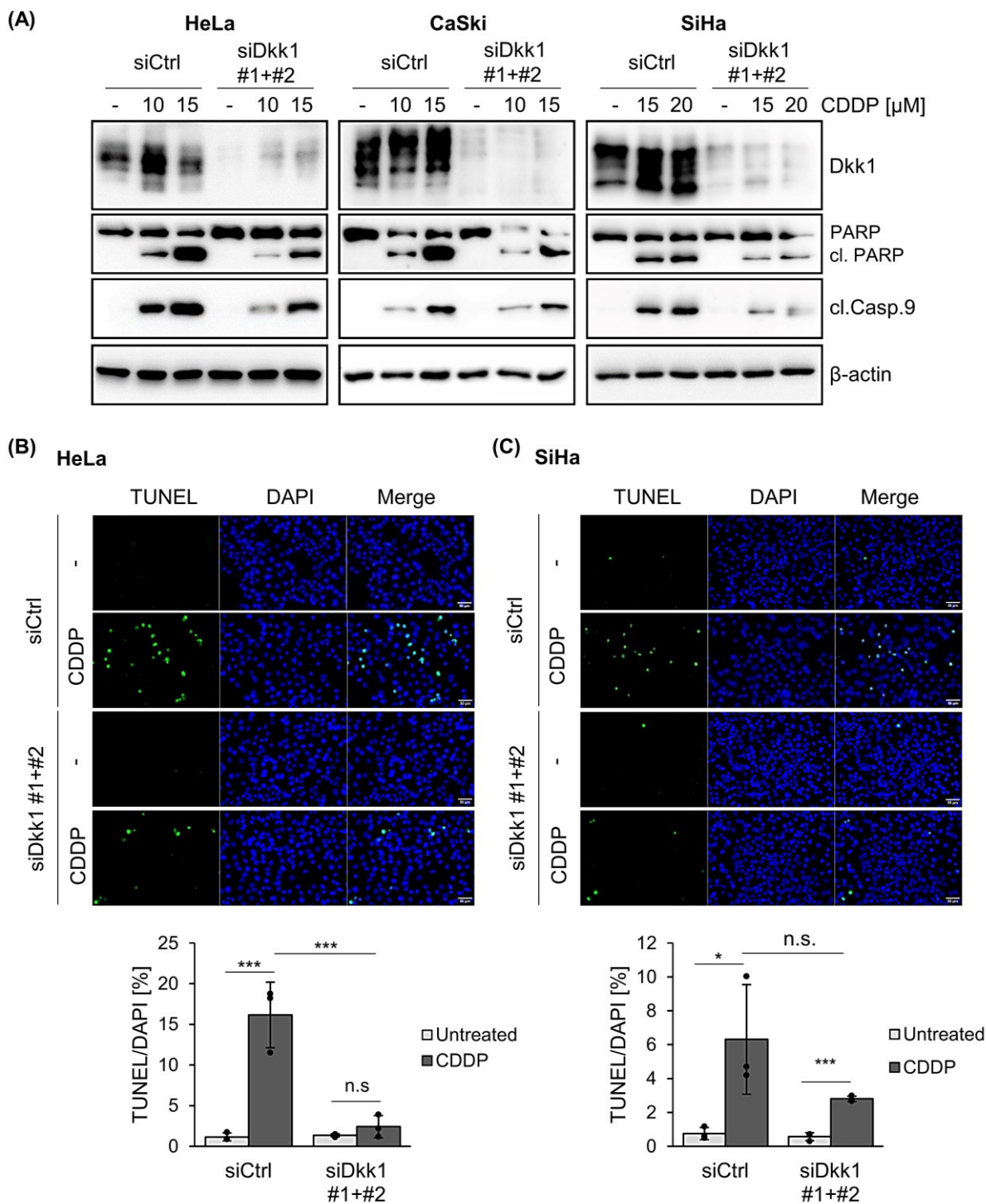


Figure 20 | Silencing of Dkk1 reduces Cisplatin-mediated apoptosis in cervical cancer cells. (A) HeLa (left panel), CaSki (central panel) and SiHa cells (right panel) were transfected with control siRNA (siCtrl) or a pool of two different *DKK1*-targeting siRNAs (siDkk1 #1+#2) and subsequently treated with two different doses of Cisplatin (CDDP) for 20 h (HeLa, CaSki) or 32 h (SiHa). Protein expression of Dkk1, PARP (cleaved (cl.) and uncleaved forms) and cl. Caspase 9 (Casp.9) was analyzed by immunoblots. β -actin: loading control. (B) HeLa cells treated with 15 μ M CDDP as described above were stained with TUNEL reagent (scale bar: 50 μ m) (upper panel) and the percentage of TUNEL-positive cells was calculated relative to the total number of cells, as determined by DAPI stainings (lower panel). Depicted are mean percentages with standard deviations and statistical significances are indicated by asterisks (***: $p < 0.001$, n.s.: not significant). (C) TUNEL assays in SiHa cells treated with 15 μ M CDDP as described for HeLa cells above (*: $p < 0.05$).

2.4.5 Cisplatin resistance of Dkk1 knockout HeLa cells

To study the role of Dkk1 for the Cisplatin response in cervical cancer cells more stringently and in more detail, I performed CRISPR/Cas9-mediated Dkk1 knockout (KO) in HeLa cells and generated four independent and stable Dkk1 KO single cell clones (Dkk1 KO #1-#4).

As observed before, treatment of parental HeLa cells with 10 μ M Cisplatin induced Dkk1 protein expression and enhanced apoptosis as shown by the increased amounts of cl. PARP and cl. Caspase 9. In stark contrast, the induction of both apoptosis markers was blocked under the same experimental conditions in all Dkk1 KO clones, indicating that the Dkk1-depleted HeLa cells are protected from Cisplatin-induced apoptosis.

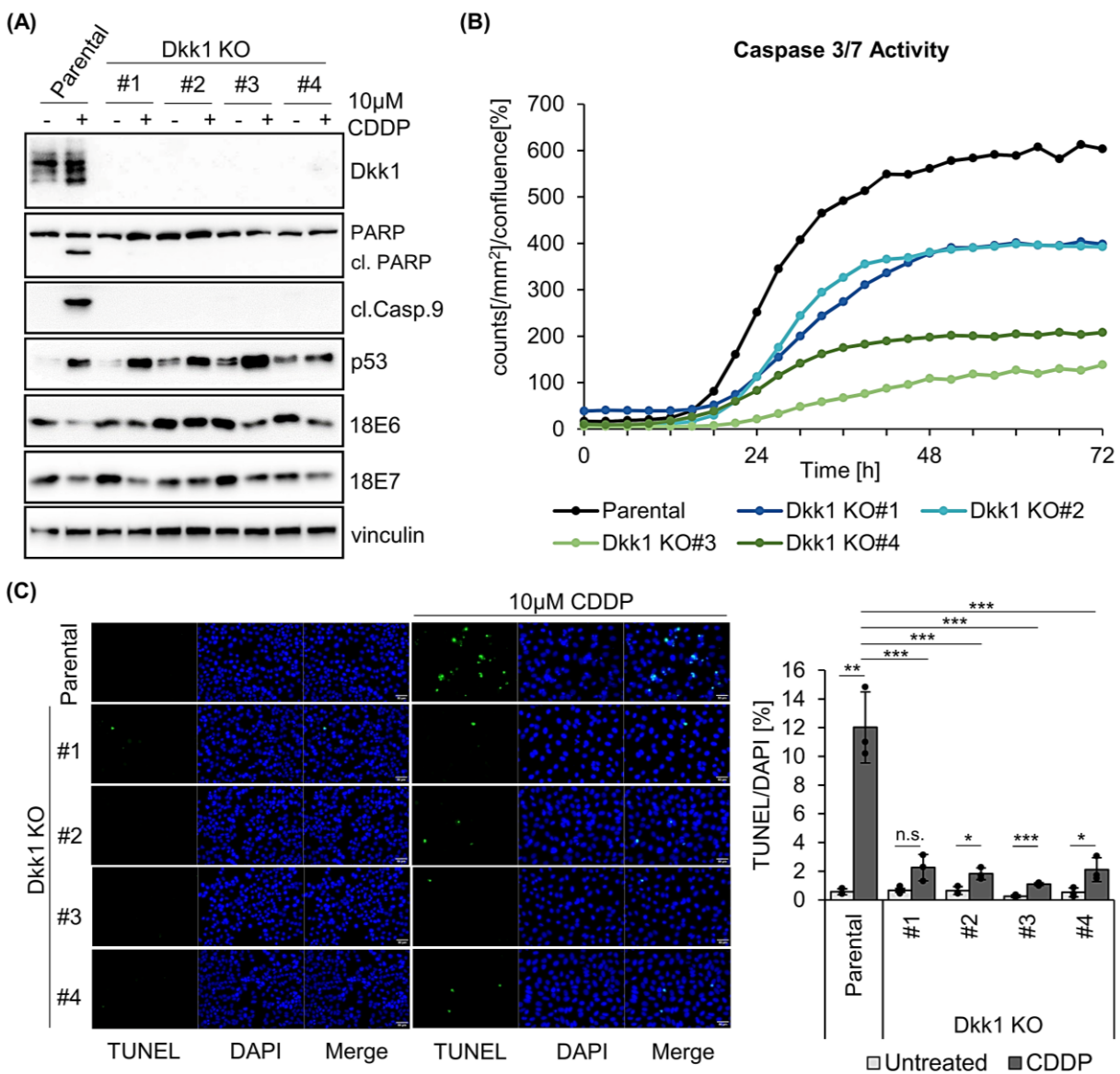


Figure 21 | (see figure legend on next page)

(see figure on previous page)

Dkk1 knockout HeLa cells exhibit increased resistance towards Cisplatin-mediated apoptosis. (A) Immunoblots of parental HeLa and CRISPR/Cas9-generated Dkk1 knockout (KO) HeLa single cell clones (Dkk1 KO #1-#4), after treatment for 24 h with 10 μ M Cisplatin (CDDP), depict protein expression of Dkk1, PARP (cleaved (cl.) and uncleaved forms), cl. Caspase 9 (Casp.9), p53 and HPV18 E6/E7 compared to the respective untreated cells. Vinculin: loading control. (B) Caspase 3/7 assay of parental HeLa cells and Dkk1 KO HeLa cells being treated with 10 μ M CDDP. Caspase 3/7 activity (counts/mm²) was measured every 2 h over 72 h using IncuCyte Live Cell Imaging and total counts were normalized to the cell confluence. Depicted are the mean counts of three technical replicates from one representative experiment. (C) TUNEL assays of untreated and CDDP-treated (10 μ M) parental HeLa and Dkk1 KO HeLa cells (scale bar: 50 μ m) (left panel). The percentage of TUNEL-positive cells was quantified relative to the respective DAPI staining, representing total cell numbers (right panel). Indicated are mean percentages with standard deviations and statistical significances are shown by asterisks (*: $p < 0.05$, **: $p < 0.01$, ***: $p < 0.001$, n.s.: not significant).

Interestingly, while the Cisplatin-induced downregulation of the HPV oncogenes was less pronounced in the Dkk1 KO HeLa cells compared to the parental HeLa cells, p53 expression was induced by Cisplatin in all cell lines irrespective of Dkk1 expression or apoptosis induction.

To confirm the differential apoptotic response of parental HeLa and Dkk1 KO HeLa cells towards Cisplatin by an independent method, caspase 3/7 activation was assessed by IncuCyte live cell imaging (Figure 21B). In line with the results obtained for the expression of the apoptosis markers cl. PARP and cl. Caspase 9, the Dkk1 KO clones also showed lower caspase 3/7 activity upon treatment with 10 μ M Cisplatin compared to parental HeLa cells. Moreover, TUNEL assays indicate that only 1-2% of the Dkk1 KO HeLa cells were stained TUNEL-positive, while in the parental cells ~12% of the cells underwent apoptosis (Figure 21C).

Collectively, in accordance with the findings based on transient RNAi-induced Dkk1 silencing (Figure 20), different apoptotic assays uncover that Dkk1 depletion renders HeLa cells more resistant towards Cisplatin-induced apoptosis and support the notion that Dkk1 is a key mediator in the apoptotic Cisplatin response in cervical cancer cells.

2.4.6 Induction of senescence in Dkk1 KO HeLa cells

Next, I aimed to analyze the cellular fate of Cisplatin-treated Dkk1 KO HeLa cells by means of their proliferative potential, following the experimental scheme in Figure 22A. Interestingly, alike parental HeLa cells, the colony formation capacity of all Dkk1 KO clones was impaired after the exposure to Cisplatin (Figure 22B), proposing the involvement of an anti-proliferative mechanism other than apoptosis.

I found that the proliferative stop of the Dkk1 KO HeLa cells after Cisplatin treatment can be explained, at least in part, by the induction of cellular senescence, as shown by the typical morphology of senescent cervical cancer cells (cellular enlargement and flattening, cytoplasmic

extensions)^{170,184} and the positive staining for the well-established senescence marker SA- β -gal¹⁸⁵ (Figure 22C). In contrast, the induction of apoptosis by Cisplatin allowed only very few of the parental HeLa cells to survive and to become senescent.

In conclusion, these results show that, as a consequence of Dkk1 depletion, HeLa cells undergo a phenotypic switch from apoptosis towards senescence in the response to Cisplatin.

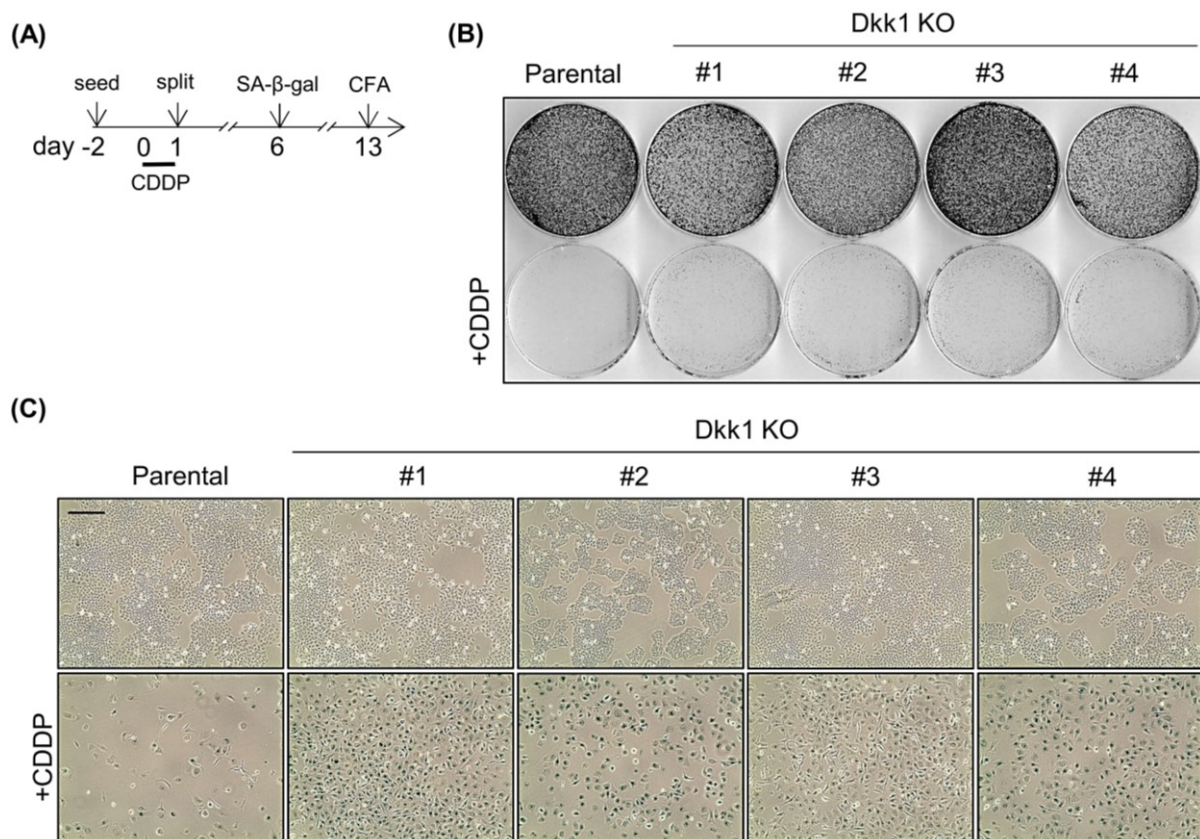


Figure 22 | Senescence induction in Cisplatin-treated Dkk1 KO HeLa cells. (A) Experimental scheme for Cisplatin (CDDP) treatment, cell splitting, colony formation assays (CFAs) and senescence-associated β -gal stainings (SA- β -gal). (B) CFAs of parental HeLa cells and Dkk1 KO HeLa cells stained with crystal violet after treatment with 10 μ M CDDP. (C) Senescence assays of parental HeLa cells and Dkk1 KO clones after treatment with 10 μ M CDDP (scale bar: 500 μ m).

2.5 Canonical Wnt signaling and the Dkk1-dependent Cisplatin response

Canonical, β -catenin-dependent Wnt signaling is known to be aberrantly activated in different cancer types⁸⁴ and was shown to increase the resistance towards a variety of therapies, including Cisplatin-based treatments.^{186,187} As Dkk1 is a well-established antagonist of the canonical Wnt pathway,⁷⁴ it was tempting to speculate that the lack of Dkk1 expression in cervical cancer cells enables an enhanced activation of this pathway upon Cisplatin treatment, which may be linked to the increased Cisplatin resistance upon Dkk1 depletion.

2.5.1 Dkk1 counteracts Wnt3a-induced canonical Wnt signaling

The TOP-/FOPflash assay, which is based on luciferase reporter plasmids containing intact or mutated β -catenin-responsive TCF-binding sites, respectively (Figure 23A), is a widely used tool to measure canonical Wnt activities.¹⁸⁸ To test the potential of secreted Dkk1 to antagonize canonical Wnt signaling, I applied this assay to HeLa cells treated with Dkk1 CM or Ctrl CM, in combination with transfection of a Wnt3a expression plasmid (pcDNA3-Wnt3a), which is a prototypical Wnt activator,⁸⁴ or vector control (pcDNA3) (Figure 23B).

In line with the data from a previous report,¹¹⁸ Ctrl-transfected HeLa cells did not exhibit basal Wnt activities, as no TOPflash activation was detectable above FOPflash activities. In contrast, upon transfection with Wnt3a, the TOPflash activities increased ~14-fold in HeLa cells treated with Ctrl CM. Notably, treatment with Dkk1 CM efficiently counteracted this effect, which indicates that Dkk1 is, in principle, able to repress Wnt3a-induced canonical Wnt signaling in HeLa cells.

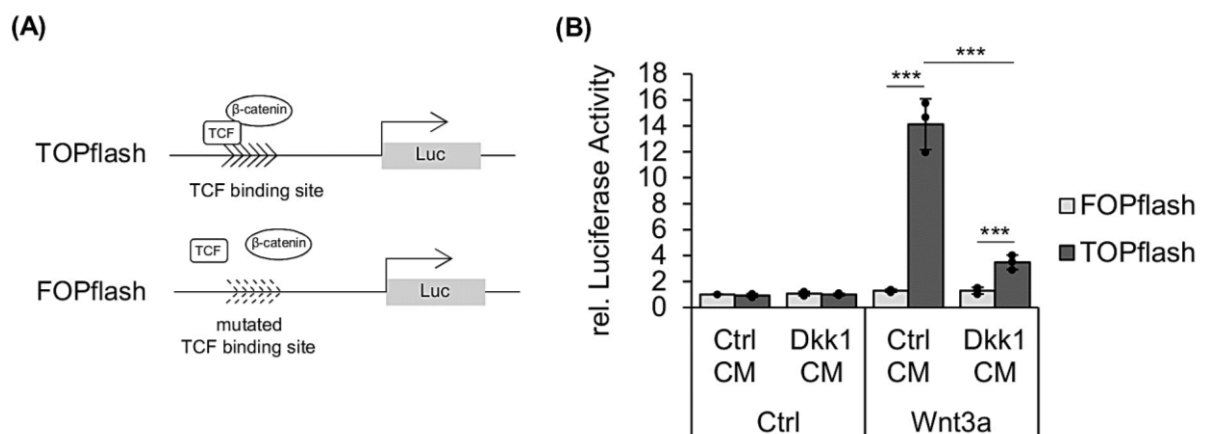


Figure 23 | Dkk1 conditioned medium counteracts Wnt3a-induced TOPflash activities. (A) TOPflash plasmids contain intact TCF-binding sites adjacent to the luciferase gene which is induced upon β -catenin binding to TCF. In FOPflash plasmids, the TCF binding sites are mutated which prohibits the binding of TCF despite the presence of β -catenin.¹⁸⁸ (B) TOP-/FOPflash assays in HeLa cells transfected with vector control pcDNA3 (Ctrl) or the expression vector pcDNA3-Wnt3a (Wnt3a) after treatment with control conditioned medium (Ctrl CM) or Dkk1 conditioned medium (Dkk1 CM) for 16 h. Depicted are the mean TOP-/FOPflash luciferase activities relative to FOPflash activities of Ctrl-transfected cells treated with Ctrl CM, along with standard deviations. Statistical significances are indicated by asterisks (***: $p < 0.001$).

2.5.2 The Dkk1-dependent Cisplatin response is uncoupled from Wnt activation

To test whether the enhanced Cisplatin-resistance of Dkk1-depleted cells is associated with an increased activation of canonical Wnt signaling, TOP-/FOPflash activities were assessed in parental HeLa cells and HeLa Dkk1 KO clones #1-#3 after Cisplatin treatment and were compared to the Wnt activities induced by ectopic Wnt3a expression (Figure 24A). Interestingly, as determined for parental HeLa cells, basal TOPflash activities were not detectable in any of the Dkk1 KO HeLa cells,

which suggests that in contrast to the repressive function of Dkk1 CM on Wnt3a-induced canonical Wnt signaling (Figure 23B), Dkk1 expression does not prohibit the endogenous canonical Wnt activities in HeLa cells.

The relative level of Wnt activation by ectopic Wnt3a expression differed between the Dkk1 KO clones which could be due to the genetic heterogeneity of the parental HeLa cell line, as discussed by Guilano et al. (2019).¹⁸⁹ Importantly, and in contrast to the positive control Wnt3a, treatment with Cisplatin did not affect TOPflash levels, neither in parental HeLa cells nor in the different Dkk1 KO HeLa cells. This indicates that the protection of Dkk1-depleted cells towards Cisplatin-induced apoptosis is not linked to a detectable increase in canonical Wnt signaling.

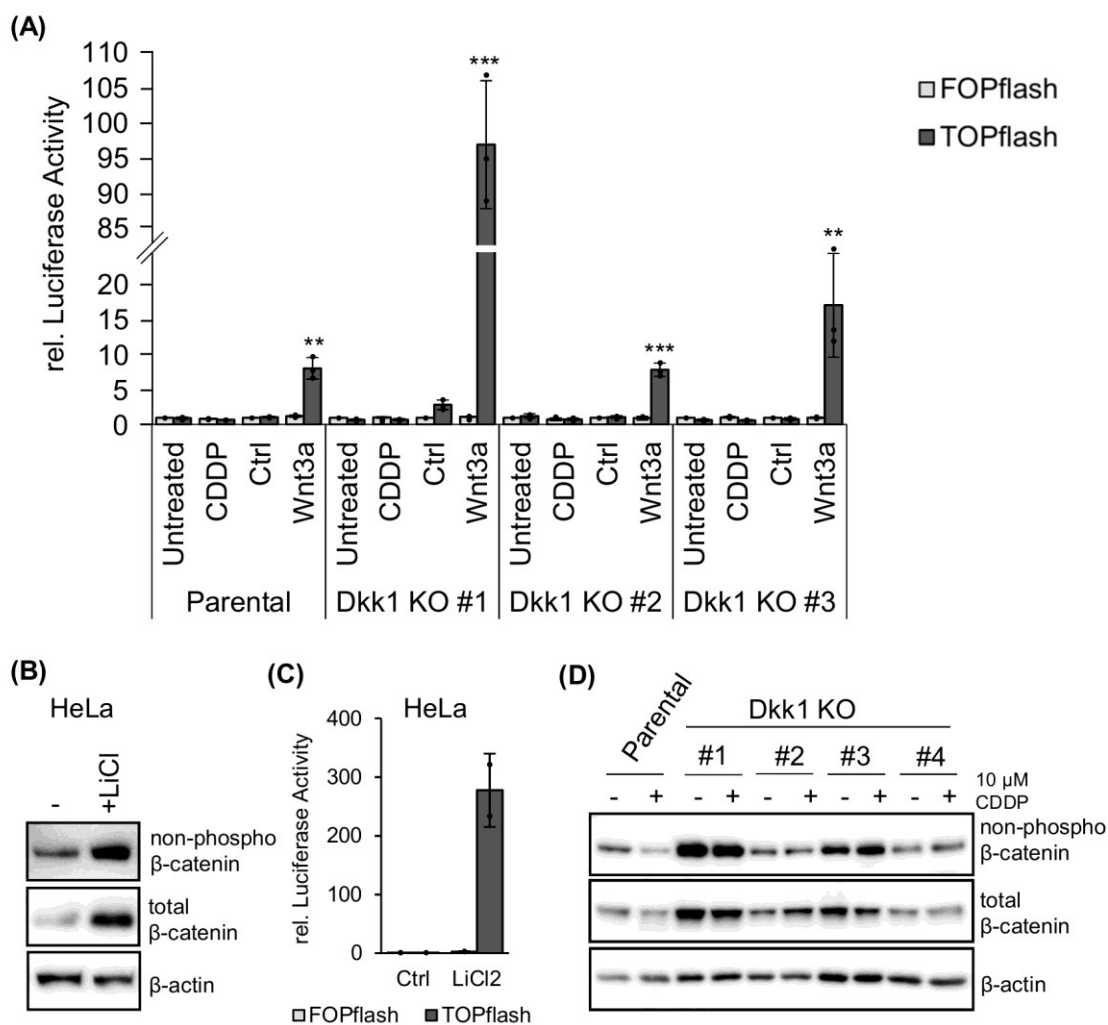


Figure 24 | Cisplatin does not affect canonical Wnt signaling activities in HeLa cells. (A) TOP-/FOPflash assays in parental HeLa and Dkk1 KO HeLa cells, which were either left untreated or treated for 16 h with 10 μM Cisplatin (CDDP), or transfected with the expression plasmid pcDNA3-Wnt3a (Wnt3a) or vector control pcDNA3 (Ctrl). Mean TOP-/FOPflash luciferase activities with standard deviations are indicated relative to the FOPflash activity of untreated or Ctrl-transfected cells, respectively. Statistical significances of Wnt3a-induced TOPflash activations are shown by asterisks (**: p<0.01, ***: p<0.001). (figure legend continued on next page)

(see figure on previous page)

(B) Parental HeLa cells were treated for 16 h with 10 mM LiCl and protein expression of unphosphorylated (non-phospho: active) β -catenin, as well as total β -catenin was analyzed by immunoblots. β -actin: loading control. (C) TOP-/FOPflash assays of parental HeLa cells treated with 10 mM LiCl. Mean luciferase activities with standard deviations (n=2) are shown relative to the FOPflash activity of untreated cells (Ctrl). (D) Immunoblots of untreated or CDDP-treated parental HeLa and Dkk1 KO HeLa cells depicting protein expression of unphosphorylated (non-phospho: active) and total β -catenin. β -actin: loading control.

To validate this observation further, I next assessed the expression of total β -catenin and non-phosphorylated β -catenin after Cisplatin treatment in immunoblots. Non-phosphorylated β -catenin represents the active form of the protein, which ultimately transduces Wnt activity to the induction of Wnt target genes.⁸⁴ In contrast to LiCl - a potent inducer of canonical Wnt signaling¹⁹⁰ which stabilized the expression levels of total and active β -catenin (Figure 24B) and increased TOPflash activities in parental HeLa cells (Figure 24C) - Cisplatin did not affect total or active β -catenin expression levels, neither in parental HeLa cells nor in any of the Dkk1 KO HeLa cells (Figure 24D).

In conclusion, these results support the notion that the protection of Dkk1-depleted cells towards Cisplatin is not linked to the induction of canonical Wnt activity in HeLa cells, which could have been caused by the evasion of this signaling cascade from Dkk1-mediated repression.

2.6 Affymetrix gene expression analyses of Cisplatin-treated HeLa cells

In order to further elucidate the regulatory role of Dkk1 in Cisplatin-mediated apoptosis in HeLa cells, gene expression profiles of parental HeLa cells and Dkk1 KO HeLa cells were assessed on Affymetrix GeneChips (Clariom™ S Assays). After extracting total RNA from the cells, transcriptome analyses were performed with the support by the DKFZ Microarray Unit of the Genomics and Proteomics Core Facility. Their service included quality controls, normalizations across all samples on the chip and the determination of differential gene expression.

2.6.1 Identification of global gene alterations

Parental HeLa cells and the cells of one selected Dkk1 KO HeLa clone - Dkk1 KO #3 - were treated according to the scheme in Figure 25A and differential gene expression was assessed by pairwise comparisons of the respective datasets. To get an overview of global transcriptional alterations, I generated volcano plots for all four comparisons (Figure 25A), which visualize the \log_2 -transformed fold changes (\log_2FC) of all 19525 genes from the chip relative to the negative decadic logarithm of the p-value as an indicator of statistical significance (Figures 25 B-E).

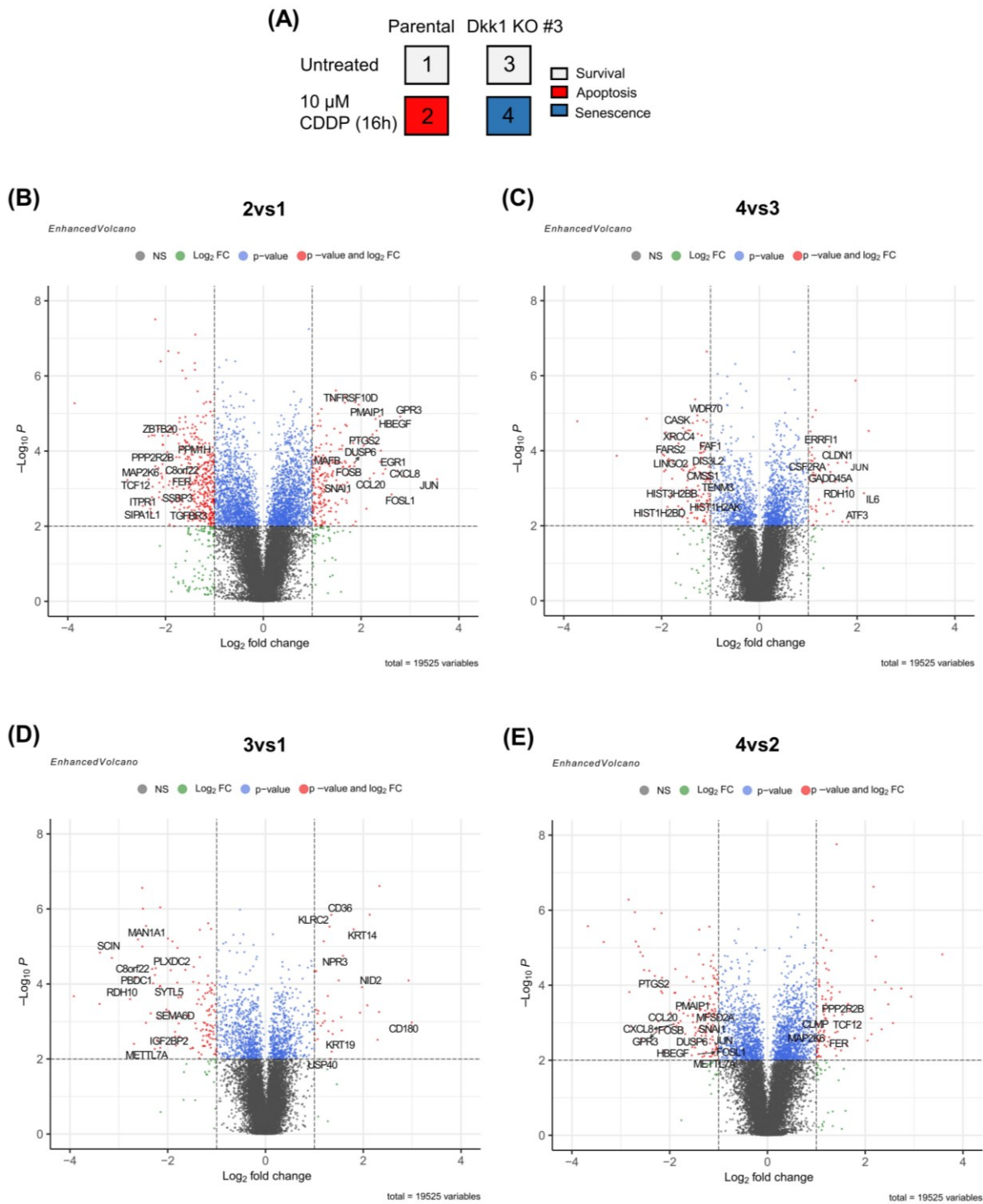


Figure 25 | Global gene alterations between Cisplatin-treated parental HeLa and Dkk1 KO HeLa cells. (A) Scheme of the experimental conditions for Affymetrix GeneChips analyses (Clariom™ S Assay) along with the respective phenotypic outcome. CDDP: Cisplatin. B)-E) Volcano plots for all pairwise comparisons of datasets. Each datapoint indicates the log₂-transformed fold change (log₂FC) of gene expression for a single gene in relation to its p-value (-log₁₀-transformed). Data cut-offs for log₂FC= |1| and p = 0.05 are depicted by dashed lines, sorting the data sets into four groups: non-significant (ns-grey), log₂FC ≥ |1| and p ≥ 0.05 (green), log₂FC < |1| and p < 0.05 (blue), log₂FC ≥ |1| and p < 0.05 (red). Gene labels indicate those genes, which were sorted based on their strongest differential regulation in between parental comparisons, as determined by Δlog₂FC, in order to exclude genes which are equally regulated in both parental HeLa and Dkk1 KO HeLa cells.

Comparison of Cisplatin-treated to untreated parental HeLa cells (2vs1) indicate major significant global transcriptional changes (Figure 25B), which was less pronounced in Dkk1 KO HeLa cells (4vs3) (Figure 25C). In more detail, in parental HeLa cells, the highlighted genes suggest the involvement of several signaling pathways in the apoptotic response to Cisplatin, as it covers genes from growth factor signaling (e.g. *GPR3*, *HBEGF*, *FER*),¹⁹¹⁻¹⁹³ inflammatory signaling (e.g. *PTGS2*, *CXCL8*, *TGFBR3*),¹⁹⁴ but also from apoptotic signaling (e.g. *PMAIP1*, *EGR1*, *TNFRSF10D*).^{127,131,195} Intriguingly, with *JUN*, *FOSL1* and *FOSB*, several members of AP-1 transcription factor complexes¹⁶² were strongly upregulated in parental HeLa cells (Figure 25B), and this effect was less noticeable in Dkk1 KO HeLa cells (Figure 25C).

A direct comparison of both untreated cell lines (3vs1) indicates that only a few number of genes was differentially, but significantly, expressed in a Dkk1-dependent manner (Figure 25D). These genes do not hint to a distinctive basal activation of a particular signaling pathway in Dkk1 KO HeLa cells and may be a result of the clonal heterogeneity of the CRISPR/Cas9-generated single cell clones.¹⁸⁹ Finally, the comparison of Cisplatin-treated Dkk1 KO HeLa cells to parental HeLa cells (4vs2) (Figure 25E) further reflects the observation that the AP-1 members *JUN*, *FOSL1* and *FOSB* were significantly lower induced in Cisplatin-treated Dkk1 KO HeLa cells compared to their parental cell line.

2.6.2 Differential activation of AP-1 signaling factors

Due to the functional role of the AP-1 complex in the induction of apoptosis,¹⁶² I decided to investigate in more detail the differential activation of this signaling pathway between parental HeLa and Dkk1 KO HeLa cells. Applying gene set enrichment analysis (GSEA)¹⁹⁶ of the Affymetrix dataset comparing Cisplatin-treated Dkk1 KO HeLa cells to parental HeLa cells (4vs2 according to Figure 25A) revealed that genes from the AP-1 transcription factor network (PID_AP1_Pathway)¹⁹⁷ were negatively enriched in Dkk1 KO HeLa cells with a normalized enrichment score (NES) of -2.05 (Figure 26A).

In total, 26 out of 69 genes from the above referenced pathway showed significant ($p < 0.05$) differential expression in this dataset. Considering all pairwise comparisons (Figure 26B), their regulation corroborates that the induction of the AP-1 members *JUN*, *ATF3*, *FOSL1*, *FOSB*, *FOS* and *JUNB* was decreased upon Cisplatin exposure in Dkk1-depleted cells compared to parental HeLa cells.

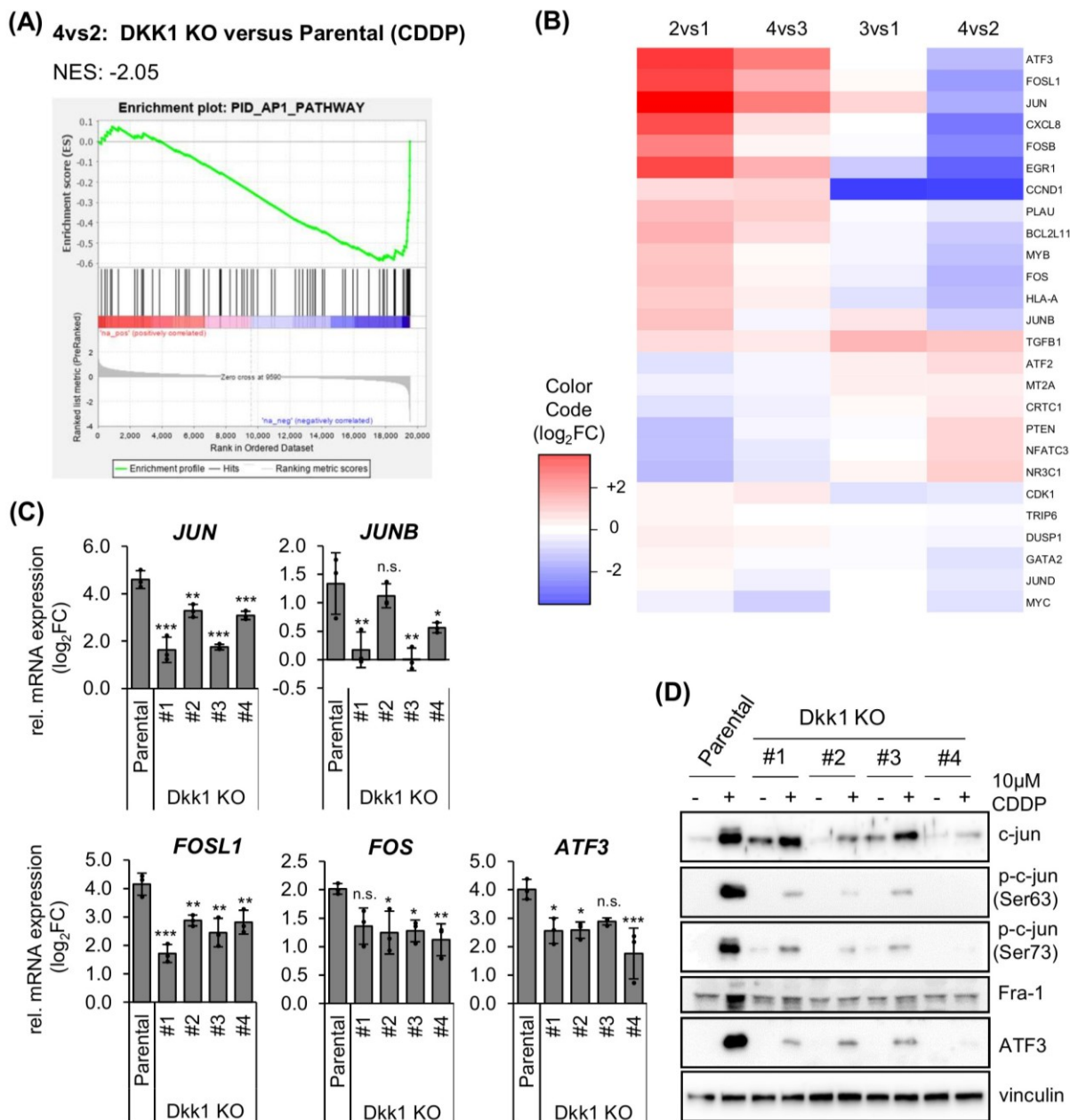


Figure 26 | Reduced activation of AP-1 signaling components in the Cisplatin response upon Dkk1 depletion. (A) Gene set enrichment analysis (GSEA)¹⁹⁶ of the PID_AP1_Pathway¹⁹⁷ comparing Cisplatin (CDDP)-treated Dkk1 KO HeLa cells to parental HeLa cells (4vs2 according to Figure 25A). NES: normalized enrichment score. (B) Heatmap of significantly ($p < 0.05$) regulated genes (4vs2) from the PID_AP-1_Pathway depicting \log_2 -transformed fold changes (\log_2FC) of those genes from all pairwise comparisons (according to Figure 25A). (C) Relative mRNA expression of AP-1 components *JUN*, *JUNB*, *FOSL1*, *FOS* and *ATF3* was analyzed by qRT-PCR for parental HeLa cells and all four Dkk1 KO clones after CDDP treatment (10 μ M, 16 h) relative to the respective untreated cells ($\log_2FC=0$). All data are indicated as mean \log_2FC with standard deviations and statistical significances of differential gene expression of Dkk1 KO HeLa cells compared to parental HeLa cells are depicted by asterisks (*: $p < 0.05$, **: $p < 0.01$, ***: $p < 0.001$, n.s.: not significant). (D) Protein expression of total c-Jun and its Ser63- and Ser73-phosphorylated forms, as well as of Fra-1 (encoded by *FOSL1*) and ATF3 were analyzed in parental HeLa and Dkk1 KO HeLa cells after CDDP exposure by immunoblots compared to untreated cells. Vinculin: loading control.

To validate that this effect was not a peculiarity of one selected Dkk1 KO clone, the transcript levels of *JUN*, *JUNB*, *FOSL1*, *FOS* and *ATF3* were next analyzed in all four Dkk1 KO HeLa cells after Cisplatin exposure compared to parental HeLa cells using qRT-PCR (Figure 26C). Although being indicated as differentially regulated by the gene expression analyses on Affymetrix GeneChips (Figure 26B), *FOSB* expression was undetectable in qRT-PCR in parental HeLa cells and was thus not included in these measurements. In accordance with the gene expression datasets for Dkk1 KO clone #3, the induction of the analyzed AP-1-related factors was less pronounced in all four Dkk1 KO clones on transcript level compared to parental HeLa cells. Immunoblots further indicate that Cisplatin strongly induced total and Ser63/73-phosphorylated c-Jun in parental HeLa cells, as well as ATF3 and Fra-1 which is the protein encoded by *FOSL1* (Figure 26D). In contrast, the induction of these proteins by Cisplatin was strongly reduced in all Dkk1 KO HeLa cells.

Overall, these data propose that the lack of Dkk1 in HeLa cells results in an impaired activation of the AP-1 signaling pathway by Cisplatin, which may be a potential reason for their resistance towards Cisplatin-induced apoptosis.

2.6.3 Validation of EGR-1 and Bim as potential AP-1 targets

Interestingly, the early growth response gene 1 (*EGR1*) and the transcript encoding the pro-apoptotic protein Bim (*BCL2L11*), which both were previously reported to be downstream effectors of AP-1 transcription factor complexes in the context of apoptosis,^{195,198} were regulated in parallel with the above analyzed AP-1 family members (Figure 26B). To further corroborate the hypothesis, that EGR1 and/or Bim are potential mediators of the Dkk1-dependent apoptotic response towards Cisplatin, I validated their protein and mRNA expressions after Cisplatin treatment in all Dkk1 KO HeLa cells compared to parental HeLa cells.

Alternative splicing of the Bim transcript *BCL2L11* leads to the formation of three major isoforms: Bim_{EL}, Bim_L and Bim_S.¹⁹⁹ In parental HeLa cells, Cisplatin strongly induced the protein levels of all three isoforms (Figure 27A), which was less pronounced in clone #2 and completely abolished in the other three Dkk1 KO clones. Notably, the Dkk1 KO clones #1 and #3 even showed a reduction of the Bim_S isoform, which accounts for the most potent variant in inducing apoptosis.¹⁹⁹ Moreover, in parental HeLa cells, for Bim_{EL} and Bim_L, a second protein band with a slightly higher apparent molecular weight was detectable, which might indicate the presence of post-translational modifications, such as phosphorylation.²⁰⁰ Contrarily, the appearance of these additional, higher migrating protein bands was also undetectable in all Dkk1 KO clones. The validation of

Bim-encoding *BCL2L11* transcripts support these results as their induction was significantly reduced in Dkk1-depleted cells (Figure 27B).

Cisplatin also strongly induced EGR1 expression on the protein (Figure 27A) and on the transcript level (Figure 27B) in parental HeLa cells, which was less pronounced in Dkk1 KO clones #1, #3 and #4, but not in clone #2.

For both, Bim and EGR1, further studies are warranted to assess their potential role in the differential response of parental HeLa and Dkk1 KO HeLa cells towards the pro-apoptotic effect of Cisplatin. Particularly Bim may represent an interesting factor for mediating the Dkk1-dependent effects on Cisplatin-induced apoptosis in cervical cancer cells, as the reduced induction of all Bim isoforms was conserved in all Dkk1 KO clones compared to parental HeLa cells.

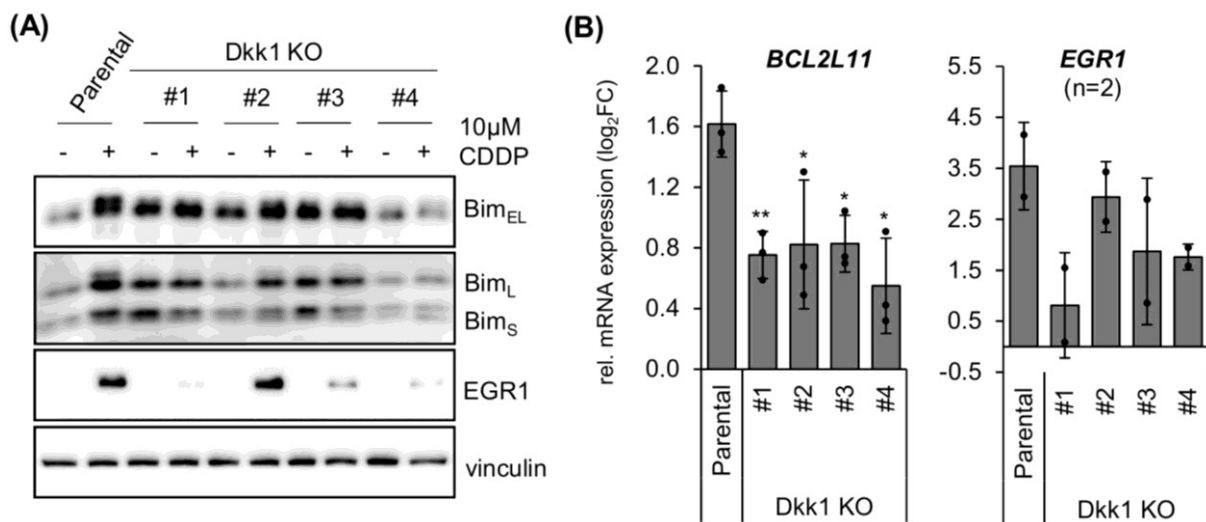


Figure 27 | Validation of Bim and EGR1 expression after Cisplatin treatment. (A) Immunoblot analyses of Bim (Bim_{EL}, Bim_L, Bim_S isoforms) and EGR1 protein expression in untreated and Cisplatin-treated parental HeLa and Dkk1 KO HeLa cells. Vinculin: loading control. (B) qRT-PCR analyses of *BCL2L11* (encoding Bim) (left panel) and *EGR1* (right panel) mRNA expression in cells treated as described above. Depicted are mean log₂-transformed fold change (log₂FC) expressions with standard deviations, relative to untreated cells (log₂FC=0). For *BCL2L11*, statistical significances of the differential expression of Dkk1 KO HeLa cells compared to parental HeLa cells are indicated by asterisks (*: p < 0.05, **: p < 0.01).

2.7 The role of JNK signaling in the Dkk1-dependent Cisplatin response

The previous findings revealed that Cisplatin-induced c-Jun phosphorylation on Ser63 and Ser73 was strongly reduced in Dkk1-depleted HeLa cells compared to parental HeLa cells (Figure 26D). As this modification is mediated by the MAPK JNK,¹⁵¹ the finding raised the question whether JNK, as a major upstream AP-1 regulator,²⁰¹ may also be a critical regulator in the Dkk1-dependent Cisplatin response in cervical cancer cells.

2.7.1 JNK activation is required for Cisplatin-induced apoptosis in HeLa cells

To investigate the potential role of JNK in mediating the differential, Dkk1-dependent Cisplatin response in HeLa cells, I first analyzed JNK activation levels, by means of the phosphorylation of its p54 and p46 isoforms, in Cisplatin-treated parental HeLa and Dkk1 KO HeLa cells. In accordance with the increased c-Jun phosphorylation (Figure 26D), JNK was also strongly phosphorylated in parental HeLa cells by Cisplatin (Figure 28A). This effect was substantially reduced in HeLa Dkk1 KO clones #1-#4. In contrast, total JNK protein levels remained unaffected and did not differ in between parental HeLa and Dkk1 KO HeLa cells.

To further study the consequences of an impaired JNK activation for Cisplatin-induced apoptosis, I next blocked JNK signaling in HeLa cells, either by transfection of a well-characterized JNK1/2-targeting siRNA²⁰² or by treatment with JNK-IN-8, a selective pan-inhibitor for JNK1, JNK2 and JNK3.²⁰³ Since JNK3 isoform expression is restricted to brain, heart and testis, I focused on the analysis of JNK1 and JNK2, which are ubiquitously expressed.¹⁵⁵

RNAi-mediated depletion of JNK1/2 efficiently repressed total JNK levels and, compared to siCtrl-transfected cells, blocked JNK phosphorylation after treatment with 10 or 15 μ M Cisplatin (Figure 28B). In contrast, the JNK inhibitor did not affect JNK expression levels nor the induction of its phosphorylation by Cisplatin, as it interferes with the catalytic site of JNKs.²⁰³

Both, RNAi-induced JNK1/2 repression and chemical JNK inhibition, prohibited the Cisplatin-induced Ser63/Ser73-phosphorylation of c-Jun and, in parallel, strongly restrained apoptosis induction, as indicated by decreased cl. PARP and cl. Caspase 9 levels (Figure 28B). In line with this observation, TUNEL assays revealed that the number of apoptotic cells was strongly reduced when JNK activity was impaired by both, genetic or chemical inhibition (Figures 28C, 28D).

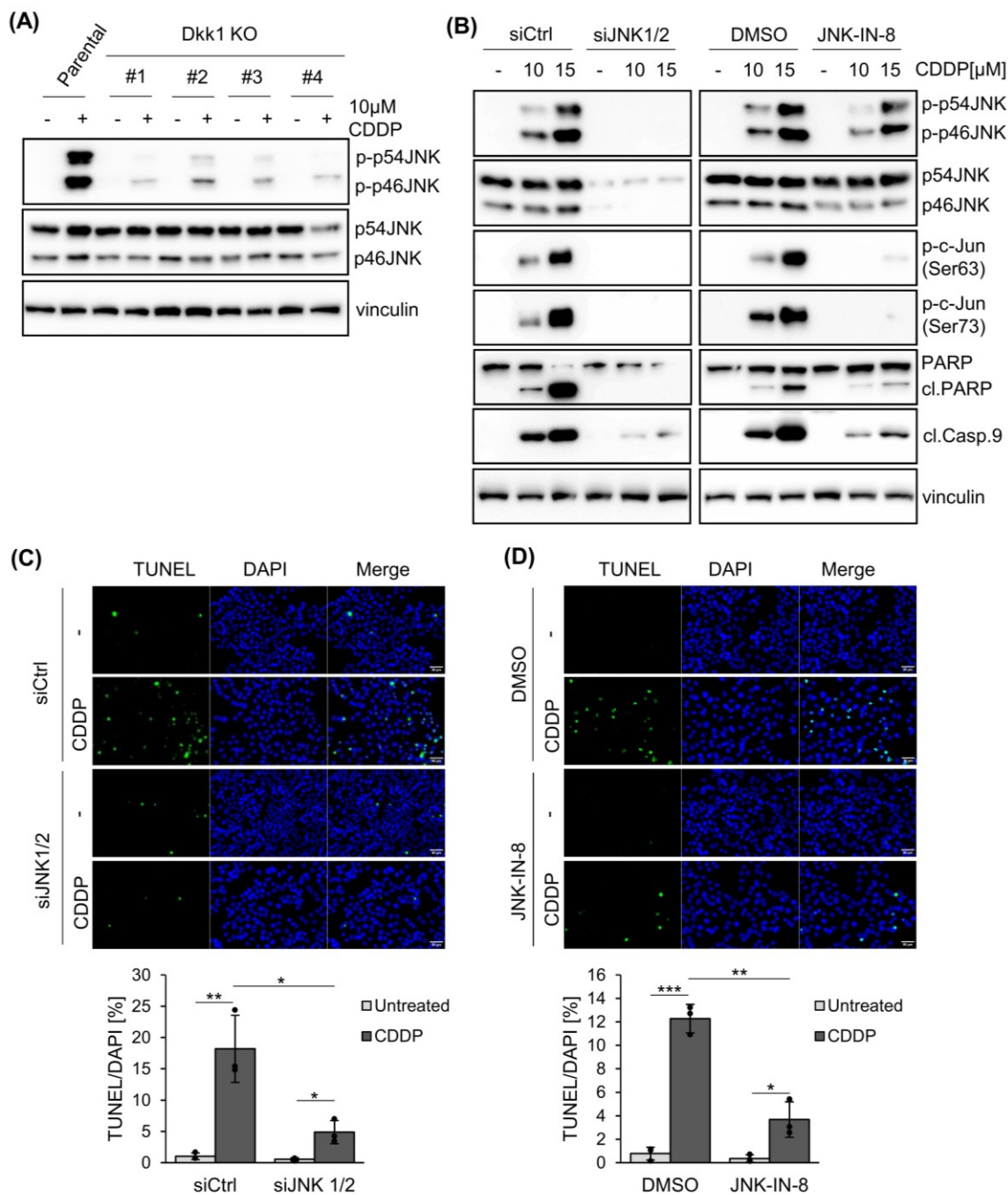


Figure 28| Impaired JNK activation in Dkk1-depleted HeLa cells contributes to Cisplatin resistance. (A) Cisplatin (CDDP)-treated and untreated parental HeLa and Dkk1 KO HeLa cells were analyzed by immunoblots for phosphorylated (p-) p46 and p54 JNK isoforms as well as total p46/p54 JNK. Vinculin: loading control. (B) HeLa cells were treated for 20 h with two doses of CDDP after transfection with control siRNA (siCtrl) or JNK1/2-targeting siRNA (siJNK1/2) (left panel) or concomitant treatment with solvent control (DMSO) or 1 μM of the JNK inhibitor JNK-IN-8 (right panel). Protein levels of phosphorylated (p-) and total p46/p54 JNK isoforms, p-c-Jun (Ser63), p-c-Jun (Ser73), PARP (cleaved (cl.) and uncleaved forms), as well as of cl. Caspase 9 (Casp.9) were analyzed by immunoblots. Vinculin: loading control. (C) TUNEL assays of siCtrl- and siJNK1/2-transfected untreated or CDDP-treated (15 μM) HeLa cells (scale bar: 50 μm) (upper panel). TUNEL-positive cells were quantified relative to the total cell number (indicated by number of DAPI stainings) and depicted are the mean percentages with standard deviations (lower panel). Asterisks represent statistical significances (*: p<0.05, **: p<0.01). (D) TUNEL assays of HeLa cells which were treated with 15 μM Cisplatin or left untreated in the presence of solvent control (DMSO) or 1 μM JNK-IN-8 (scale bar: 50 μm) (upper panel). Quantifications were performed as described above (***: p<0.001) (lower panel).

In more detail, Cisplatin treatment and concomitant RNAi-induced JNK1/2 silencing (Figure 28C) or JNK-IN-8 treatment (Figure 28D) resulted in a ~3.8-fold or ~3.4-fold decrease of apoptotic cells compared to Cisplatin exposure alone, respectively.

Collectively, these results indicate that the reduction of Cisplatin-induced JNK activation, which was observed in Dkk1-depleted HeLa cells, enhances their resistance towards Cisplatin-induced apoptosis.

2.7.2 JNK signaling in Cisplatin-mediated apoptosis in SiHa and CaSki cells

Cisplatin resistance upon RNAi-induced Dkk1 silencing was not a peculiarity of HeLa cells and was also observed in SiHa and CaSki cervical cancer cells (Figure 20). Thus, I aimed to investigate whether the interference with JNK activity is also linked to an increase in apoptosis resistance towards Cisplatin in these two cell lines. To this end, two different doses of Cisplatin were applied to SiHa and CaSki cells, which were either previously transfected with siJNK1/2 or co-treated with JNK-IN-8.

In siCtrl-transfected cells, Cisplatin efficiently induced JNK p46 and p54 phosphorylation in both cell lines while the expression levels of the total protein remained unaffected for both JNK isoforms (Figures 29A). Moreover, Ser63 and Ser73 phosphorylation of c-Jun was increased and in parallel, the expression of cl. PARP and cl. Caspase 9 enhanced, indicating an efficient induction of apoptosis. In line with the findings in HeLa cells (Figure 28), these effects were strongly reduced upon RNAi-mediated JNK1/2 silencing in SiHa and CaSki cells (Figure 29A).

Similarly, chemical JNK inhibition, which prohibited JNK-mediated phosphorylation of c-Jun on Ser63 and Ser73 by Cisplatin, also diminished the increase in cl. PARP and cl. Caspase 9 levels in both SiHa and CaSki cells (Figure 29B), indicating protection from apoptosis. In accordance, TUNEL assays in SiHa cells revealed a significant decrease in the number of apoptotic cells when Cisplatin treatment was combined with the chemical JNK inhibitor (Figure 29C).

Based on these results, it can be concluded that JNK activation plays a critical role for Cisplatin-induced apoptosis not only in HeLa, but also in SiHa and CaSki cells and that overall, by interfering with pro-apoptotic JNK activation, Dkk1 repression provides cervical cancer cells with increased resistance towards Cisplatin-induced apoptosis.

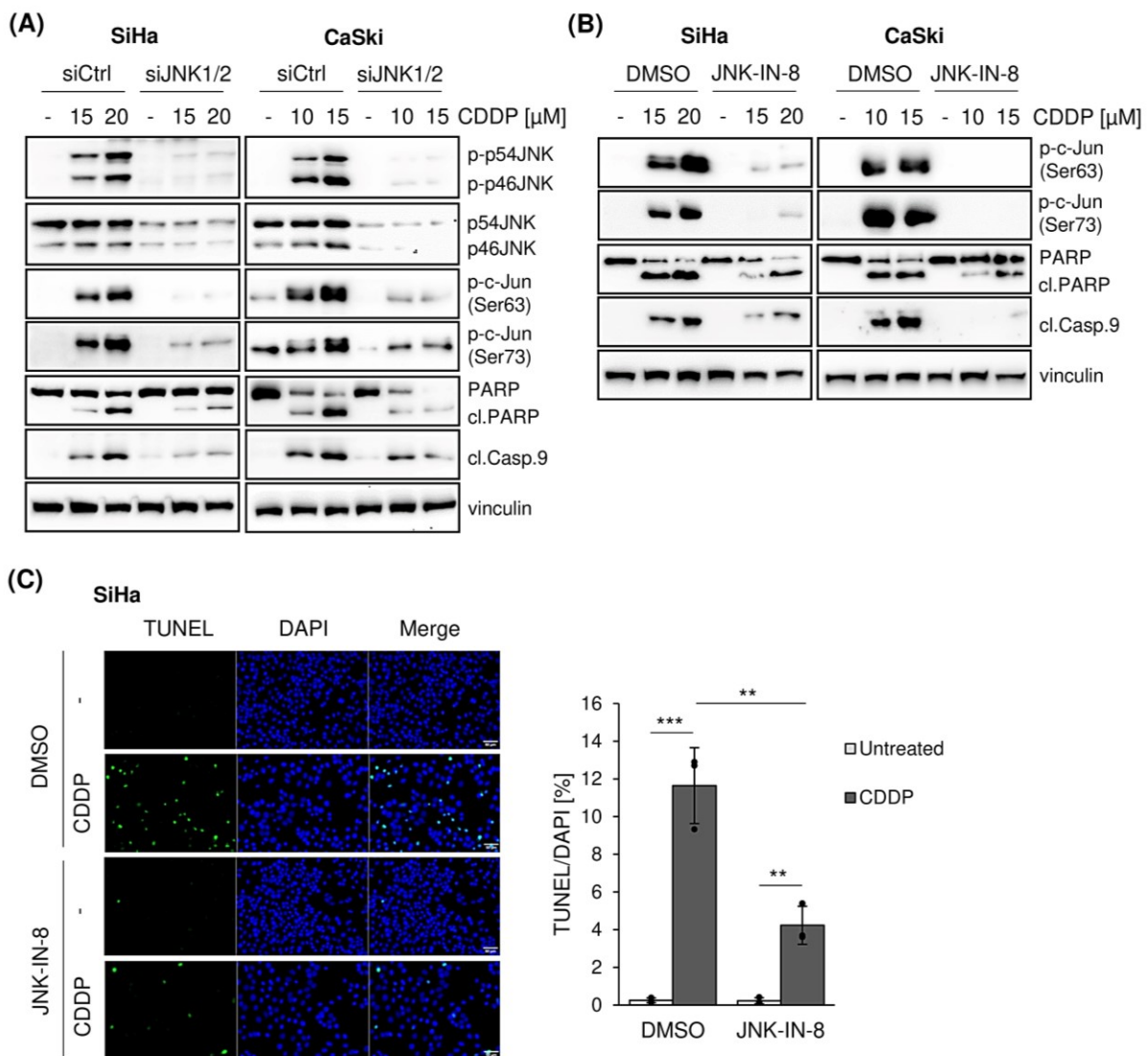


Figure 29 | JNK activity is required for Cisplatin-induced apoptosis in SiHa and Caski cells. (A) SiHa (left panel) and CaSki cells (right panel) were transfected with control siRNA (siCtrl) or JNK1/2-specific siRNA (siJNK1/2) and treated with two doses of Cisplatin (CDDP) for 32 h or 20 h, respectively. Immunoblot analyses show protein expression of phosphorylated (p)-p46 and p54 JNK isoforms, total p46/p54 JNK, p-c-Jun (Ser63), p-c-Jun (Ser73), PARP (cleaved (cl.) and uncleaved forms), as well as of cl. Caspase 9 (Casp.9). Vinculin: Loading control. (B) Cisplatin treatment was combined with the treatment of SiHa (left panel) and CaSki cells (right panel) with 1 μ M JNK-IN-8 or DMSO as a solvent control. Protein levels of p-c-Jun (Ser63), p-c-Jun (Ser73), PARP (cl. and uncleaved forms), as well as of cl. Casp. 9 were analyzed by immunoblots. Vinculin: loading control. (C) TUNEL assays of SiHa cells treated with 15 μ M Cisplatin in the presence of 1 μ M JNK-IN-8 or solvent control (DMSO) as described above (scale bar: 50 μ m) (left panel). Mean percentages of TUNEL-positive cells relative to DAPI stainings (representing the total number of cells) are indicated with standard deviations (right panel) and statistical significances are represented by asterisks (**: $p < 0.01$, ***: $p < 0.001$).

CHAPTER 3
DISCUSSION

3. Discussion

Sustained expression of the HPV *E6/E7* oncogenes drives the malignant growth of cervical cancers. Via their interference with major tumor suppressive signaling pathways, E6 and E7 play a central role in inducing an unscheduled cell cycle progression along with the protection of genome integrity from stress- or damage-induced signals.³⁰ My thesis revealed that Dkk1 is a novel, indirect target of the HPV oncogenes, with HPV E6 being a key mediator of its repression in cervical cancer cells. Moreover, it was uncovered that Dkk1 plays a major role in the apoptotic response towards Cisplatin in cervical cancer cells, as Dkk1 depletion protects against Cisplatin-induced apoptosis by modulating JNK/AP-1 signaling.

3.1 Dkk1 expression in cervical cancer cells

3.1.1 HPV-oncogene driven Dkk1 repression

RNAi-mediated silencing of the HPV *E6/E7* oncogenes was associated with an intracellular increase of Dkk1 expression on the protein and transcript level in HPV18-positive HeLa as well as in HPV16-positive SiHa and CaSki cells. This was accompanied by an increase of secreted Dkk1 in the cell supernatant, which is interesting, as Dkk1 is known to exert its signaling functions via extracellular interactions with plasma membrane receptors.⁷⁴ Therefore, these results suggest that the continuous expression of the HPV oncogenes restricts Dkk1 concentrations in cervical cancer cells, and consequently also its active role in signal transduction pathways. Notably, Dkk1 induction upon E6 or E6/E7 repression was dependent on p53 stabilization in cervical cancer cells, since it was abolished upon concomitant RNAi-induced silencing of p53. Based on the key role of HPV E6 in p53 degradation, this finding indicates that E6 is the main driver of Dkk1 repression, which is further supported by the notion that E6 silencing alone is sufficient to release Dkk1 from the negative control by the HPV oncogenes.

The present work is the first to show a connection of HPV oncogene expression and Dkk1 levels in cervical cancer cells. Previous studies presented inconsistent data regarding Dkk1 expression in cervical cancer and other HPV-positive cancer entities: On the one hand, Dkk1 was reported to be epigenetically silenced in cervical cancers,¹¹¹ while on the other hand, cervical cancer patients were shown to have elevated Dkk1 serum levels.²⁰⁴ Moreover, a recent study proposed that elevated Dkk1 expression is positively correlated with the HPV status of penile cancer cells and that enhanced Dkk1 levels are associated with an increased aggressiveness of the tumor.²⁰⁵ These discrepancies might be explainable by several aspects, including the choice of cell lines or tissues

for analysis. Importantly, enhanced Dkk1 expression may not necessarily be directly linked to oncogenic activities, as for instance it is thinkable that cells could induce tumor suppressive factors in an attempt to compensate oncogenic stimuli.

Divergent reports concerning Dkk1 expression have also been reported for other cancer entities. For instance, in breast cancer, Dkk1 is primarily regarded as a tumor suppressor,²⁰⁶ however whether Dkk1 is up- or downregulated compared to untransformed cells varies in between cell lines and further depends on the tumor stage and the subtype of cancer.^{206,207} Importantly, in the present work, cervical cancer cells expressing two different HPV types (HPV18 and HPV16) were used. These are derived from distinct histological origins which further differ in their molecular profiles, as HeLa cells have been originally acquired from an adenocarcinoma and SiHa and CaSki cells from squamous cell carcinomas.^{208,209} Consequently, this suggests that the interrelation between HPV oncogene and Dkk1 expression is conserved between different oncogenic HPV types and takes place in cervical carcinoma cells derived from different histological backgrounds.

3.1.2 Dkk1 expression in hypoxic cervical cancer cells

Surprisingly, siE6/E7-mediated Dkk1 induction at normoxic conditions differs from the observation that, under hypoxia, Dkk1 is downregulated despite an efficient repression of the HPV oncogenes.⁵⁵ Further validation studies in this thesis revealed that Dkk1 was repressed after 24 h of hypoxic cultivation in HeLa and CaSki cells, as well as in HPV-negative A549 lung cancer and HCT116 colon cancer cells, indicating that hypoxic Dkk1 downregulation is not a peculiarity of HPV oncogene-expressing cells. Moreover, cell line-dependent discrepancies in the effect of increased glucose availability and AKT inhibition on Dkk1 expression, which both are known to counteract hypoxic E6/E7 repression in a panel of cervical cancer cells,⁵⁵ further argue against a direct correlation of Dkk1 and HPV oncogene expression under hypoxia.

Although Dkk1 has emerged as an important factor in cancer development and progression, only few studies have focused on its hypoxic regulation. In line with the hypoxic Dkk1 repression observed in the present work, a study in osteoblasts also revealed a decrease of Dkk1 protein and mRNA expression at 1 % O₂, which was recuperated after prolonged treatments.²¹⁰ Additionally, when U87MG glioma and bone marrow-derived mesenchymal stem cells were cultivated for three days under hypoxia, Dkk1 levels were increased.²¹¹ Interestingly, this recuperation of Dkk1 expression was also observed in the present study in HeLa cells after hypoxic treatments for up to 48 h, while HPV E6/E7 levels remained suppressed. Hence, my findings support the concept of a

biphasic Dkk1 regulation under hypoxia. However, this regulation may also be to some extent cell type and context-dependent, as for instance in multiple myeloma cells, Dkk1 expression was shown to increase already after short term hypoxic treatments of 6 to 24 h.²¹²

In the present study, HIF-1 α expression was in part regulated in parallel with Dkk1 under hypoxia: After a rapid initial increase, HIF-1 α protein levels decreased along with those of Dkk1 and they were also re-induced after 48 h. As a major transcription factor under hypoxic conditions, HIF-1 α drives gene expression by binding to hypoxia response elements (HREs) in gene promoters.⁵¹ Although a HRE consensus site (5'-A/GCGTG-3') can be found ~ 1 kb upstream of the transcription start site in the Dkk1 promoter which was described by Wang et al.,¹¹⁴ it is so far unknown whether HIF-1 α is a direct upstream regulator of Dkk1. It was however reported, that HIF-1 α -dependent activation of the histone methyltransferase MMSET can modify histone methylation at the Dkk1 promoter region and thereby can enhance its transcription under hypoxic conditions.²¹²

My results further showed that hypoxic Dkk1 repression was dependent on glucose availability in both HPV-positive and HPV-negative cell lines. Interestingly, chemical OXPHOS inhibition under normoxic conditions also repressed Dkk1 levels in a glucose-dependent manner in HeLa and SiHa cells, suggesting that Dkk1 downregulation under hypoxia could be an indirect consequence of the hypoxic switch from OXPHOS to increased glycolysis. As this switch is to a great extent supported by the HIF-1 α -mediated induction of glycolysis-related factors,⁵² this finding provides another possible explanation for the parallel hypoxic regulation of Dkk1 with HIF-1 α by an indirect effect of HIF-1 α -mediated metabolic adaptations to the hypoxic environment.

Collectively, several results obtained in this thesis suggest that Dkk1 regulation under hypoxia is uncoupled from the HPV oncogene-driven control observed under normoxia. Although the detailed mechanisms, which drive the biphasic regulation of Dkk1 under hypoxia remain to be elucidated, global cellular adaptations to the hypoxic environment may act dominant over E6-induced Dkk1 repression in cervical cancer cells.

3.1.3 The role of p53 in regulating Dkk1 expression

DKK1 was previously reported to be a transcriptional target gene for p53, as it contains a p53 response element which was bound by wildtype p53 and ectopic p53 expression further induced the activity of the *DKK1* promoter.¹¹⁴ Consequently, my finding that Dkk1 induction after RNAi-mediated silencing of E6 or E6/E7 was dependent on the release of p53 from its E6-induced negative regulation suggests that p53 is a key driver of Dkk1 expression in cervical cancer cells.

It should be noted that not every potential p53 target gene is under the control of E6 in cervical cancer cells. More specifically, although approximately 3500 genes are postulated to be p53 target genes,¹³⁹ HPV oncogene silencing affects only the expression of a small subset of those genes.^{213,214} One possible explanation for this observation could be that a significant number of the so-called p53-responsive genes was identified by ectopic overexpression of p53, which may have resulted in unphysiologically high p53 levels. In this context, it is important to note that the cellular abundance of p53 determines its binding to low- or high-affinity gene promoters,²¹⁵ thereby triggering a differential transactivation of genes, which further may result in different phenotypic outcomes.²¹⁶ However, the present work clearly shows that *Dkk1* represents a relevant p53 target gene in HPV-positive cervical cancer cells, which is restrained via the E6 oncoprotein and reactivated by the endogenous p53 amounts that are reconstituted after the release from the E6-dependent negative regulation.

In contrast to the clear role of p53 in HPV-oncogene driven *Dkk1* repression under normoxic conditions, the significance of p53 for the regulation of *Dkk1* under hypoxia remains ambiguous. Several results from this thesis disclosed similarities between *Dkk1* and p53 levels under hypoxia: The expression of both factors was uncoupled from the negative regulation by HPV E6 and they further exhibited a parallel expression pattern in a time course experiment under hypoxia, as they were both transiently repressed after short-term hypoxic treatments and re-induced after long-term treatments. However, silencing of p53 using RNAi in combination with hypoxia revealed discrepant results regarding hypoxic *Dkk1* expression on the protein and RNA level. Immunoblot analyses suggested that the recuperation of *Dkk1* after a pro-longed hypoxic exposure is dependent on p53. However, *DKK1* transcript levels were efficiently re-induced despite p53 silencing, which would be counterintuitive if *DKK1* is transcriptionally driven by p53. An earlier study reporting a biphasic regulation of p53 under hypoxia showed that its induction after prolonged exposure to 1 % O₂ resulted in the parallel increase of several p53-responsive genes,¹⁷⁸ indicating that p53 can be transcriptionally active under these conditions, although this activity was not required for *DKK1* activation in the present study.

Collectively, my results suggest that in contrast to the key role for p53 in activating *Dkk1* expression under normoxia, *Dkk1* transcript levels may be regulated under hypoxia via p53-independent mechanisms. These could include Wnt-related feedback loops⁸⁸ or epigenetic alterations,¹¹¹ which both have previously been linked to the regulation of *Dkk1* expression.

3.1.4 Epigenetic Dkk1 regulation

In the present investigations, the treatment of HeLa, SiHa and CaSki cells with the HDAC inhibitor TSA was consistently shown to induce Dkk1 expression at normoxic conditions and therefore suggests that in addition to HPV oncogene-mediated Dkk1 repression, Dkk1 is also downregulated in cervical cancer cells by the means of histone deacetylation.

In contrast, exposure to the hypomethylating agent 5-Azacytidine resulted in cell-line dependent effects. In HeLa cells, Dkk1 concentrations remained largely unaffected, while in SiHa cells Dkk1 protein and RNA expression were strongly increased. In contrast, Dkk1 levels were greatly reduced in 5-Azacytidine-treated CaSki cells, which is counterintuitive as DNA methylation is usually associated to gene silencing¹⁷⁹ and therefore, chemical inhibition of this epigenetic mark would be expected to increase gene transcription. The Dkk1 promoter contains three CpG islands¹¹¹ which in theory can be methylated by DNMTs.¹⁷⁹ An earlier study revealed that Dkk1 promoter methylation is indeed increased in exfoliated cells of cervical cell carcinomas compared to healthy cervical cells.²¹⁷ However, *in vitro* analyses in cervical cancer cells indicated that of the three analysed cell lines in this thesis, only HeLa cells, but not SiHa and CaSki cells, were characterized by an increased methylation of the CpG islands in the Dkk1 promoter.¹¹¹ If 5-Azacytidine was specifically prohibiting DNA methylation, it should therefore not affect Dkk1 expression in the two latter cell lines, which was, however, observed in the present work. Hence, the respective up- or downregulation of Dkk1 in SiHa or CaSki cells may be due to indirect effects mediated by other 5-Azacytidine-affected genes. In accordance, 5-Azacytidine can affect the expression of genes with originally unmethylated promoters, as described by Komashko et al. (2010),²¹⁸ who found that the exposure of cells to 5-Azacytidine unspecifically increased the global levels of repressive histone H3 methylation marks. This may result in histone-methylation- but not DNA-methylation-dependent epigenetic effects on gene expression.

The histone methyltransferase enhancer of zeste homolog 2 (EZH2), which catalyzes the trimethylation of the lysine residue 27 of histone 3 (H3K27me3),²¹⁹ represents a potential enzyme being involved in epigenetic Dkk1 repression. Its recruitment to the Dkk1 promoter was associated to an increase of H3K27me3 marks in this region and its expression restricted the amounts of Dkk1 levels in lung cancer cells.²²⁰ An enhanced occupancy of H3K27me3 upon binding of EZH2 to the Dkk1 promoter region was also reported for CaSki cervical cancer cells, which was dependent on the expression of the long noncoding RNA *SNHG7*.²²¹ Interestingly, EZH2 expression is known to be induced by the HPV E7-mediated release of E2F transcription factors in cervical cancer cells,²²²

and thus may present a link between HPV oncogene-mediated and epigenetic modulation of Dkk1 expression beyond the E6/p53/Dkk1 axis, which was identified in this thesis.

HPV E6 and E7 were both further reported to interact with the histone acetyltransferase p300/CBP,²²³ which was proposed to activate Dkk1 expression.²²⁴ This correlation of histone acetylation and Dkk1 activation is in line with the finding from the present work, showing that histone deacetylation restricts Dkk1 levels in cervical cancer cells. Notably, HPV E6 was described to interfere with the catalytic activity of p300/CBP and thereby also to decrease the p300-dependent transactivation of p53-responsive genes.²²⁵ Hence, an additional involvement of p300/CBP for the E6-induced Dkk1 repression via its interference with p53 function provides a starting point for future investigations about the regulatory principles behind the control of Dkk1 expression in cervical cancer cells, linking HPV oncogene expression to epigenetic mechanisms.

In contrast to their effects on Dkk1 expression under normoxia, at hypoxic conditions, 5-Azacytidine or TSA did not affect Dkk1 repression in HeLa, SiHa or CaSki cells at least at the herein tested conditions. This indicates that hypoxic Dkk1 downregulation is probably independent from histone deacetylation or DNA methylation, potentially due to the altered epigenetic mechanisms at low oxygen concentrations.²²⁶

3.2 The pro-apoptotic role of Dkk1 in the Cisplatin response of cervical cancer cells

3.2.1 Cisplatin-induced Dkk1 induction and apoptosis

Previous studies indicated that Dkk1 can respond to a variety of pro-apoptotic and DNA-damaging agents, such as UV radiation, hydrogen peroxide or ceramide, and to chemotherapeutic compounds including Doxorubicin, Camptothecin and Cisplatin.^{98,114,115,118} In line, the present work showed that Dkk1 expression was induced on the protein and RNA level in cervical cancer cells by Cisplatin treatment, although this effect was influenced in a cell- and concentration-dependent manner. When HeLa cells were exposed to Cisplatin doses which only slightly induced apoptosis, Dkk1 expression was strongly enhanced. In contrast, higher concentrations, resulting in more severe apoptosis rates, did not affect Dkk1 expression. This latter finding may be explained by the fact that in its advanced stages, apoptosis can lead to a global decrease of cellular protein concentrations due to an enhanced mRNA decay and translation inhibition.²²⁷ These mechanisms could account for the reduced Dkk1 expression levels at late stages of apoptosis besides its potential involvement in Cisplatin-induced apoptosis at earlier stages.

While Cisplatin treatment consistently induced Dkk1 levels in CaSki cells, protein analyses of SiHa cells demonstrated even more pronounced differences of Dkk1 expression in the response to Cisplatin in this thesis. In initial experiments, 24 h of Cisplatin exposure reduced Dkk1 levels irrespective of apoptosis induction in these cells, but in experiments combining RNAi with Cisplatin treatment, the chemotherapeutic agent efficiently induced Dkk1 protein concentrations. This suggests that differences in the experimental setup account for the discrepancies in Dkk1 expression levels. First of all, in the RNAi experiments, SiHa cells were treated for 32 h instead of 24 h with Cisplatin, which may affect overall Dkk1 concentrations similarly to the time-dependent Dkk1 regulation observed under hypoxic treatments. Moreover, during the transfection process, medium was exchanged multiple times, which may have resulted in a different metabolic state of the cells when initiating the exposure to Cisplatin. As found in the present studies, Dkk1 expression strongly relies on the availability of glucose, as it was restricted by OXPHOS inhibition in a glucose-dependent manner under normoxia, and under hypoxia, Dkk1 repression was counteracted by high glucose concentrations. Importantly, apoptosis is an energy-demanding process¹³² and may therefore be associated with an increased glucose consumption, which could result in Dkk1 downregulation at late stages.

The dependence of Dkk1 expression on the cellular glucose metabolism might also be of significance for the effects of pro-apoptotic metabolic agents such as OXPHOS inhibitors. If these were used in combination with Cisplatin, Dkk1 concentrations may be reduced, which could potentially interfere with their pro-apoptotic function. As an example, our group has identified the antifungal agent Ciclopirox (CPX) to induce apoptosis in HPV-positive cancer cells.²²⁸ However, CPX exerts its pro-apoptotic effect by its OXPHOS inhibiting properties,²²⁹ which - according to the findings from this thesis - rather result in Dkk1 repression in cervical cancer cells. It will be therefore be interesting to investigate in future studies whether Dkk1 expression levels may also determine the cellular response to other therapeutic agents, including metabolic drugs such as CPX.

Importantly, the observed discrepancies in Dkk1 levels upon Cisplatin exposure may be explicable by its dynamic expression pattern dependent on the cellular metabolism and therefore do not necessarily exclude its involvement in Cisplatin-induced apoptosis which was clearly determined in the present studies by Dkk1 depletion (discussed in chapter 3.2.2) or treatment with Dkk1 CM. Therefore, my results further strongly support the tumor suppressive role of Dkk1 in cervical cancer cells, which was originally proposed by Mikheev et al. (2004): By injecting HeLa cells with

ectopic Dkk1 expression into nude mice, they showed that tumor formation required the loss of Dkk1 and that Dkk1 expression further enhanced the sensitivity of these cells towards UV-induced apoptosis.¹¹⁸

Cisplatin treatment of HeLa cells in combination with Dkk1 CM medium was shown to enhance apoptosis rates, which not only emphasizes the pro-apoptotic role of Dkk1 in cervical cancer cells, but also supports that Dkk1 exerts its signaling functions in its secreted form via extracellular binding to cell surface receptors. It remains to be studied which receptors are involved in the transmission of the Dkk1-induced pro-apoptotic signals. Upon binding to its prototypic Lrp5/6 and Fzd or Kremen receptors, the Dkk1-receptor complexes are known to be internalized by endocytosis.^{92,93} My observation that Dkk1 CM treatment of HeLa cells resulted in the intracellular accumulation of Dkk1 argues for an involvement of these receptors in Dkk1-dependent signaling. Importantly, alternative cellular signaling options for Dkk1, beyond its ability to bind to Wnt-related receptors, have been proposed in different cellular contexts: as a novel Dkk1 receptor, CKAP4 was identified to trigger activation of the PI3K/AKT cascade and Dkk1 binding to CKAP4 also leads to its internalization.¹⁰⁰ Moreover, a portion of Dkk1 was found to be localized to cell nuclei of colorectal cancer cells, where it was involved in the activation of genes linked to the detoxification of chemotherapeutic drugs.²³⁰

3.2.2 Dkk1 depletion protects against Cisplatin-induced apoptosis

In accordance with the apoptosis-sensitizing effect of ectopic Dkk1 expression in HeLa cells, transient RNAi-mediated Dkk1 repression in HeLa, SiHa and CaSki cells, as well as stable Dkk1 depletion in CRISPR/Cas9-generated Dkk1 KO HeLa cells, efficiently suppressed Cisplatin-induced apoptosis. This was determined by the assessment of several hallmarks of late apoptosis stages: Dkk1 silencing reduced the Cisplatin-induced expression of the apoptosis markers cl. PARP and cl. Caspase 9, as well as the staining of apoptosis-induced double-strand breaks in TUNEL assays and the activity of the effector caspases 3/7 in live cell imaging experiments.^{136,137,231}

In the literature, reduced Dkk1 expression has been associated with both, increased resistance or sensitization towards Cisplatin, dependent on the cellular context. In line with my results, a Cisplatin-resistant variant of the oral human head and neck carcinoma cell line Cal27 was characterized by reduced Dkk1 expression.¹¹⁵ In contrast, lung cancer and ovarian cancer cells showed decreased survival rates upon Cisplatin exposure in combination with RNAi-mediated

Dkk1 silencing.²³² These discrepancies might be associated to the varying tumor suppressive or oncogenic roles of Dkk1 in different cancer types, as in contrast to the herein supported tumor suppressive function in cervical cancer cells, Dkk1 is primarily considered as an oncogene in lung and ovarian cancer cells.^{233,234}

Altogether, these data reveal that Dkk1 depletion efficiently protects cervical cancer cells against Cisplatin-mediated apoptosis, suggesting that Dkk1 repression can be a major risk factor for Cisplatin resistance in these cells.

3.2.3 Dkk1 KO HeLa cells acquire a senescent phenotype

It was highly interesting that besides resisting Cisplatin-induced apoptosis, the Dkk1 KO HeLa cells adopted a senescent phenotype in long-term cultivations after Cisplatin treatment. This was shown by the repression of their colony formation capacity, as well as by the emergence of the typical morphological characteristics of senescent cells and positive staining for the senescence marker SA- β -gal.¹⁷⁰ In order to acquire this phenotype, it was sufficient to expose the cells once for 24 h to Cisplatin, as afterwards they were cultured in standard medium without the drug. This suggests that Cisplatin induces irreversible cellular changes in both parental HeLa and Dkk1 KO HeLa cells, which in the first case result in the execution of apoptosis and in the latter case in senescence induction.

Cisplatin is mostly known as a pro-apoptotic agent, but was also reported to be able to induce senescence in previous studies, especially when lower doses were applied.^{235,236} In general, higher doses of chemotherapeutics are known to trigger apoptosis, while lower ones lead to senescence, and it is assumed that this could be directly associated to the amount of DNA damage induced by the respective drug.¹⁶⁷ Consequently, upon Dkk1 depletion, cervical cancer cells may be able to tolerate either higher Cisplatin doses and/or increased amounts of DNA damage, which ultimately protects them from apoptosis induction. Despite the well-established role of Dkk1 in the amplification of pro-apoptotic signals induced by DNA damaging agents in the literature,⁹⁸ no data is thus far available about a pro-senescent effect of Dkk1 repression.

Although, as discussed below, induction of apoptosis or senescence by an anti-tumorigenic agent could be critical for the clinical outcome, the detailed mechanisms behind the decision between these two phenotypic responses of the cell are still poorly understood and may include differentially activated signaling pathways or metabolic effects.^{167,237} As an example, our group recently found that the iron chelator and OXPHOS inhibitor CPX induced apoptosis in cervical

cancer cells under glucose-restricted conditions, while it acted pro-senescent under increased glucose availability.²²⁹ Among the signaling pathways involved in senescence and apoptosis induction, tumor suppressive pathways involving p53 may be of particular interest for the differential phenotypic outcome of parental HeLa and Dkk1 KO HeLa cells. Despite the strong protective effect of Dkk1 depletion on apoptosis induction identified in this thesis, p53 levels were induced irrespective of the Dkk1 status upon Cisplatin exposure, suggesting that p53 could be decisive in the switch between apoptosis and senescence, for instance by a differential transactivation of downstream targets.²³⁸ As an example, the activation of the p53-target gene p21 is linked to senescence induction, while low p21 levels are associated to apoptosis.²³⁹

Both, senescence and apoptosis induction block the proliferation of cancer cells and therefore, in principle, represent desired therapeutic phenotypes. However, the induction of senescence may also have disadvantageous effects, since the secretion of SASP factors from senescent cells can exert pro-tumorigenic effects on non-senescent tumor cells and further increase their therapeutic resistance.^{167,240} For example, the secretion of the SASP-associated factors IL-6 and IL-8 establish an inflammatory and immunosuppressive microenvironment and enhance epithelial to mesenchymal transition.²⁴⁰ Moreover, senescent cells which survive immune system clearance have been reported to re-enter the cell cycle, which potentially results in the formation of even more aggressive tumors.²⁴¹ Therefore, the induction of senescence in Dkk1-depleted cells may also lead to an unfavourable outcome after Cisplatin exposure and strengthens the advantage of Dkk1-dependent apoptosis in the Cisplatin response of cervical cancer cells.

Overall, elucidating the mechanisms behind the Dkk1-dependent switch between senescence and apoptosis in cervical cancer cells should not only result in a better understanding of the cellular response towards Cisplatin treatment, but also may provide in general novel insights into the complex choice between therapy-induced apoptosis or senescence.

3.2.4 Cellular mechanisms behind the Dkk1-dependent Cisplatin response

TOP-/FOPflash reporter assays, as well as the analysis of β -catenin expression levels in the present work indicated that Cisplatin did not induce canonical Wnt signaling activities neither in parental HeLa nor in Dkk1 KO HeLa cells. As a consequence, an increased activity of Wnt signaling, which has previously been associated to Cisplatin resistance,¹⁸⁶ and is additionally known to be enhanced by HPV oncogene expression,²⁴² is most likely not causative for the protective function of Dkk1 repression towards Cisplatin-induced apoptosis in cervical cancer cells. This contrasts the findings

in other cell models proposing that canonical Wnt activation mediates Cisplatin-induced apoptosis in a Dkk1-dependent manner.^{98,115} Differences in cell types or experimental conditions may account for these discrepancies. However, the findings in the present study are further corroborated by a previous study in HeLa cells, reporting that the modulation of Dkk1 expression did not lead to alterations in β -catenin-dependent transcriptional activation or in canonical Wnt-associated factors.¹¹⁸

As a consequence, alternative pathways need to account for the profound difference in the Dkk1-dependent Cisplatin response of cervical cancer cells. In the present work, transcriptome analyses using Affymetrix GeneChips revealed that Cisplatin treatment of parental HeLa cells resulted in major transcriptomic changes compared to Dkk1 KO HeLa cells. Gene expression was assessed after 16 h of Cisplatin exposure, just before the first phenotypic hallmarks of apoptosis, including cell shrinkage and membrane blebbing,¹²⁵ became detectable. This time point represents a relatively late stage of the apoptotic process, when effector caspases have started to execute the irreversible cellular reprogramming towards death. Along with cleaving and thereby downregulating their substrates, caspases further affect transcriptional pathways,²⁴³ indicating that the strong alterations in the number of differentially regulated transcripts in between Cisplatin-treated parental HeLa and Dkk1 KO HeLa cells may be in part an indirect result of the apoptotic process.

Surprisingly, however, only few factors which are directly associated to the apoptotic process were found to be differentially regulated in Cisplatin-treated HeLa cells in a Dkk1-dependent manner - among them the pro-apoptotic factor *PMAIP1* which encodes the BH3-only protein Noxa,¹³¹ and the TRAIL receptor 4 transcribed from the *TNFRSF10D* gene.¹²⁷ However, the activity of many apoptosis-related factors, including those of the Bcl-2 family of proteins, is largely driven by their post-translational modifications, interaction partners and their cellular localization,¹³¹ which cannot be detected by the herein analysed transcriptional alterations. Besides the differential activation of growth factor signaling-related factors, which may act as upstream regulators of apoptotic pathways,²⁴⁴ and Cisplatin-induced pro-inflammatory proteins, which are known to mediate Cisplatin nephrotoxicity,²⁴⁵ my finding that a number of different AP-1 components was stronger induced by Cisplatin in parental HeLa cells compared to Dkk1 KO HeLa cells was particularly conspicuous.

In accordance, GSEA analyses of the Affymetrix data revealed a significant negative enrichment of AP-1 pathway-related genes by the comparison of the transcriptome of Cisplatin-treated Dkk1 KO HeLa cells to parental HeLa cells. This differential activation was subsequently confirmed in all individual Dkk1 KO clones for the expression of c-Jun, Fra-1 (encoded by *FOSL1*) and ATF3 on the protein and transcript level, as well as for *JUNB* and *FOS* on the transcript level. This strongly emphasizes an involvement of AP-1 activation in the Dkk1-dependent pro-apoptotic Cisplatin response of cervical cancer cells. The AP-1 transcription factor complex has been associated to both, cellular survival and apoptosis, and the ultimate decision between these two phenotypes relies on the complex dimerization patterns of its protein subfamilies.¹⁶² Previous reports found that Cisplatin can activate AP-1 related proteins, such as c-Jun and ATF3, in different cancer cell lines.²⁴⁶⁻²⁴⁸ Moreover, mouse embryonic fibroblasts lacking c-Jun expression were characterized by an increased Cisplatin resistance compared to parental cells,²⁴⁹ which supports the notion that a reduced AP-1 activation accounts for the Cisplatin-resistant phenotype of Dkk1-depleted cells.

As potential AP-1 downstream effectors, the transcriptome analyses revealed a decreased induction of the pro-apoptotic proteins Bim and EGR1 by Cisplatin in Dkk1-depleted HeLa cells. While validation experiments showed that the regulation of EGR1 was most likely clone-dependent, the expression of Bim transcripts (*BCL2L11* gene), as well as the induction of the three Bim protein isoforms Bim_{EL}, Bim_L and Bim_S were strongly impaired in Cisplatin-treated Dkk1 KO HeLa cells.

As a BH3-only protein, Bim interacts with pro-survival Bcl-2 family members to prevent their antagonistic effect on apoptosis induction.¹⁹⁹ From the literature, decreased Bim expression in CaSki and HeLa cells was associated with a reduced Cisplatin sensitivity, although it remained unclear in that study whether the protective effect is directly mediated by Bim or the API1/FGFR (fibroblast growth receptor)/ERK axis, which was proposed to regulate Bim expression.²⁵⁰ However, for instance in ovarian cancer cells, RNAi-induced Bim silencing was shown to strongly decrease Cisplatin-mediated apoptosis.²⁵¹ c-Jun-dependent activation of Bim resulting in the induction of apoptosis was previously described after nerve growth factor (NGF) withdrawal in neurons,²⁵² exposure of HeLa cells to the BH3 mimetic ABT-737¹⁹⁸ as well as after glucocorticoid treatment of leukemia cells.²⁵³ The latter report provided some evidence that this effect may be mechanistically linked to the recruitment of c-Jun to the AP-1 binding site of the Bim promoter, which ultimately drives Bim expression. It is, however, important to note that Bim expression is also regulated by other transcription factors, such as FOXO3a, E2F1 or Runx 1/2/3, which are all

known to be activated upon cellular stress. Furthermore, post-translational modifications, including its phosphorylation by the ERK, p38 or JNK MAPKs, play a major role in determining Bim activity.²⁰⁰ As discussed in detail in the following chapter (3.2.5), JNK was identified in this thesis to be critically involved in Dkk1-dependent apoptosis induction by Cisplatin and thus provides an additional potential mechanism behind the differential Bim induction observed between parental HeLa and Dkk1 KO HeLa cells.

Collectively, as a pro-apoptotic effector protein downstream of JNK /AP-1 signaling, Bim represents an interesting factor for future studies to further elucidate the molecular mechanisms of Cisplatin-induced apoptosis in cervical cancer cells.

3.2.5 JNK signaling activation in Cisplatin-induced apoptosis

A previous study reported that Cisplatin treatment of the breast cancer cell line BT474 resulted in the promoter activation of 269 different genes induced by the AP-1 factors c-Jun and ATF2.²⁵⁴ This number emphasizes the complexity of potential AP-1 downstream pathways, which may be involved in the Dkk1-dependent Cisplatin response of cervical cancer cells. In the present study, Cisplatin-induced phosphorylation on Ser63 and Ser73 of c-Jun, which represents one of the most abundant transactivators of the AP-1 family,²⁵⁵ was shown to be strongly suppressed in Dkk1 KO HeLa cells compared to parental HeLa cells. The same regulation was observed for the phosphorylation of the c-Jun upstream kinase JNK, which catalyzes c-Jun phosphorylation on these two residues.¹⁵¹ Besides c-Jun, activated JNK can also stimulate several other AP-1 complex members, either directly by phosphorylation or indirectly via the multitude of feedback regulation mechanisms in between the factors.^{161,201} For instance, the ATF3 promoter contains an AP-1 binding site which confers transcriptional stimulation via c-Jun²⁵⁶ and interestingly, ATF3 was reported to be a mediator in Cisplatin-induced apoptosis in lung cancer cells.²⁵⁷ Similarly, Fra-1, the protein encoded by the *FOSL1* gene, is also activated via an AP-1 binding site²⁵⁸ and was described to be induced in a JNK-dependent manner.²⁵⁹ Consequently, JNK represents an overarching signaling hub in regulating the complex transcriptional activity of AP-1 and therefore, the role of JNK for the Cisplatin response of cervical cancer cells was investigated in more detail in this thesis.

My results revealed that inhibition of JNK activity using JNK1/2-specific siRNA or the chemical inhibitor JNK-IN-8 efficiently abolished Cisplatin-mediated apoptosis in HeLa, SiHa and CaSki cells, which strongly suggests that JNK signaling plays a critical role for an efficient induction of apoptosis in cervical cancer cells in response to Cisplatin treatment. In the literature, JNK activation

has been linked to both pro-survival and pro-apoptotic functions dependent on the cellular context, the type and duration of the external stimulus and the crosstalk to other signaling pathways.²⁶⁰ This also includes a bipartite and tumor-dependent role in the context of Cisplatin-induced apoptosis.²⁶¹ However, in strong support of my findings in the present work, impaired JNK/AP-1 signaling was linked in a previous study to the reduced apoptotic response of a Cisplatin-resistant HeLa variant, which was generated by chronic exposure to the drug.²⁶² Altogether, these data indicate that the Dkk1-dependent activation of pro-apoptotic JNK signaling is a major reason for the enhanced Cisplatin resistance of cervical cancer cells when Dkk1 expression is abolished.

A possible functional link between Dkk1 and JNK has also been reported in other cancer cell lines,¹⁰⁵ although it remains to be investigated in more detail how Dkk1 can activate JNK signaling. A previous study in osteosarcoma cells, which positively correlated Dkk1 expression with JNK phosphorylation, described that alterations in the non-canonical Wnt/PCP pathway may account for a Dkk1-mediated JNK activation.²⁶³ This pathway is unrelated to β -catenin and involves Rac1- or RhoA-mediated JNK activation in response to Wnt ligand binding to Fzd receptors.⁹⁶ In a review, Kagey et al. (2017) proposed that Dkk1 binding to the Lrp5/6 co-receptor, which blocks canonical Wnt activation,⁷⁴ could induce a shift of Wnt ligands and its receptors to the activation of non-canonical pathways.¹⁰⁵ By using *in silico* modulation of the 3D structure of Dkk1 it was further suggested that Dkk1 could directly bind to Fzd receptors via its N-terminal domain in a similar way as described for its binding to the Kremen receptor, thus possibly being able to induce Fzd-mediated, but β -catenin-independent Wnt pathways.²⁶⁴ Non-canonical Wnt signaling is far less studied compared to its canonical counterpart, however the increasing number of reports relating Dkk1 to cancer progression in a JNK-dependent manner, emphasizes the importance to investigate this pathway in more detail.

The correlation of Dkk1 with pro-apoptotic JNK signaling may further provide novel insights into potential downstream pathways which could be involved in the Dkk1-dependent apoptotic response towards Cisplatin in cervical cancer cells. The above referenced study from Brozovic et al. (2004) using Cisplatin-resistant HeLa cells, established by long-term Cisplatin exposure, linked their resistance not only to JNK/AP-1 activation, but also to a reduced expression of FasL, which induces the extrinsic pathway of apoptosis.²⁶² Interestingly, FasL contains two AP-1 binding sites in its promoter²⁶⁵ and c-Jun was shown to be indispensable for FasL expression and FasL-associated apoptosis,²⁶⁶ which both hints to an involvement of the extrinsic apoptosis pathway in JNK/AP-1-induced apoptosis. In response to TNF α , JNK signaling was further shown

to be required for the cleavage of the Bcl-2 family protein Bid in HeLa cells,²⁶⁷ which acts downstream of the extrinsic apoptosis-associated caspase 8 and serves as a link to the intrinsic, mitochondrial pathway of apoptosis.¹³¹ Both, JNK-mediated phosphorylation and AP-1-induced transactivation of Bcl-2 family members, have also previously been linked to the latter apoptosis pathway,^{260,268} including the JNK/c-Jun-dependent regulation of the pro-apoptotic protein Bim, which was herein identified to be differentially activated in the response to Cisplatin in a Dkk1-dependent manner.

Overall, these considerations suggest that the Dkk1-mediated activation of JNK/AP-1 signaling in Cisplatin-treated cervical cancer cells may act pro-apoptotic on different levels of the apoptotic machinery, which could provide a basis for future studies aiming to elucidate in more detail the apoptotic response to Cisplatin via the Dkk1/JNK/AP-1 axis.

3.3 Implications of Dkk1 and JNK/AP-1 in cancer therapy

Dkk1 levels are restrained under normoxic conditions by the expression of HPV E6 and additionally, at least short-term hypoxic exposures result in Dkk1 downregulation, as was observed in the present study not only in cervical cancer cells, but also in colon and lung cancer cells. Importantly, Dkk1 repression strongly impairs Cisplatin-induced apoptosis in cervical cancer cells, suggesting that restrained Dkk1 levels in cervical cancer tissue may be a risk factor for an increased resistance towards Cisplatin-based therapies.

It will be highly interesting to study in more detail the mechanisms behind the cellular switch from apoptosis to senescence in the response to Cisplatin when Dkk1 is depleted. As discussed above, therapy-induced senescence can negatively affect the outcome of cancer therapies,²⁴¹ suggesting that Dkk1 repression does not only interfere with an efficient elimination of cervical cancer cells by apoptosis during Cisplatin treatment, but also that it potentially could promote the expression of pro-tumorigenic SASP factors and the survival of more aggressive cell types via the induction of senescence. This finding could also be of interest for the treatment of other cancer entities in which Dkk1 is considered as an oncogenic factor and therapeutic target.¹⁰¹ For instance, current clinical trials testing the efficacy of Dkk1-neutralizing antibodies were combined with Cisplatin treatment.²⁶⁹ It would be interesting to investigate on cellular level, whether the correlation of Dkk1 silencing and senescence induction in the response to Cisplatin, which is observed in the present thesis, may also restrain the efficiencies of these types of therapies. Conversely, Dkk1 could exert therapy-supportive activities in other tumor types considering its critical role in

Cisplatin-mediated apoptosis not only in cervical cancer, as found here, but also for instance in head and neck cancer cells.¹¹⁵ Thus, it will be interesting to study the potentially enhanced anti-tumorigenic effect of reinforced Dkk1 expression levels on cancer therapy in tumor cell models where Dkk1 is rather believed to act as a tumor suppressor.

The results in this thesis revealed that Dkk1 expression can be indeed stimulated in cervical cancer cells by certain drugs. For example, expanding the findings of a previous study,¹¹¹ I could show that Dkk1 was efficiently induced in cervical cancer cells after treatment with the HDAC inhibitor TSA, at least under normoxic conditions. Interestingly, FDA-approved HDAC inhibitors such as Belinostat or Vorinostat were reported to exert anti-tumorigenic effects in cervical cancer cell lines,²⁷⁰ and the latter drug was further shown to act synergistically with Cisplatin in apoptosis induction.²⁷¹ As another approach, Dkk1 expression was described to be transcriptionally stimulated by the vitamin D metabolite $1\alpha,25$ -dihydroxyvitamin D₃ [1,25(OH)₂D₃ or Calcitriol] in colon cancer cells,²⁷² and a combination treatment of Calcitriol with Cisplatin has been linked to an improved cellular response towards Cisplatin in several cancer entities.²⁷³

Moreover, my data suggests that an enhanced JNK activation may be beneficial for the outcome of Cisplatin-based therapies. Intriguingly, the small molecule inhibitor ABT-737, which antagonizes the activity of anti-apoptotic proteins, was shown to induce the pro-apoptotic protein Bim via JNK and c-Jun activation in HeLa cells and to further enhance radiation-induced apoptosis in this cell line.¹⁹⁸ In osteosarcoma cells, the combination of ABT-737 with Cisplatin resulted in an efficient induction of apoptosis²⁷⁴ and it will be interesting to study a potential positive correlation of these two compounds also in cervical cancer cells.

Overall, the findings from this thesis provide novel insights into the mechanism of Cisplatin-mediated apoptosis, which also possess relevance for currently applied therapies of cervical cancer patients. Since the critical role of Dkk1 in the activation of pro-apoptotic JNK/AP-1 signaling seems to be a decisive factor for apoptosis induction by Cisplatin, the molecular principles identified in this thesis may serve as a basis for the development of novel treatment regimens, especially for novel combinatory approaches with Cisplatin.

3.4 Conclusions

The present work revealed novel insights into the virus/host cell crosstalk in HPV-positive cervical cancer cells, showing that the expression of the putative tumor suppressor Dkk1 is strongly restricted by oncogenic HPVs and revealing that Dkk1 is a critical determinant of the pro-apoptotic Cisplatin response by affecting the JNK/AP-1 signaling pathway.

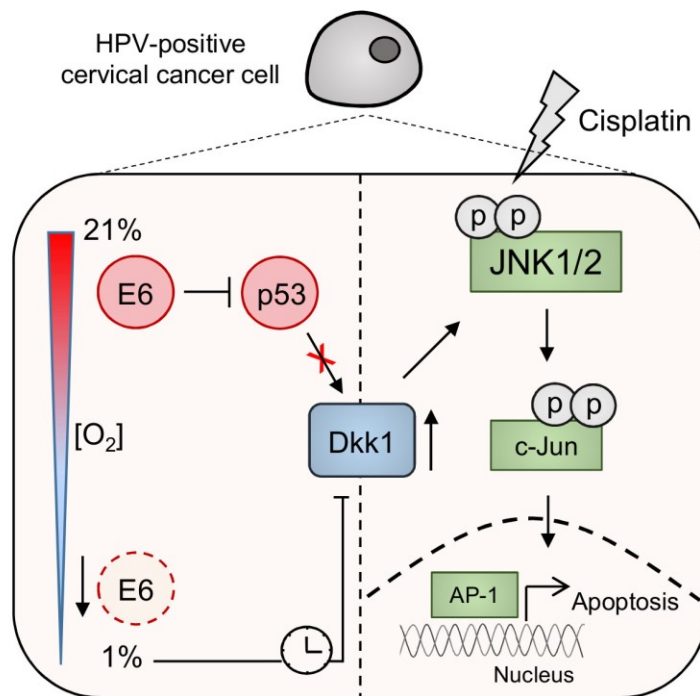


Figure 30 | Schematic model of Dkk1 regulation and its function in Cisplatin-induced apoptosis. Left panel: Under normoxic conditions (21% O₂) Dkk1 levels are restricted by HPV E6-mediated interference with the transcriptional activity of p53 on Dkk1 expression. Besides efficient downregulation of the HPV oncogenes under hypoxic conditions (1% O₂), Dkk1 is transiently repressed, which suggests that hypoxic Dkk1 regulation is uncoupled from the negative control of HPV E6. Right panel: Cisplatin-induced JNK phosphorylation and activation is dependent on Dkk1 induction. Dkk1/JNK signaling further enhances c-Jun phosphorylation and the activation of other AP-1-related factors, which may act pro-apoptotic in a Dkk1- and JNK-dependent manner.

As illustrated in Figure 30, sustained expression of the HPV E6 oncoprotein under normoxia in HPV-positive cervical cancer cells continuously restricts Dkk1 concentrations by its negative impact on p53 levels. In contrast, under hypoxic conditions, Dkk1 levels are repressed in a time-dependent manner by mechanisms which are uncoupled from HPV oncogene expression. Importantly, low Dkk1 levels provide cervical cancer cells with increased Cisplatin resistance, as Dkk1 is required for Cisplatin-induced pro-apoptotic JNK signaling, which ultimately triggers an efficient therapeutic response towards the chemotherapeutic agent, for example through the activation of pro-apoptotic AP-1 factors.

CHAPTER 4
MATERIALS AND
METHODS

4. Materials and Methods

4.1 Reagents

Where possible, molecular biology grade reagents were applied. Standard materials and reagents were purchased by the suppliers listed in Table 1. Non-standard reagents are specified in the text. If not mentioned otherwise, buffers and solutions were prepared with ddH₂O.

Table 1 | Suppliers of standard reagents and materials.

Company	Location
Bio-Rad	Munich, Germany
Carl Roth	Karlsruhe, Germany
GE Healthcare	Chicago, IL, USA
Merck	Darmstadt, Germany
New England Biolabs (NEB)	Frankfurt, Germany
Roche	Basel, Switzerland
Sartorius	Göttingen, Germany
Sigma-Aldrich	St. Louis, M, USA
Thermo Fisher Scientific	Waltham, MA, USA
Qiagen	Hilden, Germany
VWR, Avantor	Radnor, PA, USA

4.2 DNA-related methods

4.2.1 Plasmid transformation

Lysogeny Broth (LB) Medium (pH 7.0)

1 % bacto tryptone
0.5 % yeast extract
170 mM NaCl

Transformation buffer (pH 6.5)

10 % polyethylene glycol 8000
15 % glycerol
5 % DMSO
50 nM MgCl₂
in LB medium

For the amplification of plasmids, the desired DNA vector was heat-shock transformed into the *E.coli* strain TG2. For the production of competent TG2, bacteria were grown in Lysogeny Broth (LB) medium overnight at 37 °C. The next day, they were centrifuged for 5 min at 800 x g and the pellets were resuspended in transformation buffer. 500 µL aliquots of TG2 bacteria were flash frozen in liquid nitrogen and kept at -80 °C until needed. For transformation, a mixture of DNA and 100 µL of competent TG2 was incubated for 30 min on ice and then placed for 1 min in a water

bath at 42 °C. The suspension was shortly chilled on ice before adding 900 µL of LB medium and incubated for another hour on a shaker at 37 °C. 100-200 µL of the suspension were streaked on a LB agar plate composed of 100 µg/mL ampicillin which was incubated overnight at 37 °C for bacterial colony growth. A list of all plasmids used in this thesis is provided in Table 2.

Table 2 | List of plasmids.

<i>Plasmid</i>	<i>ID</i>	<i>Source</i>
M50 Super 8x TOPflash	Addgene #12456	Randall Moon ²⁷⁵
M51 Super 8x FOPflash	Addgene #12457	Randall Moon ²⁷⁵
pBluescript II	-	Stratagene, La Jolla, CA, USA
pcDNA3	#V79020	Thermo Fisher Scientific
pcDNA3-Wnt3a	Addgene #35908	Marian Waterman ²⁷⁶
pCS2	-	-
pCS2-hDkk1-Flag	Addgene #15494	Sergei Sokol ⁷⁵
pCMV-Gal	-	Butz et al. ²⁷⁷
pLentiCRISPR-v1	Addgene #49535	Feng Zhang ²⁷⁸
pLentiCRISPR-Dkk1gRNA_1	-	-

4.2.2 Plasmid DNA isolation

Solution 1 (pH 6.7)

50 mM glucose
25 mM Tris
10 mM EDTA

Solution 2

0.2 M NaOH
1 % SDS
freshly prepared

Solution 3

3 M potassium acetate
11.5 % acetic acid

TE buffer (pH 8.0)

10 mM Tris
1 mM EDTA

Plasmid DNA was isolated from transformed bacteria using the QIAprep Spin Miniprep Kit (Qiagen) or the PureLink™ HiPure Plasmid Filter Midiprep Kit (Thermo Fisher Scientific) according to the manufacturer's instructions. For this purpose, bacterial colonies were inoculated from the agar plate to 4 mL or 50 mL LB medium, respectively, supplemented with 100 µg/mL ampicillin, and grown on a shaker overnight at 37 °C.

Larger amounts of plasmid DNA were produced by cesium chloride/ ethidium bromide maxi-preparation, according to the protocol from Sambrook and Russel.²⁷⁹ After transformation, bacteria were grown in 250 mL LB medium and pelleted by centrifugation (10 min; 4,000 rpm;

4 °C). The pellets were resuspended in 10 mL of solution 1, lysed in 20 mL of solution 2 and neutralized in 15 mL of solution 3. All steps were carried out on ice. The suspension was centrifuged (10 min; 4,500 rpm; 4 °C) to remove bacterial debris. The supernatant was transferred to a fresh tube, mixed with one volume of isopropanol and incubated for 30 min on ice. Precipitated plasmid DNA was pelleted in a centrifuge (30 min; 6,000 rpm; 4 °C) and resuspended in 4 mL TE buffer. For removal of RNA, 4 mL of 5 M LiCl were added and chilled on ice for 30 min, followed by centrifugation (5 min; 4,000 rpm; 4 °C). Next, the supernatant was mixed with two volumes of 100 % EtOH and was incubated for 30 min on ice to precipitate DNA. After centrifugation (30 min; 6,000 rpm; 4 °C) the DNA pellet was resuspended in 4 mL TE buffer and mixed with 4.4 g cesium chloride and 120 μ L 10 mg/mL ethidium bromide solution (Thermo Fisher Scientific). The mixtures were pipetted into 6 mL Ultracrimp tubes (Thermo Fisher Scientific) and centrifuged in an OTD 75B Sorvall Ultracentrifuge (16-18 h; 48,000 rpm; 20 °C). Ethidium bromide incorporates to lesser extent into plasmid DNA compared to chromosomal DNA, which leads to differences in DNA densities and thus allows the separation by density gradient centrifugation. The lower band containing the more dense, supercoiled plasmid DNA was extracted from the tubes and for removal of ethidium bromide, extraction with water-saturated 1-butanol was performed until the suspension became destained. The plasmid DNA was precipitated in two volumes of 100 % EtOH for one hour at -20 °C and after pelleting (30 min; 4,500 rpm; 4 °C), it was resuspended in 4 mL TE buffer supplemented with 160 μ L 5 M NaCl. Final precipitation was performed as described in the previous step and the purified DNA was resuspended in 300-500 μ L TE buffer.

4.2.3 Agarose gel electrophoresis

<u>Electrophoresis buffer</u> (pH 7.8)	<u>6x DNA loading buffer</u>
40 mM Tris	0.25 % bromophenol blue
5 mM sodium acetate	0.25 % xylene cyanol
1 mM EDTA	30 % glycerol

Separation of DNA plasmid fragments according to their size was performed on agarose gels. 1-2 % of agarose were dissolved in electrophoresis buffer and boiled in a microwave. The PeqGREEN non-toxic DNA/RNA dye (VWR, Avantor) was added for visualization of DNA. The solution was poured into a gel tray and when it cooled down it was placed into a PerfectBlue™ gel system (VWR, Avantor).

The DNA - diluted in 6x DNA loading buffer - was loaded onto the gel next to 5 μ L of DNA SmartLadder (Eurogentec, Belgium). Dependent on the size of DNA fragments, gel runs were performed for 45-90 min at 80-100 V. UV transillumination using a gel imaging system (Intas Science Imaging Instruments, Göttingen, Germany) allowed the visualization of DNA fragments. For subsequent cloning, DNA was extracted from the gel using the QIAquick Gel Extraction Kit (Qiagen) according to the manufacturer's instructions.

4.2.4 Plasmid DNA validation

Validation of plasmid DNA (e.g. after molecular cloning) was performed using restriction digestion, followed by agarose gel electrophoresis and sequencing. For the first step, NEB restriction endonucleases suitable for the corresponding DNA vector were mixed with 0.5-1 μ g of plasmid DNA in the provided restriction buffer in a total volume of 20 μ L. Usually, the mixture was incubated for 1 h at 37 °C in a water bath, unlike indicated otherwise for an enzyme according to the manufacturer's instructions. DNA fragments were analyzed by agarose gel electrophoresis as described in chapter 4.2.3 and plasmids, which could be successfully digested, were sequenced using the service from Eurofins Genomics (Louisville, KY, USA). The obtained sequences were compared with the corresponding plasmid map with the help of the Basic Local Alignment Search Tool (BLAST) by the National Center for Biotechnology Information.

4.2.5 Molecular cloning strategies

4.2.5.1 Cloning of Dkk1-targeting gRNA for CRISPR/Cas9 knockout (KO)

Stable HeLa Dkk1 KO cells were generated using the CRISPR (clustered regularly interspaced short palindromic repeats)/Cas9 (CRISPR-associated protein 9) method. The CRISPR system, which has its origin in a prokaryotic defense mechanism against phage infection, is based on the concerted action of a Cas nuclease with a gene-targeting guideRNA (gRNA).²⁸⁰ The 20 nucleotide-long gRNA sequence is selected to bind a genome locus adjacent to a Cas-specific Protospacer Adjacent Motif (PAM) sequence (for Cas9 nuclease: NGG). Upon binding of Cas (herein: Cas9) to the PAM sequence, Cas9 can induce DNA double-strand breaks in the genomic target sequence. As these damage sites are repaired mostly by the error-prone non-homologous end joining pathway (NHEJ), small nucleotide insertions or deletions can result in alterations in the reading frame and consequently to an impaired gene expression in the cell.²⁸¹

The herein used pLentiCRISPR-v1 vector (Table 2) allows the simultaneous expression of Cas9 and a gene-targeting gRNA. Dkk1-specific gRNAs were selected using the online tool CRISPOR

developed by Jean-Paul Concordet and Maximilian Haeussler (UCSC, Santa Cruz, CA, USA)²⁸² and ordered as oligonucleotides encoding the gRNA sequence. After testing different potential *DKK1*-targeting gRNAs, the pLentiCRISPR-v1 vector containing the gRNA sequence composed of the following forward (for) and reverse (rev) oligonucleotides was selected for ensuing single cell cloning (described in chapter 4.3.7):

for 5' -CACCTACCCGGGTCTTTGTGCGCA-3'
rev 5' -AAACTTCGCGACAAAGACCCGGGTA-3'

Cloning was performed according to a protocol from the Zhang lab.²⁷⁸ The single oligonucleotides, which contain additional 5' overhangs for efficient molecular cloning (as indicated by underlined nucleotides), were phosphorylated by T4 polynucleotide kinase (PNK) in the presence of 1 mM ATP for 30 min at 37 °C in a MJ Research PTC-2000 Thermal Cycler (Marshall Scientific, USA). Immediately after this step, the mixture was incubated for 5 min at 95 °C, followed by step-wise cooling-down to 25 °C by 5 °C/min to allow annealing of the single oligonucleotides. At the same time, 3 µg of the pLentiCRISPR-v1 vector were digested using BsmBI for 1 h at 55 °C to cut out a 1885 bp filler cassette. 5'-dephosphorylation of the linearized vector was performed by addition of 10 units of calf intestinal alkaline phosphatase (CIP) and subsequent incubation for 1 h at 37 °C. After purification by agarose gel electrophoresis, the annealed oligonucleotides were ligated with a 5-fold molar excess into 100 µg of the vector using 2 units of T4 ligase (NEB) in the supplied T4 ligase buffer in a total volume of 20 µL. The mixture was incubated for 2 h at 21 °C, followed by a DNA ligase-inactivating step for 10 min at 65 °C.

4.2.5.2 pCS2 subcloning

The pCS2-hDkk1-Flag plasmid served as a template to generate a corresponding empty control vector (pCS2). For this purpose, 10 µg of the Dkk1-containing plasmid were digested using EcoRI and XhoI in the provided NEB buffer for 2 h at 37 °C, cutting out the Dkk1-Flag fragment. The linearized vector was separated from its insert via agarose gel electrophoresis and was extracted from the gel. Protruding termini were blunted using T4 DNA Polymerase (NEB) in the presence of 2 mM dNTP mix and the provided reaction buffer in a total volume of 20 µL. The mixture was incubated at RT for 5 min and the reaction was stopped by 10 min incubation at 70 °C. The blunted vector was precipitated in 2.5 volumes of 100 % ethanol for at least 30 min at -20 °C. After pelleting in a centrifuge, DNA was resuspended in nuclease-free H₂O and the vector was re-ligated using T4 DNA Ligase.

4.3 Cell-related methods

4.3.1 Cell culture

HPV-positive SiHa, CaSki and HeLa cells, including HeLa Dkk1 KO clones and the HeLa* variant, were cultured in Gibco™ Dulbecco's minimal essential medium (DMEM) (Thermo Fisher Scientific) containing 1 g/L glucose (5 mM). HPV-negative HCT116 colon cancer cells were maintained for standard cultivation in Gibco™ McCoy's 5A and A549 lung cancer cells in Gibco™ RPMI 1640 medium (Thermo Fisher Scientific). For hypoxic treatments, medium of HCT116 and A549 cells was changed to DMEM. All media were supplemented with 10 % fetal bovine serum (FBS) (PAN-Biotech, Aidenbach, Germany), 2 mM L-glutamine, 100 U/mL penicillin and 100 µg/mL streptomycin. Cell stocks were cultivated at 37 °C and 5 % CO₂ at 21 % O₂ in a humidified incubator if not indicated otherwise. Every 3-4 days, they were washed with PBS, detached with 0.25 % Trypsin-EDTA (Thermo Fisher Scientific), and split into fresh cell culture flasks.

For experiments, after trypsinization, viable cells were counted using 0.4 % Trypan Blue Solution in the Countess™ Automated Cell Counter (Thermo Fisher Scientific) and seeded in 60 mm cell culture dishes, unlike indicated otherwise. If not described in another way, experiments were performed at the same conditions as described for standard cell culture (21 % O₂, 37 °C and 5 % CO₂). Hypoxic incubations (1 % O₂, 37 °C, 5 % CO₂) were applied in the InvivoO₂ 400 physiological oxygen workstation (Ruskin Technology Ltd, Bridgend, UK). For high glucose conditions, DMEM supplemented with 4.5 g/L glucose (25 mM) was used.

4.3.2 Long-term preservation of cells

After trypsinization, cells were centrifuged for 5 min at 800 x g and resuspended in freezing medium consisting of 30 % FBS and 10 % DMSO as a cryoprotectant. 1 mL aliquots of the cell suspension were divided into Nalgene™ cryogenic tubes (Thermo Fisher Scientific) and frozen for a few days at -80 °C in isopropanol-filled Mr.Frosty™ freezing containers (Thermo Fisher Scientific), before moving them into liquid nitrogen for long-term storage. For thawing of cells, the aliquoted cryotubes were warmed in a water bath at 37 °C and the thawed cells were resuspended in standard cell culture medium in cell culture flasks. After one day, when cells have attached to the flask, medium was exchanged.

4.3.3 Transfection with siRNA

Synthetic siRNAs (Silencer® Select, Thermo Fisher Scientific) were diluted in nuclease-free water to 10 μ M stock solutions. All siRNA sequences used are listed in Table 3 which further indicates the use of siRNA pools if applicable. The cells were seeded the day before transfection to reach a confluence of 30-40 % and prior to transfection, cell culture medium was replaced with 1.6 mL of antibiotic-free DMEM containing 10 % FBS. For transfection of 10 nM siRNA, 2 μ L of the stock solution were mixed with 198 μ L Gibco™ Opti-MEM™ (Thermo Fisher Scientific). In parallel, 4 μ L (HeLa) or 6 μ L (SiHa, CaSki) of the transfection agent DharmaFECT™ I (Horizon Discovery, UK) were mixed into a final volume of 200 μ L Opti-MEM. After 5 min of incubation at RT, the DharmaFECT I solution was added to the siRNA solution and the mixture was incubated for another 20 min at RT. The transfection mix was added dropwise to the cells, which were then incubated under standard cell culture conditions. After 24 h medium was exchanged to standard cell culture medium and further treatments were performed.

Dependent on the cellular target, an efficient downregulation can be achieved between 48 and 96 h after transfection and for further downstream analyses (e.g. protein or RNA analyses) cells were harvested 72 h after transfection if not indicated otherwise.

Table 3 | Synthetic siRNAs (Silencer® Select).

<i>Target</i>	<i>siRNA</i>	<i>Target sequence (5' -> 3')</i>	<i>Pool</i>
Control	siCtrl-1	CAGUCGCGUUUGCGACUGG	-
HPV 16E6	si16E6-4	ACCGUUGUGUGAUUUGUUA	si16E6
HPV 16E6	si16E6-246	GGGAUUUAUGCAUAGUAUA	
HPV 16E6	si16E6-321	UUAGUGAGUAUAGACAUA	
HPV 16E6/E7	si16E6/E7-2	CCGGACAGAGCCCAUUACA	si16E6/E7
HPV 16E6/E7	si16E6/E7-575	CACCUACAUUGCAUGAAUA	
HPV 16E6/E7	si16E6/E7-617	CAACUGAUCUCUACUGUUA	
HPV 18E6	si18E6-340	GACAUUAUUCAGACUCTGU	si18E6
HPV 18E6	si18E6-349	CAGACUCUGUGUAUGGAGA	
HPV 18E6	si18E6-353	CUCUGUGUAUGGAGACACA	
HPV 18E6/E7	si18E6/E7	CCACAACGUCACACAAUGU	si18E6/E7
HPV 18E6/E7	si18E6/E7-563	CAGAGAAACACAAGUAUAA	
HPV 18E6/E7	si18E6/E7-846	UCCAGCAGCUGUUUCUGAA	
Dkk1	siDkk1 #1	GCUUCACACUUGUCAGAGA	siDkk1
Dkk1	siDkk1 #2	CUCAAUCCUAAGGAUAUAC	
JNK1/2	siJNK1/2	GAAAGAAUGUCCUACCUUC	-
p53	sip53	GACUCCAGUGGUAUUCUAC	-

4.3.3.1 Combined E6/E7 and p53 repression

For the combined silencing of E6/E7 and p53, 10 nM of sip53 was transfected one day after seeding as described in chapter 4.3.3. Instead of replacing the medium, after 24 h, the cells were immediately transfected with 15 nM of E6 or E6/E7-targeting siRNA and 5 nM of sip53 using the same protocol. For silencing of p53 alone, 5 nM of sip53 were filled up with 15 nM of siCtrl to have equal siRNA amounts in between conditions. After another 8 h at standard culture conditions, medium was exchanged to standard cell culture medium and harvesting and downstream analyses were performed 72 h after the first transfection.

4.3.4 Plasmid Transfection

2x BES buffer (pH 6.95)

50 mM BES

280 mM NaCl

1.5 mM Na₂HPO₄

filter-sterilized

Plasmids were transfected into cells using calcium phosphate transfection according to Chen and Okayama:²⁸³ Plasmid DNA co-precipitates with calcium phosphate, which promotes DNA binding to the cell surface and leads to the uptake of DNA via cellular endocytosis. In brief, cells were seeded the day before transfection in 60 mm cell culture plates in 3 mL of cell culture medium to be ~30 % confluent. For efficient transfection, 6 µg of total DNA needed to be transfected. If necessary, plasmid DNA was filled up to reach this amount by addition of pBluescript II vector (Stratagene, Germany). DNA was first mixed with 150 µL of 0.25 M CaCl₂, followed by the immediate addition of 150 µL 2x BES buffer. The transfection mix was incubated for 20-30 min at RT and was added dropwise to the cells, which were then incubated for 16-18 h in a humidified incubator at 35 °C and 3 % CO₂. Afterwards, medium was discarded, cells were washed twice with PBS and 3 mL of fresh culture medium were added. Transfected cells were further cultured under standard conditions to perform subsequent experiments. For further downstream analyses, cells were harvested 48 h after transfection if not indicated otherwise.

4.3.5 Preparation of Dkk1 CM

For the production of Dkk1 CM (or the respective Ctrl CM), cells of a laboratory HeLa variant without detectable Dkk1 expression (HeLa*) were seeded in 100 mm cell culture dishes in 10 mL of cell culture medium the day before transfection to be ~30 % confluent the next day. 3 µg of

pCS2-hDkk1-Flag or pCS2 (Table 2) were mixed with 17 μ g pBluescript II and were transfected into the cells according to chapter 4.3.4. For the experimental set up in 100 mm cell culture dishes, 500 μ L of each CaCl₂ and 2xBES buffer were used. 16-18 h after transfection, cells were washed twice with PBS and 20 mL of standard cell culture medium were added. After 32 h, medium was collected from the cells, centrifuged for 5 min at 800 x g to remove cell debris and stored at -80 °C. When needed, the medium was thawed at 37 °C and mixed in a ratio of 5:1 with cell culture medium containing 25 mM glucose to add fresh cell culture medium components, as well as enough glucose to the conditioned media for subsequent experiments.

4.3.6 Chemical treatments

One or two days after seeding, chemical compounds (Table 4) were diluted directly into the cell medium. Usually, medium was exchanged prior to treatments, unless it had previously been exchanged on the same day (e.g. after transfections). Final concentrations and details of treatments are indicated for each experiment.

Table 4 | Compounds for chemical treatment of cells.

<i>Compound</i>	<i>Abbreviation</i>	<i>Stock concentration</i>	<i>Solvent</i>	<i>Manufacturer</i>
5-Azacytidine	5-Aza	3 mM/ 15 mM	50% (v/v) Acetic Acid	Sigma-Aldrich
AKT inhibitor VIII	AKTIVIII	10 mM	DMSO	Sigma-Aldrich
Cisplatin	CDDP	1.5 mM	0.9% NaCl/H ₂ O	MedChem Express, USA
JNK inhibitor XVI	JNK-IN-8	1 mM	DMSO	MedChem Express, USA
Metformin	-	250 mM	DMEM	Enzo Life Sciences, Lörrach,D
Rotenone	-	50 μ M	DMSO	MP Biomedicals, Santa Ana,CA
Trichostatin A	TSA	1 mM	DMSO	Enzo Life Science, USA

4.3.6.1 5-Azacytidine

5-Azacytidine (5-Aza) is incorporated into DNA or RNA during replication as a cytidine analog which is irreversibly bound by DNMT1. Loss of DNMT1 results in hypomethylated DNA strands after ongoing replication.¹⁸⁰ To enable an efficient loss of methylation, cells were treated for 72 h with the drug and due to the low stability of the component, medium supplemented with fresh 5-Azacytidine was replaced every 24 h.

4.3.6.2 Cisplatin treatment in conditioned media

For combined Cisplatin and Dkk1 CM or Ctrl CM treatments, medium was replaced by 3 mL of conditioned medium one day after seeding the cells (chapter 4.3.5). After pre-incubation for

48 h, medium was replaced with fresh conditioned medium and Cisplatin was added for another 24 h, when cells were harvested for ensuing analyses.

4.3.7 CRISPR/Cas9-mediated generation of HeLa Dkk1 KO clones

The Dkk1-targeting vector pLentiCRISPR-Dkk1gRNA_1 (Table 2) (molecular cloning described in chapter 4.2.5.1) was transfected into HeLa cells as described in chapter 4.3.4. In parallel, one additional cell plate was MOCK-transfected as a negative control. 36 h after transfection, cell medium was replaced by fresh cell culture medium containing 1 µg/mL puromycin to select for successfully transfected cells. The next day, all surviving cells were splitted into a 100 mm cell culture dish in the presence of 1 µg/mL puromycin and kept under selection for three more days until all cells in the MOCK control were dead. The surviving cells were trypsinized and serial cell dilutions were seeded into 96-well plates in standard cell culture medium to generate single-cell clones. Single cells were validated using IncuCyte Life Cell Imaging (Sartorius). When cells were confluent enough, they were transferred into bigger cell culture dishes until enough cells could be collected for validation and cryopreservation. Dkk1 KO in single-cell clones was confirmed on the protein level using immunoblot analyses.

4.3.8 TUNEL assay

DNA double strand breaks induced by endonuclease cleavage during apoptosis can be detected using the terminal deoxynucleotidyl transferase dUTP nick end labeling (TUNEL) method.²³¹ Cells were seeded on coverslips in 60 mm cell culture dishes and treatments were applied as indicated. At the desired time after treatment, the coverslips were collected from the dish, washed with PBS and fixed for 30 min in 4 % paraformaldehyde (PFA). After washing with PBS, the cells were stored in 80 % EtOH at -20 °C or immediately stained with the TUNEL reagent. For the latter, the fixed cells were permeabilized in 0.1 % Triton/ 0.1 % sodium citrate and were washed twice with PBS. The cells were stained with 25 µL solution of the In Situ Cell Death Detection Kit, Fluorescein (Roche) and incubated for 90 min in a humidified chamber at 37 °C in the dark. After staining, the cells were dipped five times briefly in PBS and were washed twice for 10 min in PBS. Cell nuclei were stained with 30 µL of 1 µg/µL DAPI (Roche) for 5 min at RT in the dark and washing was performed with PBS as described after TUNEL stainings. The coverslips were once dipped in H₂O, once in 100 % EtOH and air-dried before mounting them with Vectashield Antifade Mounting Medium (Vector Laboratories Inc., USA) on microscope slides.

Images were taken the next day or later with a Cell Observer.Z1 with LED module Colibri.2 using the 20x / 0.4 LD PlnN Ph2 DICII objective (Zeiss, Germany). For longer storage, the microscope slides were kept at 4 °C in the dark. For each condition, at least five images were taken. TUNEL-positive cells were quantified relative to the number of DAPI stainings which account for the total cell number, using a macro for ImageJ - kindly provided by the DKFZ Light Microscope Core Facility (Damir Kronic).

4.3.9 Caspase 3/7 Assay

To detect caspase-3 and caspase-7 activity as an apoptosis marker, IncuCyte Caspase-3/7 Green Reagent for Apoptosis (Sartorius) in combination with Incucyte Life Cell Imaging was used. When adding the reagent to the cell culture medium, the cells take up the DNA-intercalating dye containing an activated caspase 3/7 recognition motif, which is cleaved by activated caspase-3/7 upon apoptosis induction. This leads to a fluorescent signal on the cellular DNA, which can be measured for quantification of apoptotic cells.

To perform this assay, 5×10^5 cells per well were seeded into 96-well plates. Two days after seeding, the cells were treated with Cisplatin in the presence of 5 μ M of the reagent in a total volume of 100 μ L cell culture medium. Caspase-3/7 activity was assessed every 2 h over a time period of three days and the counts from four images in one well were normalized to the cell confluence. Measurements were performed in technical triplicates.

4.3.10 Senescence Assay

Fixation Buffer

2% PFA

0.2% glutaraldehyde

Senescence Assay Buffer (pH 6.0)

40 mM citric acid

150 mM NaCl

2 mM MgCl₂

Freshly added:

5 mM K₃[Fe(CN)₆]

5 mM K₄[Fe(CN)₆]

1 mg/mL X-Gal in DMF

Senescent cells exhibit β -galactosidase activity at pH 6.0,¹⁷⁰ which can be detected by a blue signal in the presence of the chromogenic substrate X-gal (5-bromo-4-chloro-3-indolyl β -galactopyranoside). 24 h after Cisplatin treatment, cells were split at a ratio of 1:2 in 60 mm cell

culture dishes and incubated for 5 more days in standard cell culture medium. Untreated cells were split in parallel at a ratio of 1:10. Medium was exchanged every 2-3 days. For staining, the cells were washed with PBS and fixed for 3 min in 1.5 mL fixation buffer. After washing with PBS, the cells were incubated overnight in a wet chamber in 1.5 mL of senescence assay buffer. Imaging was conducted using the EVOS™ CL Core Cell Imaging System (Thermo Fisher Scientific) with 10 x magnification.

4.3.11 Colony Formation Assay

Crystal violet

12 mM crystal violet

29 mM NaCl

3% formaldehyde

22% EtOH

The clonogenic growth of cells after Cisplatin treatment was evaluated by colony formation assays (CFAs). To this end, cells were split 24 h after Cisplatin exposure at a ratio of 1:100 in 60 mm cell culture dishes in standard cell culture medium and cultured for 13 more days while the medium was exchanged every 3-4 days. On day 13, the cells were washed with PBS and immediately fixed and stained with 250 μ L PFA/crystal violet solution for 5 min. The staining solution was removed with water and CFAs were dried at 37 °C overnight. Images were acquired with an Epson Perfection 4990 Flatbed scanner (Epson, Suwa, Japan).

4.3.12 TOP-/FOPflash luciferase assay

Triphosphate lysis buffer

25 mM Tris (pH 7.8)

4 mM EGTA

10% glycerin

1% Triton X-100

Luciferase buffer (pH 7.8)

25 mM glycylglycine

15 mM MgSO₄

5 mM ATP *freshly added*

0.25 M luciferin *freshly added*

Canonical Wnt signaling activity was determined using TOP-/FOPflash reporter luciferase plasmids (Table 2). The plasmids contain either intact or mutated Wnt-responsive TCF binding sites in front of the firefly luciferase gene. Luciferase enzyme activity is indicative for the activity of the canonical Wnt pathway and is assessed by measuring the emitted light of luciferin (562 nm), which is oxidized in an ATP-dependent manner upon luciferase induction.

One day after seeding, cells were transfected via calcium phosphate co-precipitation (chapter 4.3.4) with 2 µg of TOP- or FOPflash plasmids and if indicated with 0.5 µg of pcDNA3 or pcDNA3-Wnt3a plasmids (Table 2). Additionally, 0.5 µg of a pCMV-gal plasmid (Table 2) were added to each transfection mix as the luciferase activity was normalized to β-galactosidase activity (described in chapter 4.3.12.1). All reactions were performed in technical duplicates. 2 days after transfection, the cells were either treated with Cisplatin or LiCl after an additional medium exchange or were cultivated in Ctrl CM or Dkk1 CM. After 16 h cells were washed with ice-cold PBS and harvested in 200 µL triphosphate lysis buffer. The samples were centrifuged for 5 min at 12,000 x g and 4 °C to pellet cell debris and 50 µL of the supernatant were transferred into flat bottom white 96 well plates. 150 µL of luciferase buffer, containing freshly added ATP and luciferin, were injected to the wells by a luminometer (LB943 Mithras², Berthold Technologies, Bad Wildbad, Germany), which immediately measures luciferase activities.

4.3.12.1 β-galactosidase assay

Galactosidase Assay Buffer (pH 7.5)

60 mM Na₂HPO₄

40 mM NaH₂PO₄

10 mM KCl

1 mM MgSO₄

1 mg/mL ortho-nitrophenyl-β-galactosidase (ONPG) *freshly added*

Active β-galactosidase (β-gal) hydrolyzes its substrate ONPG, which leads to the production of o-nitrophenol. The absorbance of this yellow-colored product can be assessed at a wavelength of 405 nm. The β-gal assay was used to normalize luciferase reporter activities to transfection efficiency- or cell number-caused variations. 50 µL of each sample from TOP-/FOPflash luciferase assays (chapter 4.3.12) were transferred into a clear 96-well plate and mixed with 200 µL galactosidase assay buffer. When the mixture turned yellow, emitted light was measured with a Multiskan EX ELISA plate reader (Thermo Electron, Germany) and unspecific absorbance, as determined by the absorbance at 620 nm, was subtracted from the β-gal values measured at 405 nm.

4.4 RNA-related methods

4.4.1 RNA isolation

Total RNA was isolated using the Spin Cartridge-based PureLink™ RNA Mini Kit (Thermo Fisher Scientific). Cells from a 60 mm plate were lysed in 600 µL of the provided lysis buffer supplemented with 1 % β-mercaptoethanol (Sigma-Aldrich) and subsequent steps were performed according to the manufacturer's instructions. As an additional step, DNA was removed from the sample using the PureLink™ DNase Set (Thermo Fisher Scientific) and as a final step, RNA was eluted from the column using 30-60 µL nuclease-free H₂O. Concentrations were measured on the NanoDrop ND-1000 spectrophotometer (VWR, Avantor) and purified RNA was stored at -80 °C.

4.4.2 Reverse transcription

Purified RNA was reverse transcribed into cDNA using the ProtoScript® II First Strand cDNA Synthesis Kit (NEB). In more detail, 0.5 µg of RNA were mixed with 1 µL of a 1:1 mixture of the supplied random and oligo dT primers and the volume was adjusted with nuclease-free H₂O to 4 µL. After a denaturation step for 5 min at 70 °C in a MJ Research PTC-2000 Thermal Cycler (Marshall Scientific, USA), tubes were placed on ice and each sample was supplemented with 5 µL of the provided 2 x reaction mix and 1 µL of the 10 x enzyme mix. Reverse transcription was completed by an initial incubation step at 25 °C, followed by incubation for 1 h at 42 °C and for 5 min at 80 °C. For subsequent qRT-PCR analysis, 40 µL of nuclease-free H₂O were added to each sample to reach a final concentration of 10 ng/µl. cDNA was stored at -20°C.

4.4.3 Quantitative real-time PCR (qRT-PCR)

Transcript levels of genes were determined by quantitative real-time PCR (qRT-PCR) in 96-well plates in technical duplicates. Reaction mixes for the desired transcript amplification contained 0.4 µL of each forward and reverse primer (5 µM; 18S ribosomal RNA (rRNA): 2.5 µM), 7.2 µL of nuclease-free H₂O and 10 µL of SYBR™ Green PCR Master Mix (Thermo Fisher Scientific) per well. 18 µL of the reaction mix were distributed on the plate and 2 µL of the previously generated cDNA (chapter 4.4.2) was added to the corresponding well. As a negative control, instead of cDNA, 2 µL of H₂O were added to the reaction mix.

qRT-PCR runs were performed using the 7300 Real Time PCR System (Thermo Fisher Scientific) by applying the program listed in Table 5. To exclude unspecific amplification, dissociation curves were generated for each primer pair. Gene expression was normalized to 18S rRNA as an internal

standard and Ct values were calculated for each reaction using the comparative Ct ($2^{-\Delta\Delta CT}$) method.²⁸⁴ All qRT-PCR primers are listed in Table 6.

Table 5 | qRT-PCR program.

Initiation	50 °C	2 min	
Polymerase Activation	95 °C	10 min	
Denaturation	95 °C	15sec	40x
Annealing and elongation	60 °C	1min	
Dissociation curve	95 °C	15sec	
	60°C	1 min	
	95°C	15 sec	
	60°C	15 sec	

Table 6 | Primer pairs for qRT-PCR analyses.

Target	Sequences	amplicon length (nt)	Source
<i>18S</i>	For: 5' -CATGGCCGTTCTTAGTTGGT-3' Rev: 5' -ATGCCAGAGTCTCGTTCGTT-3'	66	Braun et al. (2020) ²²⁸
<i>ATF3</i>	For: 5' -AAGAACGAGAAGCAGCATTGAT-3' Rev: 5' -TTCTGAGCCCGACAATACAC-3'	71	Bottone et al. (2005) ²⁸⁵
<i>DKK1</i>	For: 5' -TCTTTGTCGCGATGGTAGCG -3' Rev: 5' -AATAGGCAGTGCAGCACCTT-3'	115	Bossler et al. (2019) ⁵⁵
<i>FOS</i>	For: 5' -AAAAGGAGAATCCGAAGGGAAA-3' Rev: 5' -GTCTGTCTCCGCTTGGAGTGTAT-3'	96	De Wilde et al. (2008) ²⁸⁶
<i>FOSL1</i>	For: 5' -CGTCGAAGGCCTTGTGAACAG-3' Rev: 5' -GAAGTCGGTCAGTTCCTTCCT-3'	120	Primer Blast (NCBI)
<i>HPV 16E6/E7</i>	For: 5' -CAATGTTTCAGGACCCACAGG-3' Rev: 5' -CTCACGTCGCAGTAACGTGTG-3'	125	Braun et al. (2020) ²²⁸
<i>HPV 18E6/E7</i>	For: 5' -ATGCATGGACCTAAGGCAAC-3' Rev: 5' -AGGTCGTCTGCTGAGCTTTC-3'	247	Braun et al. (2020) ²²⁸
<i>JUN</i>	For: 5' -TCGACATGGAGTCCCAGGA-3' Rev: 5' -GGCGATTCTCTCCAGCTTCC-3'	101	De Wilde et al. (2008) ²⁸⁶
<i>JUNB</i>	For: 5' -TGGTGGCCTCTCTACACGA-3' Rev: 5' -GGGTCGGCCAGGTTGAC-3'	66	De Wilde et al. (2008) ²⁸⁶
<i>TP53</i>	For: 5' -CTGAGGTTGGCTCTGACTGT-3' Rev: 5' -CAAAGCTGTTCCGTCCTCCAGT-3'	144	Braun et al. (2020) ²²⁸

4.4.3.1 Quality control of qRT-PCR primers

Before being included in qRT-PCR experiments, all primers were tested by generating standard curves. Primers were diluted to a concentration of 5 μ M in nuclease-free water and were tested in qRT-PCR by a serial dilution of cDNA (undiluted, 1:10, 1:100, 1:1000) using the same program as

described in Table 5. Absolute Ct values were plotted against the negative logarithm of the dilution factor and the slope of the line through the data points was calculated. Efficient primers were selected based on a slope between 3.1-3.6 and on dissociation curves indicating no unspecific amplification.

4.4.4 Gene expression analyses on Affymetrix GeneChips

Microarray-based gene expression analyses of untreated and Cisplatin-treated parental HeLa and HeLa Dkk1 KO #3 cells was performed in cooperation with the DKFZ Microarray Unit (Genomics and Proteomics Core Facility). Affymetrix GeneChips are generated by photolithographic-based oligonucleotide synthesis on a quartz wafer and they hold up a large number of 25-mer-oligonucleotides which represent human transcript sequences from various public sources. To reduce the risk of unspecific signals, for each gene, sixteen different oligonucleotides are coupled to the surface, representing one probe set.²⁸⁷ In more detail, gene expression was herein assessed in Clariom™ S assays (Thermo Fisher Scientific) which enable the determination of over 20,000 well-annotated genes. To this end, cells were treated two days after seeding with 10 μ M Cisplatin or left untreated for control. For statistical purposes, all treatments were performed in biological triplicates and after 16 hours, total RNA was extracted from the cells (chapter 4.4.1).

The following steps were carried out by the DKFZ Microarray Unit: For labeling, the cDNA derived by total RNA was *in vitro* transcribed to cRNA with all uracil bases being tagged with biotin. The labeled cRNA was fragmented into random pieces of 30-400 base pairs, which were then added to the array. The cRNA fragments hybridize to the oligo probes on the chip whenever they are complementary to each other. Unbound RNA was removed by a washing step and the chip was stained with a fluorescent dye (Cy5-streptavidin) that binds to the incorporated biotin on hybridized samples. Fluorescence intensities on the chip surface were measured with a laser scanner and are representative for the level of expression of a certain gene in the sample. At all steps, experimental quality was monitored by the DKFZ Microarray Unit which also provided basic data analysis. This included the quantitative analysis of raw data, quantile normalization over all hybridizations and differential analyses of gene expression data between the given treatments.

Volcano plots for all log₂-transformed fold changes (log₂FC) of the four comparisons were generated in R studio using the *EnhancedVolcano* package.²⁸⁸ Gene set enrichment analysis (GSEA)¹⁹⁶ of the PID_AP1_Pathway¹⁹⁷ was performed using GSEA v. 4.0.3, testing differential gene

expression by their log₂FC values between Cisplatin-treated parental HeLa and Dkk1 KO #3 cells. Statistically significant ($p < 0.05$) differentially regulated genes from the PID_AP1_Pathway of this comparison were plotted in a heatmap for all four pairwise comparison in R studio using the *gplots* package.²⁸⁹

4.5 Protein-related methods

4.5.1 Protein isolation and protein sample preparation

<u>RIPA lysis buffer</u> (pH 7.5)	<u>4x Loading buffer</u>
10 mM Tris	250 mM Tris-HCl
150 mM NaCl	40 % glycerol
1 mM EDTA	20 % β -mercaptoethanol
1 % NP-40	8 % SDS
0.5 % Sodium Deoxycholate	0.008 % bromophenol blue
0.1 % SDS	

Proteins were extracted from cells for immunoblot analyses by chemical lysis using RIPA lysis buffer, which was freshly supplemented with 100 μ L PhosSTOP phosphatase inhibitor cocktail (Roche), 25 μ L Pefabloc (Merck) and 10 μ L P8340 protease inhibitor cocktail (Sigma-Aldrich) per 900 μ L RIPA at the time of harvest. After normoxic incubations, the cells inside the cell culture dishes were washed once in PBS and scraped in PBS into a 1.5 mL tube. The cells were briefly pelleted in a centrifuge (10 s; 13,000 \times g) and were resuspended in 50-100 μ L of RIPA lysis buffer per 60 mm plate. After hypoxic incubations, cells were washed with ice-cold PBS and 150 μ L of RIPA lysis buffer was immediately added to the cells before scraping and transferring them into 1.5 mL tubes. Cells were incubated in lysis buffer on ice and after 30 min cell debris was removed by centrifugation (5 min; 13,000 \times g, 4 °C). The supernatant containing the proteins was transferred into a fresh 1.5 mL tube on ice.

Protein concentrations were determined based on the Bradford method, using the Protein Assay Dye Reagent (BioRad). The concentrated reagent was diluted with water in a ratio of 1:5 and 2 μ L of the protein solution were mixed with 1 mL of the Bradford dye in a Brand® semi-micro disposable cuvette (Merck). After being incubated for 5 min at RT, the absorption of the solution at 595 nm was determined with a photometer (BioPhotometer D30, Eppendorf, Germany). Protein concentrations were calculated using a previously generated standard curve by BSA. The protein

lysates were diluted with 4 x loading buffer to the desired protein concentration and the mixtures were boiled for 5 min at 95 °C. Proteins were stored at -80°C until used for immunoblots.

4.5.2 Protein sample preparation from cell supernatants

For analyses of secreted Dkk1 protein levels, 1 mL of the cell supernatant was transferred into a 1.5 mL tube before harvesting the cells. The supernatant was first centrifuged for 5 min at 1,000 x g to remove residual cells and then transferred to a fresh 1.5 mL tube, followed by another centrifugation step at 13,000 x g for 5 min and 4 °C. 120 µL of the supernatant were mixed with 40 µL of 4 x loading buffer and the mixture was boiled for 5 min at 95 °C. Supernatants were stored at -80 °C and when used for immunoblots, the volume loaded onto the gel was calculated relative to the protein concentration of the corresponding cells as determined in chapter 4.5.2.

4.5.3 SDS polyacrylamide gel electrophoresis (SDS-PAGE)

Tris-Glycine SDS Running buffer

2.5 mM Tris

19.2 mM glycine

0.1 % SDS

SDS polyacrylamide gel electrophoresis (SDS-PAGE) according to Laemmli allows the separation of proteins from cell lysates according to their molecular weight. Polyacrylamide gels were prepared as described in Table 7 in glass plates which had been previously sealed with 1 % agarose. After polymerization, gels were placed in an XCell SureLock™ Mini-Cell Electrophoresis System (Thermo Fisher Scientific) which was filled with Tris-Glycine SDS running buffer. 18-30 µg of protein per sample were loaded onto the gels and 1.5 µL of peqGOLD pre-stained Protein Marker IV (VWR, Avantor) was applied next to the sample as a size marker. Gels were run at 100-120 V for 1.5-2h.

Table 7 | Recipes for polyacrylamide gels for SDS-PAGE.

Stacking Gel	2 Gels (4 %)	Resolving Gel	2 Gels (12 %)
H ₂ O	2 mL	H ₂ O	5.7 mL
0.47 M Tris pH 6.7	1.2 mL	3 M Tris pH 8.9	1.8 mL
30 % acrylamide/bisacrylamide	620 µL	30 % acrylamide/bisacrylamide	5.5 mL
10 % SDS	45.8 mL	10 % SDS	137.5 mL
TEMED	1.8 µL	TEMED	3.4 µL
10 % APS	183.3 µL	10 % APS	176 µL

4.5.4 Immunoblots

<u>Towbin transfer buffer</u> (pH 8.3)	<u>Blocking solution</u> (in PBS)
2.5 mM Tris	5 % skim milk powder
19.2 mM glycine	1 % BSA
20 % methanol	0.2 % Tween-20

Immediately after running gels by SDS-PAGE, proteins were transferred from the gel onto an Immobilon-P PVDF (polyvinylidene fluoride) membrane (Merck) using a Trans-Blot® SD Semi-Dry Electrophoretic Transfer Cell (BioRad). The PVDF membrane was activated in methanol and was subsequently soaked in Towbin transfer buffer together with eight Whatman papers (GE Healthcare). Starting at the anode at the bottom of the transfer system, the blot sandwich was prepared in the following order: four Whatman papers, PVDF membrane, gel, four Whatman papers. After assembling the top part of the blot system composed of the cathode, proteins were transferred to the membrane for 1 h at 20 V, and afterwards the membrane was incubated in blocking solution for 1 h while shaking.

Primary antibodies were prepared in blocking solution according to Table 8 and were incubated on the membranes at 4 °C overnight. After three 10 min-long washing steps in 0.2 % Tween-20-supplemented PBS (PBS-T), the corresponding horseradish-peroxidase (HRP)-conjugated secondary antibody (Table 8) was diluted in blocking solution and was incubated on the membrane for 1-2 h at RT. The membrane was washed as described after primary antibody incubation in PBS-T and protein signals were obtained via enhanced chemiluminescence (ECL) using the ECL™ Prime Western Blotting Detection Reagent (GE Healthcare) or the WesternBright Sirius HRP Substrate (Advansta, San Jose, CA, USA) according to the manufacturer's instructions. Finally, blot images were acquired using the Fusion SL Detection System (Vilber Lourmat, Germany).

4.6 Statistical Analyses

If not indicated otherwise, all experiments were conducted at least thrice as biological replicates with consistent results. Transcript expression determined by qRT-PCR was log₂-transformed for further analyses. Mean values for qRT-PCR, TOP-/FOPflash luciferase activities and TUNEL quantifications, as well as standard deviations were calculated in Microsoft Excel (Microsoft Office 2010). Statistical one-way ANOVA tests were performed using SigmaPlot Software and statistical significances based on p-values are indicated by asterisks (p<0.05 (*), <0.01 (**), <0.001(***)).

Statistical testing of Affymetrix Gene Expression analyses was conducted by the DKFZ Microarray Core Facility.

Table 8 | Primary and secondary antibodies used for immunoblots.

Target	Source	Dilution	Source	Product ID
β-actin	Mouse	1:50,000	Santa Cruz	sc-47778
AKT, phospho (Ser473)	Rabbit	1:1000	Cell Signaling Technology	4058
ATF3	Mouse	1:250	Santa Cruz	sc-81189
β-catenin	Mouse	1:500	BD Pharmingen	610153
active β-catenin (non-phospho)	Rabbit	1:1000	Cell Signaling Technology	8814
BIM	Rabbit	1:1000	Cell Signaling Technology	2933
Caspase 9, cleaved (Asp330)	Rabbit	1:1000	Cell Signaling Technology	7237
c-jun	Rabbit	1:1000	Santa Cruz	sc-74543
c-jun, phospho (Ser63)	Rabbit	1:1000	Cell Signaling Technology	2361S
c-jun, phospho (Ser73)	Rabbit	1:1000	Cell Signaling Technology	9164S
Dkk1	Rabbit	1:500	Cell Signaling Technology	4687
DNMT1	Mouse	1:250	Santa Cruz	sc-271729
EGR1	Rabbit	1:500	Cell Signaling Technology	4153
Fra-1	Rabbit	1:1000	Santa Cruz	sc-605x
HIF-1α	Mouse	1:1,000	BD Pharmingen	610959
HPV 16E6	Mouse	1:2,000	Arbor Vita Corporation (Sunnyvale, CA, USA)	-
HPV 16E7	Mouse	1:1,000	Kind gift from Dr. Müller, DKFZ Heidelberg	-
HPV 18E6	Mouse	1:2,000	Arbor Vita Corporation (Sunnyvale, CA, USA)	-
HPV 18E7	Chicken	1:2,000	Zentgraf, DKFZ Heidelberg	B(28)#47 31.10.-11.11.95
JNK/SAPK	Rabbit	1:1,000	Cell Signaling Technology	9252
JNK/SAPK, phospho (Thr183/Tyr185)	Rabbit	1:1,000	Cell Signaling Technology	4668S
p53 (DO-1)	Mouse	1:1,000	Santa Cruz	sc-126
PARP, cleaved (Asp214)	Mouse	1:1,000	Cell Signaling Technology	9546
Tubulin, acetylated	Mouse	1:1,000	Sigma Aldrich	T6793
Tubulin	Mouse	1:1,5000	Sigma Aldrich	CP06
Vinculin	Mouse	1:4,000	Santa Cruz	sc-73614

HRP-conjugated secondary antibodies

Target	Dilution	Source	ID
Chicken	1:10,000	Santa Cruz	sc-2428
Mouse	1:5,000	Santa Cruz	sc-2005
Rabbit	1:5,000	Santa Cruz	sc-2004

APPENDIX

Appendix

List of Figures

Figure 1 Cancers attributable to HPV infection in 2018.	4
Figure 2 HPV genome organization and life cycle in the progression to cancer.	5
Figure 3 Cooperative effect of HPV E6 and E7 to disrupt tumor suppressor pathways.	7
Figure 4 Schematic representation of Cisplatin-related cellular mechanisms.	10
Figure 5 Domain structure and lengths (aa: amino acids) of Dkk1-4 and the Dkk3-related factor soggy.	11
Figure 6 Modulation of Wnt signaling by Dkk1.	13
Figure 7 Extrinsic and intrinsic apoptosis pathways and interference with HPV E6/E7.	17
Figure 8 Silencing of the HPV oncogenes induces Dkk1 expression in cervical cancer cells.	26
Figure 9 siE6/E7-mediated induction of Dkk1 is dependent on p53 stabilization.	27
Figure 10 Dkk1 downregulation does not affect HPV E6 or HPV E7 expression.	28
Figure 11 Hypoxic Dkk1 regulation in HPV-positive and HPV-negative cancer cells.	29
Figure 12 OXPHOS inhibition represses Dkk1 in a glucose-dependent manner.	31
Figure 13 Dkk1 is transiently repressed in parallel with p53 under hypoxia.	32
Figure 14 p53 affects Dkk1 regulation under hypoxia on the protein but not on the transcript level.	33
Figure 15 The effect of 5-Azacytidine and Trichostatin A on Dkk1 regulation.	34
Figure 16 5-Azacytidine or TSA treatments do not counteract hypoxic Dkk1 repression.	36
Figure 17 Effect of Cisplatin on Dkk1 expression in cervical cancer cells.	37
Figure 18 Apoptosis induction in HeLa* cells upon Dkk1 overexpression.	38
Figure 19 Dkk1 conditioned medium enhances Cisplatin-induced apoptosis in HeLa cells.	39
Figure 20 Silencing of Dkk1 reduces Cisplatin-mediated apoptosis in cervical cancer cells.	41
Figure 21 Dkk1 knockout HeLa cells exhibit increased resistance towards Cisplatin-mediated apoptosis.	42
Figure 22 Senescence induction in Cisplatin-treated Dkk1 KO HeLa cells.	44
Figure 23 Dkk1 conditioned medium counteracts Wnt3a-induced TOPflash activities.	45
Figure 24 Cisplatin does not affect canonical Wnt signaling activities in HeLa cells.	46
Figure 25 Global gene alterations between Cisplatin-treated parental HeLa and Dkk1 KO HeLa cells.	48

Figure 26 Reduced activation of AP-1 signaling components in the Cisplatin response upon Dkk1 depletion.	50
Figure 27 Validation of Bim and EGR1 expression after Cisplatin treatment.	52
Figure 28 Impaired JNK activation in Dkk1-depleted HeLa cells contributes to Cisplatin resistance.	54
Figure 29 JNK activity is required for Cisplatin-induced apoptosis in SiHa and Caski cells.	56
Figure 30 Schematic model of Dkk1 regulation and its function in Cisplatin-induced apoptosis.	75

List of Tables

Table 1 Suppliers of standard reagents and materials.	79
Table 2 List of plasmids.	80
Table 3 Synthetic siRNAs (Silencer® Select).	85
Table 4 Compounds for chemical treatment of cells.	87
Table 5 qRT-PCR program.	93
Table 6 Primer pairs for qRT-PCR analyses.	93
Table 7 Recipes for polyacrylamide gels for SDS-PAGE.	96
Table 8 Primary and secondary antibodies used for immunoblots.	98

Abbreviations

5-Aza	5-Azacytidine
aa	amino acids
AP-1	activator protein 1
APAF-1	apoptotic protease-activating factor 1
APC	adenomatous-polyposis-coli
ATF	activating transcription factor
ATP	adenosine triphosphate
ATR	ataxia telangiectasia and Rad3-related protein
β-gal	β-galactosidase
BH3	Bcl-2 homology
BLAST	basic local alignment search tool
BMP	bone morphogenetic protein
bp	base pair
bZIP	basic-region leucine zipper
Cas9	CRISPR-associated protein 9
CDDP	Cisplatin [cis-diamminedichloroplatinum(II)]
cDNA	complementary deoxyribonucleic acid
CFA	colony formation assay
CIN	cervical intraepithelial neoplasia

CIP	calf intestinal alkaline phosphatase
CK1 α	casein kinase 1 α
CKAP4	cytoskeleton associated protein 4
CM	conditioned medium
CRE	cAMP response element
CRISPR	clustered regularly interspaced short palindromic repeats
CPX	Ciclopirox
Ct	cycle threshold
Ctr1	copper transporter 1
Ctrl	Control
CytC	cytochrome c
DISC	death inducing signaling complex
DMEM	Dulbecco's Modified Eagle's Medium
DNA	deoxyribonucleic acid
DNMT1	DNA methyltransferase 1
dNTPs	deoxynucleotide triphosphates
Dkk	Dickkopf
DR4/5	death receptor 4/5
DREAM	dimerization partner, RB-like, E2F and multi-vulval class B
Dvl	Dishevelled
E6AP	E6-associated protein
ECL	enhanced chemiluminescence
EGR1	early growth response gene 1
ERK	extracellular-signal regulated kinase
EZH2	enhancer of zeste homolog 2
FasL	Fas ligand
FasR	Fas receptor
FBS	fetal bovine serum
FGFR	fibroblast growth factor receptor
Fzd	Frizzled
gRNA	guide ribonucleic acid
GSEA	Gene Set Enrichment Analysis
GSH	glutathione
GSK-3 β	glycogen synthase kinase 3 β
HDAC	histone deacetylase
HIF-1 α	hypoxia-inducible factor 1 α
HPV	human papillomavirus
HRE	hypoxia response element
HRP	horse redish peroxidase
HSPG	heparan sulfate proteoglycan
IAP	inhibitor of apoptosis
IL	interleukin
JNK	c-Jun N-terminal kinase
KO	knockout
Krm	Kremen
LB	Lysogeny Broth
LCR	long coding region
LRP5/6	low density lipoprotein reprotor 5/6
MAP2K	mitogen-activated protein kinase kinase

MAP3K	mitogen-activated protein kinase kinase kinase
MAPK	mitogen-activated protein kinase
MAREs	Maf recognition elements
MKK4/7	mitogen-activated protein kinase kinase 4/7
MOMP	mitochondrial outer membrane permeabilization
mTORC2	mammalian target of rapamycin complex 2
mRNA	messenger ribonucleic acid
NES	normalized enrichment score
NGF	nerve growth factor
NHEJ	non-homologous end joining pathway
ONPG	ortho-nitrophenyl β -galactosidase
ORF	open reading frame (ORF)
OXPHOS	oxidative phosphorylation
p53RE	p53 response element
PAM	protospacer adjacent motif
PARP	poly (ADP-ribose)-polymerase
PCP	planar cell polarity
PD-1	programmed cell death protein 1
PFA	paraformaldehyde
PI3K	phosphoinositide 3-kinase
PNK	polynucleotide kinase
PLC	phospholipase C
pRb	retinoblastoma protein
PV	papillomavirus
PVDF	polyvinylidene flouride
qRT-PCR	quantitative real time – polymerase chain reaction
RIPA	radioimmunoprecipitation buffer
RNA	ribonucleic acid
RNAi	RNA interference
ROCK	Rho kinase
rRNA	ribosomal ribonucleic acid
RT	room temperature
SA	senescence assay
SA- β -gal	senescence-associated β -galactosidase
SASP	senescence-associated secretory phenotype
SDS	sodium dodecyl sulfate
SDS-PAGE	sodium dodecyl sulfate-polyacrylamide gel electrophoresis
siRNA	small interfering ribonucleic acid
Smac	second mitochondria-derived activator of caspase
TCF/LEF	T-cell factor/lymphoid enhancer factor
TGF β	transforming growth factor β
TNF	tumor necrosis factor
TNFR	tumor necrosis factor receptor
TPA	12-O-Tetradecanoylphorbol-13-acetate
TRAIL	tumor necrosis factor related apoptosis inducing ligand
TRE	12-O-Tetradecanoylphorbol-13-acetate DNA response element
TSA	Trichostatin A
TUNEL	terminal deoxynucleotidyl transferase dUTP nick end labeling
URR	upstream regulatory region

VEGFR	vascular endothelial growth factor receptor
X-Gal	5-bromo-4-chloro-3-indolyl β -galactosidase

Nucleotides are named by the one-letter code and amino acids by their three-letter code according to declarations by the International Union of Pure and Applied Chemistry (IUPAC).

Units

<i>Symbol</i>	<i>Unit</i>
%	percent
°C	degree Celsius
d	day
Da	Dalton
<i>g</i>	gravitational acceleration
g	gram
h	hour
L	liter
M	molar
m	meter
min	minute
rpm	revolutions per minute

Prefixes

<i>Symbol</i>	<i>Prefix</i>	<i>Factor</i>
n	nano	10^{-9}
μ	micro	10^{-6}
m	milli	10^{-3}
k	kilo	10^3

References

1. Sung H, Ferlay J, Siegel RL, et al. Global Cancer Statistics 2020: GLOBOCAN Estimates of Incidence and Mortality Worldwide for 36 Cancers in 185 Countries. *CA Cancer J Clin.* 2021;71(3):209-249.
2. de Magalhaes JP. How ageing processes influence cancer. *Nat Rev Cancer.* 2013;13(5):357-365.
3. Khan N, Afaq F, Mukhtar H. Lifestyle as risk factor for cancer: Evidence from human studies. *Cancer Lett.* 2010;293(2):133-143.
4. Basu AK. DNA Damage, Mutagenesis and Cancer. *Int J Mol Sci.* 2018;19(4).
5. De Flora S, Bonanni P. The prevention of infection-associated cancers. *Carcinogenesis.* 2011;32(6):787-795.
6. de Martel C, Georges D, Bray F, Ferlay J, Clifford GM. Global burden of cancer attributable to infections in 2018: a worldwide incidence analysis. *Lancet Glob Health.* 2020;8(2):e180-e190.
7. Schiffman M, Castle PE, Jeronimo J, Rodriguez AC, Wacholder S. Human papillomavirus and cervical cancer. *Lancet.* 2007;370(9590):890-907.
8. Bernard HU, Burk RD, Chen Z, van Doorslaer K, zur Hausen H, de Villiers EM. Classification of papillomaviruses (PVs) based on 189 PV types and proposal of taxonomic amendments. *Virology.* 2010;401(1):70-79.
9. Doorbar J, Quint W, Banks L, et al. The biology and life-cycle of human papillomaviruses. *Vaccine.* 2012;30 Suppl 5:F55-70.
10. Bouvard V, Baan R, Straif K, et al. A review of human carcinogens--Part B: biological agents. *Lancet Oncol.* 2009;10(4):321-322.
11. Doorbar J, Egawa N, Griffin H, Kranjec C, Murakami I. Human papillomavirus molecular biology and disease association. *Rev Med Virol.* 2015;25 Suppl 1:2-23.
12. de Sanjose S, Quint WG, Alemany L, et al. Human papillomavirus genotype attribution in invasive cervical cancer: a retrospective cross-sectional worldwide study. *Lancet Oncol.* 2010;11(11):1048-1056.
13. Hildesheim A, Herrero R, Castle PE, et al. HPV co-factors related to the development of cervical cancer: results from a population-based study in Costa Rica. *Br J Cancer.* 2001;84(9):1219-1226.
14. Moreno V, Bosch FX, Munoz N, et al. Effect of oral contraceptives on risk of cervical cancer in women with human papillomavirus infection: the IARC multicentric case-control study. *Lancet.* 2002;359(9312):1085-1092.
15. Munoz N, Franceschi S, Bosetti C, et al. Role of parity and human papillomavirus in cervical cancer: the IARC multicentric case-control study. *Lancet.* 2002;359(9312):1093-1101.
16. Yang X, Jin G, Nakao Y, Rahimtula M, Pater MM, Pater A. Malignant transformation of HPV 16-immortalized human endocervical cells by cigarette smoke condensate and characterization of multistage carcinogenesis. *Int J Cancer.* 1996;65(3):338-344.
17. Ronco G, Dillner J, Elfstrom KM, et al. Efficacy of HPV-based screening for prevention of invasive cervical cancer: follow-up of four European randomised controlled trials. *Lancet.* 2014;383(9916):524-532.
18. Harper DM, DeMars LR. HPV vaccines - A review of the first decade. *Gynecol Oncol.* 2017;146(1):196-204.
19. Drolet M, Benard E, Perez N, Brisson M, Group HPVVIS. Population-level impact and herd effects following the introduction of human papillomavirus vaccination programmes: updated systematic review and meta-analysis. *Lancet.* 2019;394(10197):497-509.
20. Drolet M, Laprise JF, Martin D, et al. Optimal human papillomavirus vaccination strategies to prevent cervical cancer in low-income and middle-income countries in the context of limited resources: a mathematical modelling analysis. *Lancet Infect Dis.* 2021;21(11):1598-1610.
21. Doorbar J. Molecular biology of human papillomavirus infection and cervical cancer. *Clin Sci (Lond).* 2006;110(5):525-541.
22. Doorbar J, Gallimore PH. Identification of proteins encoded by the L1 and L2 open reading frames of human papillomavirus 1a. *J Virol.* 1987;61(9):2793-2799.

23. Venuti A, Paolini F, Nasir L, et al. Papillomavirus E5: the smallest oncoprotein with many functions. *Mol Cancer*. 2011;10:140.
24. White EA. Manipulation of Epithelial Differentiation by HPV Oncoproteins. *Viruses*. 2019;11(4).
25. Giroglou T, Florin L, Schafer F, Streeck RE, Sapp M. Human papillomavirus infection requires cell surface heparan sulfate. *J Virol*. 2001;75(3):1565-1570.
26. Richards RM, Lowy DR, Schiller JT, Day PM. Cleavage of the papillomavirus minor capsid protein, L2, at a furin consensus site is necessary for infection. *Proc Natl Acad Sci U S A*. 2006;103(5):1522-1527.
27. Horvath CA, Boulet GA, Renoux VM, Delvenne PO, Bogers JP. Mechanisms of cell entry by human papillomaviruses: an overview. *Viol J*. 2010;7:11.
28. Smith PP, Friedman CL, Bryant EM, McDougall JK. Viral integration and fragile sites in human papillomavirus-immortalized human keratinocyte cell lines. *Genes Chromosomes Cancer*. 1992;5(2):150-157.
29. zur Hausen H. Papillomaviruses and cancer: from basic studies to clinical application. *Nat Rev Cancer*. 2002;2(5):342-350.
30. Hoppe-Seyler K, Bossler F, Braun JA, Herrmann AL, Hoppe-Seyler F. The HPV E6/E7 Oncogenes: Key Factors for Viral Carcinogenesis and Therapeutic Targets. *Trends Microbiol*. 2018;26(2):158-168.
31. Bernard BA, Bailly C, Lenoir MC, Darmon M, Thierry F, Yaniv M. The human papillomavirus type 18 (HPV18) E2 gene product is a repressor of the HPV18 regulatory region in human keratinocytes. *J Virol*. 1989;63(10):4317-4324.
32. McBride AA, Warburton A. The role of integration in oncogenic progression of HPV-associated cancers. *PLoS Pathog*. 2017;13(4):e1006211.
33. Dooley KE, Warburton A, McBride AA. Tandemly Integrated HPV16 Can Form a Brd4-Dependent Super-Enhancer-Like Element That Drives Transcription of Viral Oncogenes. *mBio*. 2016;7(5).
34. Tang S, Tao M, McCoy JP, Jr., Zheng ZM. The E7 oncoprotein is translated from spliced E6*1 transcripts in high-risk human papillomavirus type 16- or type 18-positive cervical cancer cell lines via translation reinitiation. *J Virol*. 2006;80(9):4249-4263.
35. Butz K, Hoppe-Seyler F. Transcriptional control of human papillomavirus (HPV) oncogene expression: composition of the HPV type 18 upstream regulatory region. *J Virol*. 1993;67(11):6476-6486.
36. Jabbar SF, Park S, Schweizer J, et al. Cervical cancers require the continuous expression of the human papillomavirus type 16 E7 oncoprotein even in the presence of the viral E6 oncoprotein. *Cancer Res*. 2012;72(16):4008-4016.
37. Butz K, Denk C, Ullmann A, Scheffner M, Hoppe-Seyler F. Induction of apoptosis in human papillomavirus-positive cancer cells by peptide aptamers targeting the viral E6 oncoprotein. *Proc Natl Acad Sci U S A*. 2000;97(12):6693-6697.
38. Butz K, Ristriani T, Hengstermann A, Denk C, Scheffner M, Hoppe-Seyler F. siRNA targeting of the viral E6 oncogene efficiently kills human papillomavirus-positive cancer cells. *Oncogene*. 2003;22(38):5938-5945.
39. Goodwin EC, DiMaio D. Repression of human papillomavirus oncogenes in HeLa cervical carcinoma cells causes the orderly reactivation of dormant tumor suppressor pathways. *Proc Natl Acad Sci U S A*. 2000;97(23):12513-12518.
40. Hall AH, Alexander KA. RNA interference of human papillomavirus type 18 E6 and E7 induces senescence in HeLa cells. *J Virol*. 2003;77(10):6066-6069.
41. Roman A, Munger K. The papillomavirus E7 proteins. *Virology*. 2013;445(1-2):138-168.
42. Zhang HS, Postigo AA, Dean DC. Active transcriptional repression by the Rb-E2F complex mediates G1 arrest triggered by p16INK4a, TGFbeta, and contact inhibition. *Cell*. 1999;97(1):53-61.

43. Boyer SN, Wazer DE, Band V. E7 protein of human papilloma virus-16 induces degradation of retinoblastoma protein through the ubiquitin-proteasome pathway. *Cancer Res.* 1996;56(20):4620-4624.
44. Rashid NN, Rothan HA, Yusoff MS. The association of mammalian DREAM complex and HPV16 E7 proteins. *Am J Cancer Res.* 2015;5(12):3525-3533.
45. Scheffner M, Huibregtse JM, Vierstra RD, Howley PM. The HPV-16 E6 and E6-AP complex functions as a ubiquitin-protein ligase in the ubiquitination of p53. *Cell.* 1993;75(3):495-505.
46. Klingelhutz AJ, Foster SA, McDougall JK. Telomerase activation by the E6 gene product of human papillomavirus type 16. *Nature.* 1996;380(6569):79-82.
47. Duensing S, Munger K. Mechanisms of genomic instability in human cancer: insights from studies with human papillomavirus oncoproteins. *Int J Cancer.* 2004;109(2):157-162.
48. Thomas M, Myers MP, Massimi P, Guarnaccia C, Banks L. Analysis of Multiple HPV E6 PDZ Interactions Defines Type-Specific PDZ Fingerprints That Predict Oncogenic Potential. *PLoS Pathog.* 2016;12(8):e1005766.
49. Hanahan D, Weinberg RA. Hallmarks of cancer: the next generation. *Cell.* 2011;144(5):646-674.
50. Bertout JA, Patel SA, Simon MC. The impact of O₂ availability on human cancer. *Nat Rev Cancer.* 2008;8(12):967-975.
51. Masoud GN, Li W. HIF-1 α pathway: role, regulation and intervention for cancer therapy. *Acta Pharm Sin B.* 2015;5(5):378-389.
52. Al Tameemi W, Dale TP, Al-Jumaily RMK, Forsyth NR. Hypoxia-Modified Cancer Cell Metabolism. *Front Cell Dev Biol.* 2019;7:4.
53. Vaupel P, Hockel M, Mayer A. Detection and characterization of tumor hypoxia using pO₂ histography. *Antioxid Redox Signal.* 2007;9(8):1221-1235.
54. Hoppe-Seyler K, Bossler F, Lohrey C, et al. Induction of dormancy in hypoxic human papillomavirus-positive cancer cells. *Proc Natl Acad Sci U S A.* 2017;114(6):E990-E998.
55. Bossler F, Kuhn BJ, Gunther T, et al. Repression of Human Papillomavirus Oncogene Expression under Hypoxia Is Mediated by PI3K/mTORC2/AKT Signaling. *mBio.* 2019;10(1).
56. Society AC. Treatment Options for Cervical Cancer, by Stage. <https://www.cancer.org/cancer/cervical-cancer/treating/by-stage.html>. Accessed March 17, 2022.
57. Rose PG, Bundy BN, Watkins EB, et al. Concurrent cisplatin-based radiotherapy and chemotherapy for locally advanced cervical cancer. *N Engl J Med.* 1999;340(15):1144-1153.
58. Choi IJ, Cha MS, Park ES, et al. The efficacy of concurrent cisplatin and 5-fluorouracil chemotherapy and radiation therapy for locally advanced cancer of the uterine cervix. *J Gynecol Oncol.* 2008;19(2):129-134.
59. Lorusso D, Petrelli F, Coinu A, Raspagliesi F, Barni S. A systematic review comparing cisplatin and carboplatin plus paclitaxel-based chemotherapy for recurrent or metastatic cervical cancer. *Gynecol Oncol.* 2014;133(1):117-123.
60. Frenel JS, Le Tourneau C, O'Neil B, et al. Safety and Efficacy of Pembrolizumab in Advanced, Programmed Death Ligand 1-Positive Cervical Cancer: Results From the Phase Ib KEYNOTE-028 Trial. *J Clin Oncol.* 2017;35(36):4035-4041.
61. Tewari KS, Sill MW, Penson RT, et al. Bevacizumab for advanced cervical cancer: final overall survival and adverse event analysis of a randomised, controlled, open-label, phase 3 trial (Gynecologic Oncology Group 240). *Lancet.* 2017;390(10103):1654-1663.
62. Rosenberg B, Vancamp L, Krigas T. Inhibition of Cell Division in Escherichia Coli by Electrolysis Products from a Platinum Electrode. *Nature.* 1965;205:698-699.
63. Dasari S, Tchounwou PB. Cisplatin in cancer therapy: molecular mechanisms of action. *Eur J Pharmacol.* 2014;740:364-378.
64. Ciarimboli G. Membrane transporters as mediators of Cisplatin effects and side effects. *Scientifica (Cairo).* 2012;2012:473829.
65. Eastman A. The formation, isolation and characterization of DNA adducts produced by anticancer platinum complexes. *Pharmacol Ther.* 1987;34(2):155-166.

66. Siddik ZH. Cisplatin: mode of cytotoxic action and molecular basis of resistance. *Oncogene*. 2003;22(47):7265-7279.
67. Zhao H, Piwnicka-Worms H. ATR-mediated checkpoint pathways regulate phosphorylation and activation of human Chk1. *Mol Cell Biol*. 2001;21(13):4129-4139.
68. Zhu H, Luo H, Zhang W, Shen Z, Hu X, Zhu X. Molecular mechanisms of cisplatin resistance in cervical cancer. *Drug Des Devel Ther*. 2016;10:1885-1895.
69. Galluzzi L, Senovilla L, Vitale I, et al. Molecular mechanisms of cisplatin resistance. *Oncogene*. 2012;31(15):1869-1883.
70. Branch P, Masson M, Aquilina G, Bignami M, Karran P. Spontaneous development of drug resistance: mismatch repair and p53 defects in resistance to cisplatin in human tumor cells. *Oncogene*. 2000;19(28):3138-3145.
71. Achkar IW, Abdulrahman N, Al-Sulaiti H, Joseph JM, Uddin S, Mraiche F. Cisplatin based therapy: the role of the mitogen activated protein kinase signaling pathway. *J Transl Med*. 2018;16(1):96.
72. Glinka A, Wu W, Delius H, Monaghan AP, Blumenstock C, Niehrs C. Dickkopf-1 is a member of a new family of secreted proteins and functions in head induction. *Nature*. 1998;391(6665):357-362.
73. Fedi P, Bafico A, Nieto Soria A, et al. Isolation and biochemical characterization of the human Dkk-1 homologue, a novel inhibitor of mammalian Wnt signaling. *J Biol Chem*. 1999;274(27):19465-19472.
74. Niehrs C. Function and biological roles of the Dickkopf family of Wnt modulators. *Oncogene*. 2006;25(57):7469-7481.
75. Krupnik VE, Sharp JD, Jiang C, et al. Functional and structural diversity of the human Dickkopf gene family. *Gene*. 1999;238(2):301-313.
76. Haniu M, Horan T, Spahr C, et al. Human Dickkopf-1 (huDKK1) protein: characterization of glycosylation and determination of disulfide linkages in the two cysteine-rich domains. *Protein Sci*. 2011;20(11):1802-1813.
77. Aravind L, Koonin EV. A colipase fold in the carboxy-terminal domain of the Wnt antagonists--the Dickkopfs. *Curr Biol*. 1998;8(14):R477-478.
78. Monaghan AP, Kioschis P, Wu W, et al. Dickkopf genes are co-ordinately expressed in mesodermal lineages. *Mech Dev*. 1999;87(1-2):45-56.
79. Kemp C, Willems E, Abdo S, Lambiv L, Leyns L. Expression of all Wnt genes and their secreted antagonists during mouse blastocyst and postimplantation development. *Dev Dyn*. 2005;233(3):1064-1075.
80. Uhlen M, Fagerberg L, Hallstrom BM, et al. Proteomics. Tissue-based map of the human proteome. *Science*. 2015;347(6220):1260419.
81. Hashimoto H, Itoh M, Yamanaka Y, et al. Zebrafish Dkk1 functions in forebrain specification and axial mesendoderm formation. *Dev Biol*. 2000;217(1):138-152.
82. Mukhopadhyay M, Shtrom S, Rodriguez-Esteban C, et al. Dickkopf1 is required for embryonic head induction and limb morphogenesis in the mouse. *Dev Cell*. 2001;1(3):423-434.
83. Glinka A, Wu W, Onichtchouk D, Blumenstock C, Niehrs C. Head induction by simultaneous repression of Bmp and Wnt signalling in *Xenopus*. *Nature*. 1997;389(6650):517-519.
84. Zhan T, Rindtorff N, Boutros M. Wnt signaling in cancer. *Oncogene*. 2017;36(11):1461-1473.
85. Pinzone JJ, Hall BM, Thudi NK, et al. The role of Dickkopf-1 in bone development, homeostasis, and disease. *Blood*. 2009;113(3):517-525.
86. Niehrs C. The complex world of WNT receptor signalling. *Nat Rev Mol Cell Biol*. 2012;13(12):767-779.
87. Kimelman D, Xu W. beta-catenin destruction complex: insights and questions from a structural perspective. *Oncogene*. 2006;25(57):7482-7491.
88. Niida A, Hiroko T, Kasai M, et al. DKK1, a negative regulator of Wnt signaling, is a target of the beta-catenin/TCF pathway. *Oncogene*. 2004;23(52):8520-8526.

89. Ahn VE, Chu ML, Choi HJ, Tran D, Abo A, Weis WI. Structural basis of Wnt signaling inhibition by Dickkopf binding to LRP5/6. *Dev Cell*. 2011;21(5):862-873.
90. Brott BK, Sokol SY. Regulation of Wnt/LRP signaling by distinct domains of Dickkopf proteins. *Mol Cell Biol*. 2002;22(17):6100-6110.
91. Bourhis E, Tam C, Franke Y, et al. Reconstitution of a frizzled8.Wnt3a.LRP6 signaling complex reveals multiple Wnt and Dkk1 binding sites on LRP6. *J Biol Chem*. 2010;285(12):9172-9179.
92. Mao B, Wu W, Davidson G, et al. Kremen proteins are Dickkopf receptors that regulate Wnt/beta-catenin signalling. *Nature*. 2002;417(6889):664-667.
93. Yamamoto H, Sakane H, Yamamoto H, Michiue T, Kikuchi A. Wnt3a and Dkk1 regulate distinct internalization pathways of LRP6 to tune the activation of beta-catenin signaling. *Dev Cell*. 2008;15(1):37-48.
94. Ellwanger K, Saito H, Clement-Lacroix P, et al. Targeted disruption of the Wnt regulator Kremen induces limb defects and high bone density. *Mol Cell Biol*. 2008;28(15):4875-4882.
95. Wang K, Zhang Y, Li X, et al. Characterization of the Kremen-binding site on Dkk1 and elucidation of the role of Kremen in Dkk-mediated Wnt antagonism. *J Biol Chem*. 2008;283(34):23371-23375.
96. Katoh M. WNT/PCP signaling pathway and human cancer (review). *Oncol Rep*. 2005;14(6):1583-1588.
97. Pandur P, Lasche M, Eisenberg LM, Kuhl M. Wnt-11 activation of a non-canonical Wnt signalling pathway is required for cardiogenesis. *Nature*. 2002;418(6898):636-641.
98. Shou J, Ali-Osman F, Multani AS, Pathak S, Fedi P, Srivenugopal KS. Human Dkk-1, a gene encoding a Wnt antagonist, responds to DNA damage and its overexpression sensitizes brain tumor cells to apoptosis following alkylating damage of DNA. *Oncogene*. 2002;21(6):878-889.
99. Grotewold L, Ruther U. The Wnt antagonist Dickkopf-1 is regulated by Bmp signaling and c-Jun and modulates programmed cell death. *EMBO J*. 2002;21(5):966-975.
100. Kimura H, Fumoto K, Shojima K, et al. CKAP4 is a Dickkopf1 receptor and is involved in tumor progression. *J Clin Invest*. 2016;126(7):2689-2705.
101. Menezes ME, Devine DJ, Shevde LA, Samant RS. Dickkopf1: a tumor suppressor or metastasis promoter? *Int J Cancer*. 2012;130(7):1477-1483.
102. Tian E, Zhan F, Walker R, et al. The role of the Wnt-signaling antagonist DKK1 in the development of osteolytic lesions in multiple myeloma. *N Engl J Med*. 2003;349(26):2483-2494.
103. Bu G, Lu W, Liu CC, et al. Breast cancer-derived Dickkopf1 inhibits osteoblast differentiation and osteoprotegerin expression: implication for breast cancer osteolytic bone metastases. *Int J Cancer*. 2008;123(5):1034-1042.
104. Hall CL, Daignault SD, Shah RB, Pienta KJ, Keller ET. Dickkopf-1 expression increases early in prostate cancer development and decreases during progression from primary tumor to metastasis. *Prostate*. 2008;68(13):1396-1404.
105. Kagey MH, He X. Rationale for targeting the Wnt signalling modulator Dickkopf-1 for oncology. *Br J Pharmacol*. 2017;174(24):4637-4650.
106. Han SX, Zhou X, Sui X, et al. Serum dickkopf-1 is a novel serological biomarker for the diagnosis and prognosis of pancreatic cancer. *Oncotarget*. 2015;6(23):19907-19917.
107. Tao YM, Liu Z, Liu HL. Dickkopf-1 (DKK1) promotes invasion and metastasis of hepatocellular carcinoma. *Dig Liver Dis*. 2013;45(3):251-257.
108. Iyer SP, Beck JT, Stewart AK, et al. A Phase IB multicentre dose-determination study of BHQ880 in combination with anti-myeloma therapy and zoledronic acid in patients with relapsed or refractory multiple myeloma and prior skeletal-related events. *Br J Haematol*. 2014;167(3):366-375.
109. Wall JA, Klempner SJ, Arend RC. The anti-DKK1 antibody DKN-01 as an immunomodulatory combination partner for the treatment of cancer. *Expert Opin Investig Drugs*. 2020;29(7):639-644.
110. Aguilera O, Fraga MF, Ballestar E, et al. Epigenetic inactivation of the Wnt antagonist DICKKOPF-1 (DKK-1) gene in human colorectal cancer. *Oncogene*. 2006;25(29):4116-4121.

111. Lee J, Yoon YS, Chung JH. Epigenetic silencing of the WNT antagonist DICKKOPF-1 in cervical cancer cell lines. *Gynecol Oncol.* 2008;109(2):270-274.
112. Sato H, Suzuki H, Toyota M, et al. Frequent epigenetic inactivation of DICKKOPF family genes in human gastrointestinal tumors. *Carcinogenesis.* 2007;28(12):2459-2466.
113. Vibhakar R, Foltz G, Yoon JG, et al. Dickkopf-1 is an epigenetically silenced candidate tumor suppressor gene in medulloblastoma. *Neuro Oncol.* 2007;9(2):135-144.
114. Wang J, Shou J, Chen X. Dickkopf-1, an inhibitor of the Wnt signaling pathway, is induced by p53. *Oncogene.* 2000;19(14):1843-1848.
115. Gosepath EM, Eckstein N, Hamacher A, et al. Acquired cisplatin resistance in the head-neck cancer cell line Cal27 is associated with decreased DKK1 expression and can partially be reversed by overexpression of DKK1. *Int J Cancer.* 2008;123(9):2013-2019.
116. Lee AY, He B, You L, et al. Dickkopf-1 antagonizes Wnt signaling independent of beta-catenin in human mesothelioma. *Biochem Biophys Res Commun.* 2004;323(4):1246-1250.
117. Peng S, Miao C, Li J, Fan X, Cao Y, Duan E. Dickkopf-1 induced apoptosis in human placental choriocarcinoma is independent of canonical Wnt signaling. *Biochem Biophys Res Commun.* 2006;350(3):641-647.
118. Mikheev AM, Mikheeva SA, Liu B, Cohen P, Zarbl H. A functional genomics approach for the identification of putative tumor suppressor genes: Dickkopf-1 as suppressor of HeLa cell transformation. *Carcinogenesis.* 2004;25(1):47-59.
119. Brill A, Torchinsky A, Carp H, Toder V. The role of apoptosis in normal and abnormal embryonic development. *J Assist Reprod Genet.* 1999;16(10):512-519.
120. Arandjelovic S, Ravichandran KS. Phagocytosis of apoptotic cells in homeostasis. *Nat Immunol.* 2015;16(9):907-917.
121. Cohen JJ. Programmed cell death in the immune system. *Adv Immunol.* 1991;50:55-85.
122. Norbury CJ, Hickson ID. Cellular responses to DNA damage. *Annu Rev Pharmacol Toxicol.* 2001;41:367-401.
123. Wong RS. Apoptosis in cancer: from pathogenesis to treatment. *J Exp Clin Cancer Res.* 2011;30:87.
124. Rock KL, Kono H. The inflammatory response to cell death. *Annu Rev Pathol.* 2008;3:99-126.
125. Kerr JF, Wyllie AH, Currie AR. Apoptosis: a basic biological phenomenon with wide-ranging implications in tissue kinetics. *Br J Cancer.* 1972;26(4):239-257.
126. Shi Y. Mechanisms of caspase activation and inhibition during apoptosis. *Mol Cell.* 2002;9(3):459-470.
127. Ashkenazi A, Dixit VM. Death receptors: signaling and modulation. *Science.* 1998;281(5381):1305-1308.
128. Pan G, Ni J, Wei YF, Yu G, Gentz R, Dixit VM. An antagonist decoy receptor and a death domain-containing receptor for TRAIL. *Science.* 1997;277(5327):815-818.
129. Kischkel FC, Hellbardt S, Behrmann I, et al. Cytotoxicity-dependent APO-1 (Fas/CD95)-associated proteins form a death-inducing signaling complex (DISC) with the receptor. *EMBO J.* 1995;14(22):5579-5588.
130. Li H, Zhu H, Xu CJ, Yuan J. Cleavage of BID by caspase 8 mediates the mitochondrial damage in the Fas pathway of apoptosis. *Cell.* 1998;94(4):491-501.
131. Kale J, Osterlund EJ, Andrews DW. BCL-2 family proteins: changing partners in the dance towards death. *Cell Death Differ.* 2018;25(1):65-80.
132. Tait SW, Green DR. Mitochondria and cell death: outer membrane permeabilization and beyond. *Nat Rev Mol Cell Biol.* 2010;11(9):621-632.
133. Riedl SJ, Shi Y. Molecular mechanisms of caspase regulation during apoptosis. *Nat Rev Mol Cell Biol.* 2004;5(11):897-907.
134. Du C, Fang M, Li Y, Li L, Wang X. Smac, a mitochondrial protein that promotes cytochrome c-dependent caspase activation by eliminating IAP inhibition. *Cell.* 2000;102(1):33-42.

135. Germain M, Affar EB, D'Amours D, Dixit VM, Salvesen GS, Poirier GG. Cleavage of automodified poly(ADP-ribose) polymerase during apoptosis. Evidence for involvement of caspase-7. *J Biol Chem.* 1999;274(40):28379-28384.
136. Crowley LC, Waterhouse NJ. Detecting Cleaved Caspase-3 in Apoptotic Cells by Flow Cytometry. *Cold Spring Harb Protoc.* 2016;2016(11).
137. Kaufmann SH, Desnoyers S, Ottaviano Y, Davidson NE, Poirier GG. Specific proteolytic cleavage of poly(ADP-ribose) polymerase: an early marker of chemotherapy-induced apoptosis. *Cancer Res.* 1993;53(17):3976-3985.
138. Yuan CH, Filippova M, Duerksen-Hughes P. Modulation of apoptotic pathways by human papillomaviruses (HPV): mechanisms and implications for therapy. *Viruses.* 2012;4(12):3831-3850.
139. Fischer M. Census and evaluation of p53 target genes. *Oncogene.* 2017;36(28):3943-3956.
140. Aubrey BJ, Kelly GL, Janic A, Herold MJ, Strasser A. How does p53 induce apoptosis and how does this relate to p53-mediated tumour suppression? *Cell Death Differ.* 2018;25(1):104-113.
141. Vogt M, Butz K, Dymalla S, Semzow J, Hoppe-Seyler F. Inhibition of Bax activity is crucial for the antiapoptotic function of the human papillomavirus E6 oncoprotein. *Oncogene.* 2006;25(29):4009-4015.
142. Borbely AA, Murvai M, Konya J, et al. Effects of human papillomavirus type 16 oncoproteins on survivin gene expression. *J Gen Virol.* 2006;87(Pt 2):287-294.
143. Jackson S, Storey A. E6 proteins from diverse cutaneous HPV types inhibit apoptosis in response to UV damage. *Oncogene.* 2000;19(4):592-598.
144. Thomas M, Banks L. Inhibition of Bak-induced apoptosis by HPV-18 E6. *Oncogene.* 1998;17(23):2943-2954.
145. Yuan H, Fu F, Zhuo J, et al. Human papillomavirus type 16 E6 and E7 oncoproteins upregulate c-IAP2 gene expression and confer resistance to apoptosis. *Oncogene.* 2005;24(32):5069-5078.
146. Filippova M, Song H, Connolly JL, Dermody TS, Duerksen-Hughes PJ. The human papillomavirus 16 E6 protein binds to tumor necrosis factor (TNF) R1 and protects cells from TNF-induced apoptosis. *J Biol Chem.* 2002;277(24):21730-21739.
147. Filippova M, Parkhurst L, Duerksen-Hughes PJ. The human papillomavirus 16 E6 protein binds to Fas-associated death domain and protects cells from Fas-triggered apoptosis. *J Biol Chem.* 2004;279(24):25729-25744.
148. Garnett TO, Duerksen-Hughes PJ. Modulation of apoptosis by human papillomavirus (HPV) oncoproteins. *Arch Virol.* 2006;151(12):2321-2335.
149. Thompson DA, Zacny V, Belinsky GS, et al. The HPV E7 oncoprotein inhibits tumor necrosis factor alpha-mediated apoptosis in normal human fibroblasts. *Oncogene.* 2001;20(28):3629-3640.
150. Severino A, Abbruzzese C, Manente L, et al. Human papillomavirus-16 E7 interacts with Siva-1 and modulates apoptosis in HaCaT human immortalized keratinocytes. *J Cell Physiol.* 2007;212(1):118-125.
151. Hibi M, Lin A, Smeal T, Minden A, Karin M. Identification of an oncoprotein- and UV-responsive protein kinase that binds and potentiates the c-Jun activation domain. *Genes Dev.* 1993;7(11):2135-2148.
152. Dong C, Davis RJ, Flavell RA. MAP kinases in the immune response. *Annu Rev Immunol.* 2002;20:55-72.
153. Logan SK, Falasca M, Hu P, Schlessinger J. Phosphatidylinositol 3-kinase mediates epidermal growth factor-induced activation of the c-Jun N-terminal kinase signaling pathway. *Mol Cell Biol.* 1997;17(10):5784-5790.
154. Dhanasekaran DN, Reddy EP. JNK signaling in apoptosis. *Oncogene.* 2008;27(48):6245-6251.
155. Davis RJ. Signal transduction by the JNK group of MAP kinases. *Cell.* 2000;103(2):239-252.
156. Gupta S, Barrett T, Whitmarsh AJ, et al. Selective interaction of JNK protein kinase isoforms with transcription factors. *EMBO J.* 1996;15(11):2760-2770.

157. Yuasa T, Ohno S, Kehrl JH, Kyriakis JM. Tumor necrosis factor signaling to stress-activated protein kinase (SAPK)/Jun NH2-terminal kinase (JNK) and p38. Germinal center kinase couples TRAF2 to mitogen-activated protein kinase/ERK kinase kinase 1 and SAPK while receptor interacting protein associates with a mitogen-activated protein kinase kinase kinase upstream of MKK6 and p38. *J Biol Chem.* 1998;273(35):22681-22692.
158. Coso OA, Chiariello M, Yu JC, et al. The small GTP-binding proteins Rac1 and Cdc42 regulate the activity of the JNK/SAPK signaling pathway. *Cell.* 1995;81(7):1137-1146.
159. Schaeffer HJ, Weber MJ. Mitogen-activated protein kinases: specific messages from ubiquitous messengers. *Mol Cell Biol.* 1999;19(4):2435-2444.
160. Dhanasekaran N, Premkumar Reddy E. Signaling by dual specificity kinases. *Oncogene.* 1998;17(11 Reviews):1447-1455.
161. Gazon H, Barbeau B, Mesnard JM, Peloponese JM, Jr. Hijacking of the AP-1 Signaling Pathway during Development of ATL. *Front Microbiol.* 2017;8:2686.
162. Shaulian E, Karin M. AP-1 in cell proliferation and survival. *Oncogene.* 2001;20(19):2390-2400.
163. Angel P, Imagawa M, Chiu R, et al. Phorbol ester-inducible genes contain a common cis element recognized by a TPA-modulated trans-acting factor. *Cell.* 1987;49(6):729-739.
164. Yang Y, Cvekl A. Large Maf Transcription Factors: Cousins of AP-1 Proteins and Important Regulators of Cellular Differentiation. *Einstein J Biol Med.* 2007;23(1):2-11.
165. Karin M. The regulation of AP-1 activity by mitogen-activated protein kinases. *J Biol Chem.* 1995;270(28):16483-16486.
166. Angel P, Hattori K, Smeal T, Karin M. The jun proto-oncogene is positively autoregulated by its product, Jun/AP-1. *Cell.* 1988;55(5):875-885.
167. Childs BG, Baker DJ, Kirkland JL, Campisi J, van Deursen JM. Senescence and apoptosis: dueling or complementary cell fates? *EMBO Rep.* 2014;15(11):1139-1153.
168. Hayflick L, Moorhead PS. The serial cultivation of human diploid cell strains. *Exp Cell Res.* 1961;25:585-621.
169. O'Sullivan RJ, Karlseder J. Telomeres: protecting chromosomes against genome instability. *Nat Rev Mol Cell Biol.* 2010;11(3):171-181.
170. Munoz-Espin D, Serrano M. Cellular senescence: from physiology to pathology. *Nat Rev Mol Cell Biol.* 2014;15(7):482-496.
171. Coppe JP, Desprez PY, Krtolica A, Campisi J. The senescence-associated secretory phenotype: the dark side of tumor suppression. *Annu Rev Pathol.* 2010;5:99-118.
172. Acosta JC, Banito A, Wuestefeld T, et al. A complex secretory program orchestrated by the inflammasome controls paracrine senescence. *Nat Cell Biol.* 2013;15(8):978-990.
173. Xue W, Zender L, Miething C, et al. Senescence and tumour clearance is triggered by p53 restoration in murine liver carcinomas. *Nature.* 2007;445(7128):656-660.
174. Laurson J, Raj K. Localisation of human papillomavirus 16 E7 oncoprotein changes with cell confluence. *PLoS One.* 2011;6(6):e21501.
175. Sarbassov DD, Guertin DA, Ali SM, Sabatini DM. Phosphorylation and regulation of Akt/PKB by the rictor-mTOR complex. *Science.* 2005;307(5712):1098-1101.
176. Fontaine E. Metformin-Induced Mitochondrial Complex I Inhibition: Facts, Uncertainties, and Consequences. *Front Endocrinol (Lausanne).* 2018;9:753.
177. Hoppe-Seyler K, Herrmann AL, Daschle A, et al. Effects of Metformin on the virus/host cell crosstalk in human papillomavirus-positive cancer cells. *Int J Cancer.* 2021;149(5):1137-1149.
178. Zhuang L, Ly R, Rosl F, Niebler M. p53 Is Regulated in a Biphasic Manner in Hypoxic Human Papillomavirus Type 16 (HPV16)-Positive Cervical Cancer Cells. *Int J Mol Sci.* 2020;21(24).
179. Fuks F. DNA methylation and histone modifications: teaming up to silence genes. *Curr Opin Genet Dev.* 2005;15(5):490-495.
180. Issa JP, Kantarjian HM, Kirkpatrick P. Azacitidine. *Nat Rev Drug Discov.* 2005;4(4):275-276.

181. Vanhaecke T, Papeleu P, Elaut G, Rogiers V. Trichostatin A-like hydroxamate histone deacetylase inhibitors as therapeutic agents: toxicological point of view. *Curr Med Chem.* 2004;11(12):1629-1643.
182. Venkatraman M, Anto RJ, Nair A, Varghese M, Karunakaran D. Biological and chemical inhibitors of NF-kappaB sensitize SiHa cells to cisplatin-induced apoptosis. *Mol Carcinog.* 2005;44(1):51-59.
183. Baldus SE, Schwarz E, Lohrey C, et al. Smad4 deficiency in cervical carcinoma cells. *Oncogene.* 2005;24(5):810-819.
184. Honegger A, Schilling D, Bastian S, et al. Dependence of intracellular and exosomal microRNAs on viral E6/E7 oncogene expression in HPV-positive tumor cells. *PLoS Pathog.* 2015;11(3):e1004712.
185. Debacq-Chainiaux F, Erusalimsky JD, Campisi J, Toussaint O. Protocols to detect senescence-associated beta-galactosidase (SA-beta-gal) activity, a biomarker of senescent cells in culture and in vivo. *Nat Protoc.* 2009;4(12):1798-1806.
186. Zhong Z, Virshup DM. Wnt Signaling and Drug Resistance in Cancer. *Mol Pharmacol.* 2020;97(2):72-89.
187. Gao Y, Liu Z, Zhang X, et al. Inhibition of cytoplasmic GSK-3beta increases cisplatin resistance through activation of Wnt/beta-catenin signaling in A549/DDP cells. *Cancer Lett.* 2013;336(1):231-239.
188. Korinek V, Barker N, Morin PJ, et al. Constitutive transcriptional activation by a beta-catenin-Tcf complex in APC-/- colon carcinoma. *Science.* 1997;275(5307):1784-1787.
189. Giuliano CJ, Lin A, Girish V, Sheltzer JM. Generating Single Cell-Derived Knockout Clones in Mammalian Cells with CRISPR/Cas9. *Curr Protoc Mol Biol.* 2019;128(1):e100.
190. Hedgepeth CM, Conrad LJ, Zhang J, Huang HC, Lee VM, Klein PS. Activation of the Wnt signaling pathway: a molecular mechanism for lithium action. *Dev Biol.* 1997;185(1):82-91.
191. Kim L, Wong TW. The cytoplasmic tyrosine kinase FER is associated with the catenin-like substrate pp120 and is activated by growth factors. *Mol Cell Biol.* 1995;15(8):4553-4561.
192. Lappano R, De Marco P, De Francesco EM, Chimento A, Pezzi V, Maggiolini M. Cross-talk between GPER and growth factor signaling. *J Steroid Biochem Mol Biol.* 2013;137:50-56.
193. Prenzel N, Zwick E, Daub H, et al. EGF receptor transactivation by G-protein-coupled receptors requires metalloproteinase cleavage of proHB-EGF. *Nature.* 1999;402(6764):884-888.
194. Cai W, Li H, Zhang Y, Han G. Identification of key biomarkers and immune infiltration in the synovial tissue of osteoarthritis by bioinformatics analysis. *PeerJ.* 2020;8:e8390.
195. Chen L, Wang S, Zhou Y, et al. Identification of early growth response protein 1 (EGR-1) as a novel target for JUN-induced apoptosis in multiple myeloma. *Blood.* 2010;115(1):61-70.
196. Subramanian A, Tamayo P, Mootha VK, et al. Gene set enrichment analysis: a knowledge-based approach for interpreting genome-wide expression profiles. *Proc Natl Acad Sci U S A.* 2005;102(43):15545-15550.
197. Schaefer CF, Anthony K, Krupa S, et al. PID: the Pathway Interaction Database. *Nucleic Acids Res.* 2009;37(Database issue):D674-679.
198. Wang H, Yang YB, Shen HM, Gu J, Li T, Li XM. ABT-737 induces Bim expression via JNK signaling pathway and its effect on the radiation sensitivity of HeLa cells. *PLoS One.* 2012;7(12):e52483.
199. O'Connor L, Strasser A, O'Reilly LA, et al. Bim: a novel member of the Bcl-2 family that promotes apoptosis. *EMBO J.* 1998;17(2):384-395.
200. Sionov RV, Vlahopoulos SA, Granot Z. Regulation of Bim in Health and Disease. *Oncotarget.* 2015;6(27):23058-23134.
201. Whitmarsh AJ, Davis RJ. Transcription factor AP-1 regulation by mitogen-activated protein kinase signal transduction pathways. *J Mol Med (Berl).* 1996;74(10):589-607.

202. Li G, Xiang Y, Sabapathy K, Silverman RH. An apoptotic signaling pathway in the interferon antiviral response mediated by RNase L and c-Jun NH₂-terminal kinase. *J Biol Chem.* 2004;279(2):1123-1131.
203. Zhang T, Inesta-Vaquera F, Niepel M, et al. Discovery of potent and selective covalent inhibitors of JNK. *Chem Biol.* 2012;19(1):140-154.
204. Jiang T, Huang L, Zhang S. DKK-1 in serum as a clinical and prognostic factor in patients with cervical cancer. *Int J Biol Markers.* 2013;28(2):221-225.
205. Bley IA, Zwick A, Hans MC, et al. DKK1 inhibits canonical Wnt signaling in human papillomavirus-positive penile cancer cells. *Transl Oncol.* 2022;15(1):101267.
206. Mikheev AM, Mikheeva SA, Maxwell JP, et al. Dickkopf-1 mediated tumor suppression in human breast carcinoma cells. *Breast Cancer Res Treat.* 2008;112(2):263-273.
207. Forget MA, Turcotte S, Beauseigle D, et al. The Wnt pathway regulator DKK1 is preferentially expressed in hormone-resistant breast tumours and in some common cancer types. *Br J Cancer.* 2007;96(4):646-653.
208. Babion I, Jaspers A, van Splunter AP, van der Hoorn IAE, Wilting SM, Steenbergen RDM. miR-9-5p Exerts a Dual Role in Cervical Cancer and Targets Transcription Factor TWIST1. *Cells.* 2019;9(1).
209. Wright AA, Howitt BE, Myers AP, et al. Oncogenic mutations in cervical cancer: genomic differences between adenocarcinomas and squamous cell carcinomas of the cervix. *Cancer.* 2013;119(21):3776-3783.
210. Genetos DC, Toupadakis CA, Raheja LF, et al. Hypoxia decreases sclerostin expression and increases Wnt signaling in osteoblasts. *J Cell Biochem.* 2010;110(2):457-467.
211. Guo KT, Fu P, Juerchott K, et al. The expression of Wnt-inhibitor DKK1 (Dickkopf 1) is determined by intercellular crosstalk and hypoxia in human malignant gliomas. *J Cancer Res Clin Oncol.* 2014;140(8):1261-1270.
212. Xu Y, Guo J, Liu J, et al. Hypoxia-induced CREB cooperates MMSET to modify chromatin and promote DKK1 expression in multiple myeloma. *Oncogene.* 2021;40(7):1231-1241.
213. Kelley ML, Keiger KE, Lee CJ, Huibregtse JM. The global transcriptional effects of the human papillomavirus E6 protein in cervical carcinoma cell lines are mediated by the E6AP ubiquitin ligase. *J Virol.* 2005;79(6):3737-3747.
214. Kuner R, Vogt M, Sultmann H, et al. Identification of cellular targets for the human papillomavirus E6 and E7 oncogenes by RNA interference and transcriptome analyses. *J Mol Med (Berl).* 2007;85(11):1253-1262.
215. Chen X, Ko LJ, Jayaraman L, Prives C. p53 levels, functional domains, and DNA damage determine the extent of the apoptotic response of tumor cells. *Genes Dev.* 1996;10(19):2438-2451.
216. Weinberg RL, Veprintsev DB, Bycroft M, Fersht AR. Comparative binding of p53 to its promoter and DNA recognition elements. *J Mol Biol.* 2005;348(3):589-596.
217. He YH, Su RJ, Zheng J. Detection of DKK-1 gene methylation in exfoliated cells of cervical squamous cell carcinoma and its relationship with high risk HPV infection. *Arch Gynecol Obstet.* 2021;304(3):743-750.
218. Komashko VM, Farnham PJ. 5-azacytidine treatment reorganizes genomic histone modification patterns. *Epigenetics.* 2010;5(3):229-240.
219. Gan L, Yang Y, Li Q, Feng Y, Liu T, Guo W. Epigenetic regulation of cancer progression by EZH2: from biological insights to therapeutic potential. *Biomark Res.* 2018;6:10.
220. Hussain M, Rao M, Humphries AE, et al. Tobacco smoke induces polycomb-mediated repression of Dickkopf-1 in lung cancer cells. *Cancer Res.* 2009;69(8):3570-3578.
221. Chi C, Li M, Hou W, Chen Y, Zhang Y, Chen J. Long Noncoding RNA SNHG7 Activates Wnt/beta-Catenin Signaling Pathway in Cervical Cancer Cells by Epigenetically Silencing DKK1. *Cancer Biother Radiopharm.* 2020;35(5):329-337.
222. Holland D, Hoppe-Seyler K, Schuller B, et al. Activation of the enhancer of zeste homologue 2 gene by the human papillomavirus E7 oncoprotein. *Cancer Res.* 2008;68(23):9964-9972.

223. Durzynska J, Lesniewicz K, Poreba E. Human papillomaviruses in epigenetic regulations. *Mutat Res Rev Mutat Res.* 2017;772:36-50.
224. Fu M, Wang C, Rao M, et al. Cyclin D1 represses p300 transactivation through a cyclin-dependent kinase-independent mechanism. *J Biol Chem.* 2005;280(33):29728-29742.
225. Patel D, Huang SM, Baglia LA, McCance DJ. The E6 protein of human papillomavirus type 16 binds to and inhibits co-activation by CBP and p300. *EMBO J.* 1999;18(18):5061-5072.
226. Camuzi D, de Amorim ISS, Ribeiro Pinto LF, Oliveira Trivilin L, Mencalha AL, Soares Lima SC. Regulation Is in the Air: The Relationship between Hypoxia and Epigenetics in Cancer. *Cells.* 2019;8(4).
227. Bushell M, Stoneley M, Sarnow P, Willis AE. Translation inhibition during the induction of apoptosis: RNA or protein degradation? *Biochem Soc Trans.* 2004;32(Pt 4):606-610.
228. Braun JA, Herrmann AL, Blase JL, et al. Effects of the antifungal agent ciclopirox in HPV-positive cancer cells: Repression of viral E6/E7 oncogene expression and induction of senescence and apoptosis. *Int J Cancer.* 2020;146(2):461-474.
229. Herrmann AL, Kuhn BJ, Holzer A, Krijgsveld J, Hoppe-Seyler K, Hoppe-Seyler F. Delineating the Switch between Senescence and Apoptosis in Cervical Cancer Cells under Ciclopirox Treatment. *Cancers (Basel).* 2021;13(19).
230. Aguilera O, Gonzalez-Sancho JM, Zazo S, et al. Nuclear DICKKOPF-1 as a biomarker of chemoresistance and poor clinical outcome in colorectal cancer. *Oncotarget.* 2015;6(8):5903-5917.
231. Gavrieli Y, Sherman Y, Ben-Sasson SA. Identification of programmed cell death in situ via specific labeling of nuclear DNA fragmentation. *J Cell Biol.* 1992;119(3):493-501.
232. Salim H, Zong D, Haag P, et al. DKK1 is a potential novel mediator of cisplatin-refractoriness in non-small cell lung cancer cell lines. *BMC Cancer.* 2015;15:628.
233. Li S, Qin X, Guo X, et al. Dickkopf-1 is oncogenic and involved in invasive growth in non small cell lung cancer. *PLoS One.* 2013;8(12):e84944.
234. Wang S, Zhang S. Dickkopf-1 is frequently overexpressed in ovarian serous carcinoma and involved in tumor invasion. *Clin Exp Metastasis.* 2011;28(6):581-591.
235. Sun X, Shi B, Zheng H, et al. Senescence-associated secretory factors induced by cisplatin in melanoma cells promote non-senescent melanoma cell growth through activation of the ERK1/2-RSK1 pathway. *Cell Death Dis.* 2018;9(3):260.
236. Wang X, Wong SC, Pan J, et al. Evidence of cisplatin-induced senescent-like growth arrest in nasopharyngeal carcinoma cells. *Cancer Res.* 1998;58(22):5019-5022.
237. Wu M, Ye H, Shao C, et al. Metabolomics-Proteomics Combined Approach Identifies Differential Metabolism-Associated Molecular Events between Senescence and Apoptosis. *J Proteome Res.* 2017;16(6):2250-2261.
238. Murray-Zmijewski F, Slee EA, Lu X. A complex barcode underlies the heterogeneous response of p53 to stress. *Nat Rev Mol Cell Biol.* 2008;9(9):702-712.
239. Zhang Y, Gao Y, Zhang G, et al. DNMT3a plays a role in switches between doxorubicin-induced senescence and apoptosis of colorectal cancer cells. *Int J Cancer.* 2011;128(3):551-561.
240. Wang L, Lankhorst L, Bernards R. Exploiting senescence for the treatment of cancer. *Nat Rev Cancer.* 2022.
241. Milanovic M, Fan DNY, Belenki D, et al. Senescence-associated reprogramming promotes cancer stemness. *Nature.* 2018;553(7686):96-100.
242. Bello JO, Nieva LO, Paredes AC, Gonzalez AM, Zavaleta LR, Lizano M. Regulation of the Wnt/beta-Catenin Signaling Pathway by Human Papillomavirus E6 and E7 Oncoproteins. *Viruses.* 2015;7(8):4734-4755.
243. Anania VG, Yu K, Gnad F, et al. Uncovering a Dual Regulatory Role for Caspases During Endoplasmic Reticulum Stress-induced Cell Death. *Mol Cell Proteomics.* 2016;15(7):2293-2307.
244. Yanamadala V, Negoro H, Denker BM. Heterotrimeric G proteins and apoptosis: intersecting signaling pathways leading to context dependent phenotypes. *Curr Mol Med.* 2009;9(5):527-545.

245. Ramesh G, Reeves WB. TNF-alpha mediates chemokine and cytokine expression and renal injury in cisplatin nephrotoxicity. *J Clin Invest.* 2002;110(6):835-842.
246. Kudo K, Gavin E, Das S, Amable L, Shevde LA, Reed E. Inhibition of Gli1 results in altered c-Jun activation, inhibition of cisplatin-induced upregulation of ERCC1, XPD and XRCC1, and inhibition of platinum-DNA adduct repair. *Oncogene.* 2012;31(44):4718-4724.
247. St Germain C, Niknejad N, Ma L, Garbuio K, Hai T, Dimitroulakos J. Cisplatin induces cytotoxicity through the mitogen-activated protein kinase pathways and activating transcription factor 3. *Neoplasia.* 2010;12(7):527-538.
248. Tsai TF, Lin JF, Lin YC, et al. Cisplatin contributes to programmed death-ligand 1 expression in bladder cancer through ERK1/2-AP-1 signaling pathway. *Biosci Rep.* 2019;39(9).
249. Sanchez-Perez I, Perona R. Lack of c-Jun activity increases survival to cisplatin. *FEBS Lett.* 1999;453(1-2):151-158.
250. Jang HS, Woo SR, Song KH, et al. API5 induces cisplatin resistance through FGFR signaling in human cancer cells. *Exp Mol Med.* 2017;49(9):e374.
251. Wang J, Zhou JY, Wu GS. Bim protein degradation contributes to cisplatin resistance. *J Biol Chem.* 2011;286(25):22384-22392.
252. Whitfield J, Neame SJ, Paquet L, Bernard O, Ham J. Dominant-negative c-Jun promotes neuronal survival by reducing BIM expression and inhibiting mitochondrial cytochrome c release. *Neuron.* 2001;29(3):629-643.
253. Heidari N, Miller AV, Hicks MA, Marking CB, Harada H. Glucocorticoid-mediated BIM induction and apoptosis are regulated by Runx2 and c-Jun in leukemia cells. *Cell Death Dis.* 2012;3:e349.
254. Hayakawa J, Mittal S, Wang Y, et al. Identification of promoters bound by c-Jun/ATF2 during rapid large-scale gene activation following genotoxic stress. *Mol Cell.* 2004;16(4):521-535.
255. Abate C, Luk D, Curran T. Transcriptional regulation by Fos and Jun in vitro: interaction among multiple activator and regulatory domains. *Mol Cell Biol.* 1991;11(7):3624-3632.
256. Liang G, Wolfgang CD, Chen BP, Chen TH, Hai T. ATF3 gene. Genomic organization, promoter, and regulation. *J Biol Chem.* 1996;271(3):1695-1701.
257. St Germain C, O'Brien A, Dimitroulakos J. Activating Transcription Factor 3 regulates in part the enhanced tumour cell cytotoxicity of the histone deacetylase inhibitor M344 and cisplatin in combination. *Cancer Cell Int.* 2010;10:32.
258. Adiseshaiah P, Papaiahgari SR, Vuong H, Kalvakolanu DV, Reddy SP. Multiple cis-elements mediate the transcriptional activation of human fra-1 by 12-O-tetradecanoylphorbol-13-acetate in bronchial epithelial cells. *J Biol Chem.* 2003;278(48):47423-47433.
259. Das KC, Muniyappa H. c-Jun-NH2 terminal kinase (JNK)-mediates AP-1 activation by thioredoxin: phosphorylation of cJun, JunB, and Fra-1. *Mol Cell Biochem.* 2010;337(1-2):53-63.
260. Liu J, Lin A. Role of JNK activation in apoptosis: a double-edged sword. *Cell Res.* 2005;15(1):36-42.
261. Yan D, An G, Kuo MT. C-Jun N-terminal kinase signalling pathway in response to cisplatin. *J Cell Mol Med.* 2016;20(11):2013-2019.
262. Brozovic A, Fritz G, Christmann M, et al. Long-term activation of SAPK/JNK, p38 kinase and fas-L expression by cisplatin is attenuated in human carcinoma cells that acquired drug resistance. *Int J Cancer.* 2004;112(6):974-985.
263. Krause U, Ryan DM, Clough BH, Gregory CA. An unexpected role for a Wnt-inhibitor: Dickkopf-1 triggers a novel cancer survival mechanism through modulation of aldehyde-dehydrogenase-1 activity. *Cell Death Dis.* 2014;5:e1093.
264. Khalili S, Rasaee MJ, Bamdad T. [3D structure of DKK1 indicates its involvement in both canonical and non-canonical Wnt pathways]. *Mol Biol (Mosk).* 2017;51(1):180-192.
265. Matsui K, Xiao S, Fine A, Ju ST. Role of activator protein-1 in TCR-mediated regulation of the murine fasl promoter. *J Immunol.* 2000;164(6):3002-3008.

266. Kolbus A, Herr I, Schreiber M, Debatin KM, Wagner EF, Angel P. c-Jun-dependent CD95-L expression is a rate-limiting step in the induction of apoptosis by alkylating agents. *Mol Cell Biol.* 2000;20(2):575-582.
267. Deng Y, Ren X, Yang L, Lin Y, Wu X. A JNK-dependent pathway is required for TNF α -induced apoptosis. *Cell.* 2003;115(1):61-70.
268. Ameyar M, Wisniewska M, Weitzman JB. A role for AP-1 in apoptosis: the case for and against. *Biochimie.* 2003;85(8):747-752.
269. Goyal L, Sirard C, Schrag M, et al. Phase I and Biomarker Study of the Wnt Pathway Modulator DKN-01 in Combination with Gemcitabine/Cisplatin in Advanced Biliary Tract Cancer. *Clin Cancer Res.* 2020;26(23):6158-6167.
270. Lourenco de Freitas N, Deberaldini MG, Gomes D, et al. Histone Deacetylase Inhibitors as Therapeutic Interventions on Cervical Cancer Induced by Human Papillomavirus. *Front Cell Dev Biol.* 2020;8:592868.
271. Jin KL, Park JY, Noh EJ, et al. The effect of combined treatment with cisplatin and histone deacetylase inhibitors on HeLa cells. *J Gynecol Oncol.* 2010;21(4):262-268.
272. Aguilera O, Pena C, Garcia JM, et al. The Wnt antagonist DICKKOPF-1 gene is induced by 1 α ,25-dihydroxyvitamin D₃ associated to the differentiation of human colon cancer cells. *Carcinogenesis.* 2007;28(9):1877-1884.
273. Ma Y, Trump DL, Johnson CS. Vitamin D in combination cancer treatment. *J Cancer.* 2010;1:101-107.
274. Zhang F, Yu X, Liu X, et al. ABT-737 potentiates cisplatin-induced apoptosis in human osteosarcoma cells via the mitochondrial apoptotic pathway. *Oncol Rep.* 2017;38(4):2301-2308.
275. Veeman MT, Slusarski DC, Kaykas A, Louie SH, Moon RT. Zebrafish prickles, a modulator of noncanonical Wnt/Fz signaling, regulates gastrulation movements. *Curr Biol.* 2003;13(8):680-685.
276. Najdi R, Proffitt K, Sprowl S, et al. A uniform human Wnt expression library reveals a shared secretory pathway and unique signaling activities. *Differentiation.* 2012;84(2):203-213.
277. Butz K, Shahabeddin L, Geisen C, Spitkovsky D, Ullmann A, Hoppe-Seyler F. Functional p53 protein in human papillomavirus-positive cancer cells. *Oncogene.* 1995;10(5):927-936.
278. Sanjana NE, Shalem O, Zhang F. Improved vectors and genome-wide libraries for CRISPR screening. *Nat Methods.* 2014;11(8):783-784.
279. Sambrook J, Russell DW. Purification of Closed Circular DNA by Equilibrium Centrifugation in CsCl-Ethidium Bromide Gradients: Discontinuous Gradients. *CSH Protoc.* 2006;2006(1).
280. Makarova KS, Haft DH, Barrangou R, et al. Evolution and classification of the CRISPR-Cas systems. *Nat Rev Microbiol.* 2011;9(6):467-477.
281. Adli M. The CRISPR tool kit for genome editing and beyond. *Nat Commun.* 2018;9(1):1911.
282. Concordet JP, Haeussler M. CRISPOR: intuitive guide selection for CRISPR/Cas9 genome editing experiments and screens. *Nucleic Acids Res.* 2018;46(W1):W242-W245.
283. Chen C, Okayama H. High-efficiency transformation of mammalian cells by plasmid DNA. *Mol Cell Biol.* 1987;7(8):2745-2752.
284. Livak KJ, Schmittgen TD. Analysis of relative gene expression data using real-time quantitative PCR and the 2^{- $\Delta\Delta$ C(T)} Method. *Methods.* 2001;25(4):402-408.
285. Bottone FG, Jr., Moon Y, Kim JS, Alston-Mills B, Ishibashi M, Eling TE. The anti-invasive activity of cyclooxygenase inhibitors is regulated by the transcription factor ATF3 (activating transcription factor 3). *Mol Cancer Ther.* 2005;4(5):693-703.
286. de Wilde J, De-Castro Arce J, Snijders PJ, Meijer CJ, Rosl F, Steenbergen RD. Alterations in AP-1 and AP-1 regulatory genes during HPV-induced carcinogenesis. *Cell Oncol.* 2008;30(1):77-87.
287. Dalma-Weiszhausz DD, Warrington J, Tanimoto EY, Miyada CG. The affymetrix GeneChip platform: an overview. *Methods Enzymol.* 2006;410:3-28.
288. Blighe K RS, Lewis M. EnhancedVolcano: Publication-ready volcano plots with enhanced colouring and labeling. <https://github.com/kevinblighe/EnhancedVolcano>. 2018.

289. Gregory R. Warnes BB, Lodewijk Bonebakker, Robert Gentleman,, Wolfgang Huber AL, Thomas Lumley, Martin Maechler, Arni, Magnusson SM, Marc Schwartz and Bill Venables. gplots: Various R Programming Tools for Plotting Data. R package version 3.1.1. <https://CRAN.R-project.org/package=gplots>. 2020.